CHEMICAL ENGINEERING SCIENCE
GENIE CHIMIQUE

VOL. 3 DECEMBER 1954 No. 6

The viscosity of pseudo-plastic fluids

JU CHIN CHU, K. C. BURRIDGE* and FRANK BROWN**
Polytechnic Institute of Brooklyn, Brooklyn 2, New York

(*Received July* 1954)

Summary—In a previous paper [5] the authors have discussed the development of a correlation for the prediction of heat transfer coefficients of pseudo-plastic fluids. For the application of the correlation to any particular problem, it is necessary to have viscosity data over the range of conditions involved. The present paper discusses the method employed for obtaining the viscosity data used in the correlation of heat transfer coefficients.

Three plastic (pseudo-) fluids were investigated covering a range of viscosities from one to thirteen centipoises. The pseudo-plastic liquids used were the aqueous solution of sodium carboxymethyl cellulose, polyvinyl alcohol, and sodium polymethacrylate. The modified Ostwald viscometer was designed and used in this work. Previous workers have used either pipe viscometers or the rotating cylinder type, both of which are cumbersome and expensive to install. The modified Ostwald viscometer maintains the condition of tubular flow and conducts the measurement at very low rates of shear. Another advantage of the modified Ostwald viscometer is that it enables viscosity measurements to be made at point values of the pressure drop across the capillary tube. This is important for pseudo-plastic fluids when the viscosity is dependent upon the rate of flow.

The results of viscosity measurement can be directly applicable to the design of heat exchangers and pressure drop calculations for the specification of the pump handling the pseudo-plastic fluids. It is probable that a similar treatment can be applied to those fluids exhibiting general non-Newtonian behaviour.

Résumé—Dans un mémoire antérieur, les auteurs ont discuté l'établissement d'une relation permettant la prévision des coefficients de transmission thermique des fluides pseudo-plastiques. Pour appliquer cette relation à un problème particulier, il faut connaître les valeurs de la viscosité dans l'étendue du domaine d'utilisation considéré. Les auteurs discutent ici la méthode qu'ils emploient pour obtenir les valeurs de la viscosité utilisées dans la corrélation des coefficients de transmission thermique.

Ils ont étudié trois fluides pseudo-plastiques couvrant des valeurs de la viscosité comprises entre une et treize centipoises. Les liquides pseudo-plastiques étaient une solution aqueuse d'oxyméthyl-cellulose-carbonate de sodium, d'alcool polyvinylique et de polyméthacrylate de sodium. Ils ont utilisé un viscosimètre d'OSTWALD convenablement modifié, tandis que les auteurs antérieurs avaient employé des viscosimètres à tube ou à cylindre rotatif, appareils encombrants et d'installation coûteuse. Le viscosimètre d'OSTWALD modifié assure un état d'écoulement laminaire et permet la mesure avec des tensions de cisaillement très faibles. L'appareil présente l'avantage supplémentaire de permettre des mesures de viscosité pour des valeurs parfaitement définies de la perte de charge à travers le capillaire : ceci est important pour les liquides pseudo-plastiques dont la viscosité varie avec la vitesse d'écoulement.

Les résultats de ces mesures sont directement applicables au dessin des échangeurs de chaleur et aux calculs des pertes de charges indispensables pour le choix des pompes pour la manutention des liquides pseudo-plastiques. Il paraît vraisemblable que le même mode de traitement serait applicable à d'autres fluides non-Newtoniens.

* Present address : Dunlop Rubber Co., Birmingham, England.
** „ „ Celanese Corp. of America, Summit, N.J.

Introduction

In a previous paper (5) the authors have developed a correlation for the prediction of heat transfer coefficients of pseudo-plastic fluids. The concept of heat transfer coefficient is based upon the assumption of a lamina flow adjacent to the wall. For both Newtonian and Non-Newtonian fluids, a knowledge of viscosity characteristics of the fluid is a prerequisite to the development of a correlation of heat transfer coefficient data.

The viscosity of a fluid is defined as the rate of a shear stress (Sg) to the rate of shearing (R_s) perpendicular to the direction of the shear stress. The rate of shearing, R_s, is expressed in terms of velocity gradient. Mathematically, the viscosity is given by :

$$\mu = Sg/R_s \tag{1}$$

This ratio is a constant independent of shear rate for a majority of fluids which are known as Newtonian Fluids. At zero stress of shear, the shear rate is equal to zero. For a flow through a channel of circular cross section, the viscosity of a fluid at the wall is given by :

$$\mu = \frac{PRg/2N}{4\overline{V}/\pi R^3} \tag{2}$$

where

$$PRg/2N = S_s \tag{3}$$

$$4\overline{V}/\pi R^3 = R_s \tag{4}$$

Eq. (2) indicates that the shear rate at the wall can be evaluated from the volumetric rate of flow of fluids and the diameter of the circular channel. The shearing stress at the wall is evaluated from the length and diameter of the channel with the data of pressure drop through the channel in a direction of flow. Since the viscosity of a Newtonian fluid is a constant for a given fluid at a given temperature and independent of shear stress, the visocity at the wall is the same as the viscosity of the fluid at any point in an isothermal flow.

On the other hand, if the ratio of shear stress to shear rate is not a constant, the fluid is called non-Newtonian. Pseudo-plastic fluids come into this general catagory. The viscosity of a pseudo-plastic fluid has a finite value at zero rate of shear, falling off asymptotically to a lower fixed value as the rate of shear increases to infinity. There is no time dependence of the viscosity on the condition of shear. Examples of these fluids are many suspensions, latices, emulsions and solutions of larger molecules.

The second class of fluids deviating from Newtonian behaviour are those known as "Bingham bodies." These materials show no evidence of flow until a certain minimum value of shear stress is achieved. Beyond this point they commence to flow and exhibit simple Newtonian behaviour providing the shear stress is maintained in excess of the yield point value. Such a material is sometimes termed an ideal plastic. In practice many materials behave as Bingham bodies insofar as they show yield points, but thereafter they behave as pseudo-plastic fluids rather than as simple Newtonian fluids. These fluids are termed by Hedstrom [8] to be general non-Newtonian fluids. Fig. 1 shows graphically the shearing stress vs. rate of shear relation for the various types of fluid discussed.

The present work is confined primarily to pseudo-plastic fluids, but it is probable that a

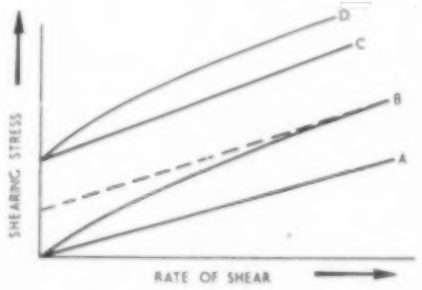

A = SIMPLE NEWTONIAN FLUID

B = PSEUDO PLASTIC FLUID

C = BINGHAM BODY

D = GENERAL NON NEWTONIAN FLUID

Fig. 1. Shear rate and stress diagram for fluids :—
A = Simple Newtonian fluid.
B = Pseudo-plastic fluid
C = Binham body
D = General non-Newtonian fluid.

VOL. 3 1954

similar treatment can be applied to those fluids exhibiting general non-Newtonian behaviour.

There are several terms with regard to the viscometric behaviour of a pseudo-plastic fluid. For the isothermal flow of pseudo-plastic fluid, WINDING has successfully used in his correlation [16-18] " apparent viscosity " which was defined by [2] [12] [16] [18] :

$$\mu_a = Sg/R_s \tag{5}$$

The rate of shear, R_s, and shearing stress Sg are calculated the same was as for a Newtonian fluid by Eqs. (3) and (4). However, the rate of shear computed from the volume by Eq. (4) can no longer be the true rate of shear at the wall because of its dependence upon the shear stress. Another term is called the differential viscosity, which is defined as the slope at any point of the curve of shear versus shear rate. Mathematically, it is given by :

$$\mu_d = \frac{dSg}{dR_s} \tag{6}$$

Fig. 2 shows the shearing stress vs. shearing rate curve of a typical pseudo-plastic fluid. It will be seen that the differential viscosity at any point X on the curve is the slope at point X, while the apparent viscosity is the ratio $\frac{XH}{OH}$.

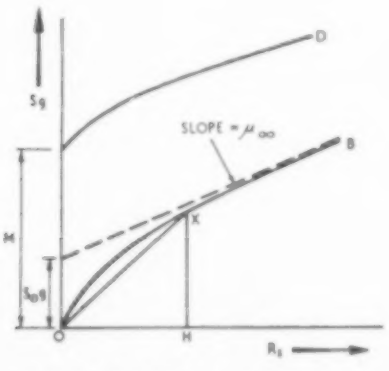

Fig. 2. Sheer rate and stress diagram for non-Newtonian fluids.
B = Curve for pseudo-plastic fluid.
D = Curve for general non-Newtonian fluid.

Although the apparent and differential viscosities are empirical quantities, they represent unique measures of the viscometric behaviour of a pseudo-plastic fluid at any selected condition of shear, and as such they are satisfactory for most engineering purposes.

There have been many attempts [1, 4, 11, 12, 13, 14, 15, 16] to derive an expression in relating the shear stress to the rate of shear for pseudo-plastic fluids. These expressions are known as the power series method [13, 14], the coefficient of structural stability method [14], the direct integration of tubular flow equation [11], and WILLIAMSONS equation [15]. Using a hyperbolic function of shear stress, BROWN and BURRIDGE [4] developed a relation which was too cumbersome to permit any practical application. WILLIAMSON's equation [15], which is the simplest relation between the shear stress and shear rate of a pseudo-plastic fluid, was used by WINDING *et al.* in the treatment of their data [16, 17, 18]. The equation is of the following form :

$$Sg/R_s = \frac{S_0 g}{a + R_s} + \mu_\infty \tag{7}$$

The constants in the equation, $S_0 g$, a, μ_∞ are functions of the system and temperature and not of rate of shear nor the dimensions of the tube.

As a consequence of the various methods of defining the coefficient of pseudo-plastic visocosity, it follows that the Reynolds number, depending as it does on viscosity, may also be expressed in several ways for a pseudo-plastic fluid. WINDING [16] recommended the use of the apparent viscosity, giving an apparent Reynolds number,

$$Re_a = \frac{DG}{\mu_a} \tag{8}$$

While the apparent viscosity is not a constant quantity across the section of a pseudo-plastic fluid in tubular flow, its use may be justified on the same basis as the use of the mass velocity, which also represents an average quantity, in the calculation of the Reynolds number [16]. In deriving the pseudo-plastic analogue of the Fanning friction factor, WINDING *et al.*

(18) found that data on *GR-S* latices were correlated better by the use of apparent viscosity at zero rate of shear.

In work on slurries behaving essentially as "Bingham bodies," BONILLA [3] and HEDSTROM [8] derived the apparent Reynolds number in terms of effective viscosity of slurry. The effective viscosity is mathematically analogous to the apparent viscosity at infinite rate of shear, μ_∞, of a pseudo-plastic fluid. In fact, WINDING [17, 18] used the apparent viscosity at infinite rate of shear in the correlation of some data particularly on heat transfer.

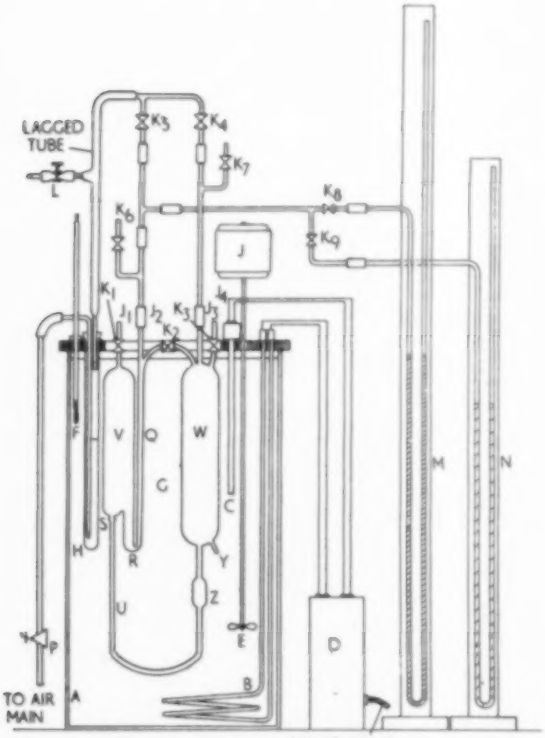

Fig. 3. General arrangement drawing of the viscosity apparatus.

EXPERIMENTAL METHOD

A. *Description of the apparatus.*

A schematic drawing of the general arrangement of the viscosity apparatus is presented in Fig. 3. Detailed dimensional drawings of the modified Ostwald viscometer used are shown in Fig. 4. A glass thermostat bath (A) was filled with water and temperature controlled to $\pm$ 0·05°C, the temperature of the bath being indicated by the precision grade mercury in glass thermometer (F) graduated in 0·1°C. The marine type impeller (E) assured vigorous agitation of the water in the bath.

In the thermostat bath were immersed the viscometer (G) and the air bubbler (H). The water level in the bath was maintained just below the cocks (K_1, K_2, and K_3) on the viscometer. The exit tubes (J_2 and J_3) of the viscometer

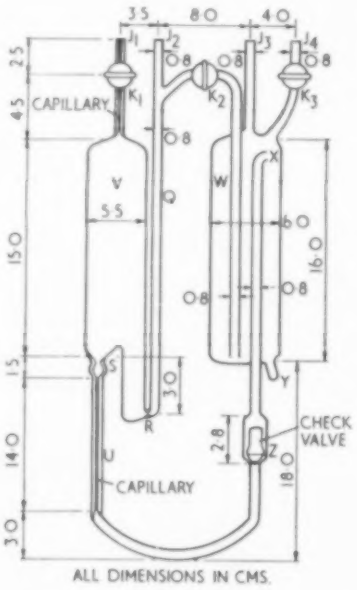

Fig. 4. Modified Ostwald viscometer.

were connected via pressure rubber tubing to the air feed and exit manifold system comprising cocks K_4, K_5, K_6, K_7, and L. This manifold system provided the flexibility of air supply, and of venting to atmospheric pressure, which was necessary for the development of a convenient experimental procedure. This manifold also had a connection via cock K_8 to the mercury manometer (M), or via cock K_9 to the water manometer (N).

Filtered compressed air was supplied from an 80 p.s.i.g. main via a reducing value (P).

Suitable adjustment of this reducing valve enabled a constant pressure on the exit side of the valve to be maintained at any value greater than 3 cm Hg gauge. For lower exit pressures the operation of the reducing valve became erratic. Constant pressures below 3 cm Hg gauge were obtained by adjusting the valve to give an exit pressure of 3 cm Hg gauge and introducing a leak to atmosphere on the exit side of the valve by adjusting the screw clip (L). The bubbler (H) was necessary to saturate the feed air at the operating temperature of thermostat in order to avoid evaporation of the sample in the viscometer. The exit pipe from the bubbler to the T-joint leading to cocks K_4 and K_5 was lagged.

B. *Experimental procedure*

The "Ostwald viscometer," used in this work differed from those used ordinarily in that the bulbs were designed to hold a sample of approximately 100 ml. This large sample size minimized the effect of any errors in measuring the time of passage of the sample when flowing through the capillary at high rate. Such measurements would not be necessary in the case of a simple Newtonian fluid but becomes essential with a pseudo-plastic fluid if its viscometric behaviour is to be established over a reasonably wide range of rates of shear. Four such viscometers were constructed. These viscometers were of essentially identical external dimensions and differed only in the bore of the capillary tube. The bore ranged from about 0·075 cm to 0·2 cm. The details of the viscometer dimensions are given in Table 1.

The capillaries were specially selected to be of uniform bore to within $\pm$ 0·4% throughout their length, and the sample volumes were measured to $\pm$ 0·1 ml.

It was necessary to obtain data from viscometers over a range of capillary diameters in order to determine the significance of the wall slippage effect in relation to capillary diameter [16]. The viscometer was filled with approximately 105 ml of liquid and placed in the thermostat bath, the latter having previously been adjusted in the thermostat bath, the latter having previously been adjusted to the required temperature. The exit tubes (J_2 and J_3) of the viscometer were connected.

To expel liquid from bulb (W) to bulb (V) (Fig. 4), cocks K_5 and K_7 were closed and cock K_6 was opened. The air pressure was applied into bulb (W) by opening cock K_4. To reverse the liquid flow, cocks K_4 and K_6 were closed, K_7 was opened, and air pressure was applied to bulb (V) by opening K_5. The air pressure thus applied to (V) was shown on either the mercury manometer (M) or the water manometer (N), depending on whether cock K_8 or cock K_9 was opened. The water manometer was used, for greater accuracy, when the applied air pressure was less than 4 cm Hg gauge.

Cock K_7 was of large bore to enable easy exit of the air to the atmosphere from bulb (W) as the liquid level in the bulb rose. The various cocks and T-joints in the manifold system were connected together with short lengths of pressure hose which allowed some flexibility and facilitated the removal of the viscometer from the thermostat bath. With the pressure rubber tubing, the viscometer could be adjusted exactly to a vertical position in the bath. About 15 minutes were required for the sample to attain the temperature of the bath, the temperature equalizing process being promoted by blowing the sample liquid to and fro between bulbs (V) and (W). The temperature equilibrium of the sample was checked by setting the feed air pressure at some arbitrary value and taking successive measurements of the time required for bulb (V) to be emptied of liquid between the graduation levels at (R) and (S). Time measurements were recorded on a stop-watch reading to 0·1 sec. Pressure differences could be read to $\pm$ 0·02 cm Hg on the mercury manometer and $\pm$ 0·1 cm water on the water manometer.

The ordinary Ostwald viscometer has limitations both as regards the range of data that can be obtained from it and also with regard to certain assumptions implicit in obtaining the data. The modified Ostwald viscometer was developed to eliminate these objections and is illustrated in Fig. 5. The sample liquid was expelled from bulb (V) through the capillary (U) into bulb (W), and the time of passage of the liquid level

from the graduation mark (R) to the graduation mark (S) was measured. (Z) was a check valve with a buoyant float to facilitate the transference back of liquid from bulb (W) to bulb (V).

To make a measurement of viscosity, the bulb (V) was completely filled up to cock K_1; then with K_1, K_2, K_4 and K_6 closed and K_7 open, the air pressure was applied down the tube (Q). In filling the bulb (V), the tube (Q) was also partially filled so that with the initial passage of air down (Q) displacing this liquid, the liquid flow out through (X) into the bulb (W) before the liquid in (Q) was displaced beyond the constriction (R). The time for the liquid to pass through the constriction (R) to constriction (S) was measured.

The object in designing the modified Ostwald viscometer was to enable the liquid to be discharged through the capillary tube under a pressure head which was constant and independent of the liquid level in either viscometer bulb. It was possible with this instrument to take measurements at pressure heads approaching zero without any low limit being imposed by either hydrostatic head in the viscometer bulbs. Since the whole of the flow for a given measurement was at one definite pressure, the rate of flow calculated from the data was for that pressure and was not an average rate of flow derived for a pressure range, which was the case when the normal Ostwald viscometer was employed.

Viscometers Nos. I, II, III and IV were used to determine the effect of wall slippage, as considered in the discussion of the results. The solution used was a 0·35% solution of sodium carboxymethyl cellulose. The modified Ostwald viscometer was subsequently employed for the whole of the viscosity data on the fluids used for the experiments on heat transfer [4, 5].

The viscosity data were obtained for the following solution. The data are treated and presented graphically in Figs. 6-8 as well as in Tables 1 to 17.

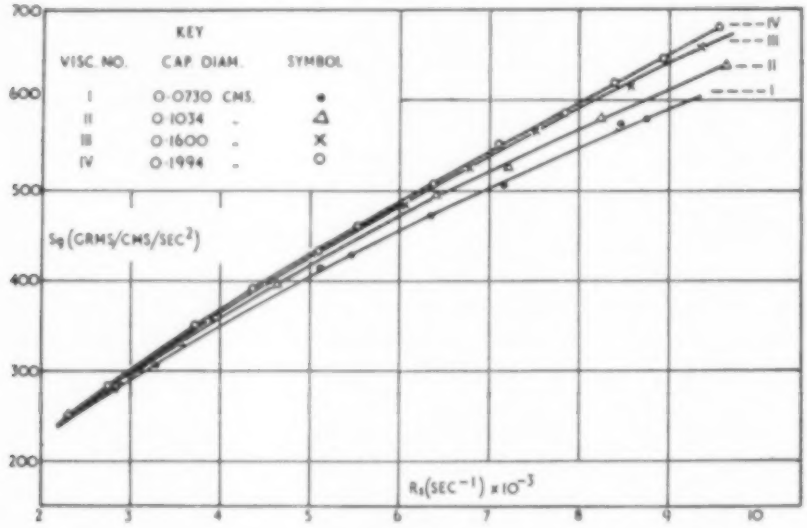

Fig. 5. Graph of the consistency variables for 0·35% CMC solution in water, showing the effect of capillary diameter.

(a) 0·25% sodium carboxymethyl cellulose (CMC) solution; data at 30°C, 35°C, 42°C, 49°C, 56°C, 63°C and 70°C.

(b) 2·5% polyvinyl alcohol (PVA) solution; data at 30°C, 40°C, 50°C, 60°C and 70°C.

(c) 0·025% sodium polymethacrylate (SPM) solution; data at 30°C, 40°C, 50°C, 60°C and 70°C.

VOL. 3 1954

Table 1. *Viscosity data of* 0·25% *CMC solution at* 30°C.

Instrument : Modified Ostwald Viscometer.

Pressure (cm Hg)	*Time (sec.)*	*N′ (cm.)*	*Sg (g/cm sec²)*	R_s *(sec⁻¹)* × 10^{-3}
0·169	2010·2	17·30	6·0	0·147
0·85	420·6	17·55	33·9	0·69
1·77	201·5	18·05	68·6	1·45
2·42	143·7	18·60	91·1	2·03
2·84	122·35	19·12	104·0	2·40
3·44	102·1	19·85	121·2	2·86
4·39	80·6	20·7	148·4	3·62
6·04	59·9	22·75	185·6	4·87
7·09	51·5	23·95	208·4	5·67
8·29	44·9	25·35	229	6·50

Instrument : Ostwald Viscometer No. IV.

6·8	19·6	18·8	237·8	6·78
8·05	17·0	20·1	264·4	7·82
9·65	14·8	22·5	283·6	8·98
10·6	13·6	23·7	296·1	9·77
11·9	12·35	24·9	316·4	10·77
12·9	11·5	26·1	327·5	11·56
14·1	10·7	27·0	345·6	12·41
14·85	10·35	27·6	351·2	12·84

Table 2. *Viscosity data of* 0·25% *CMC solution at* 35°C.

Instrument : Modified Ostwald Viscometer.

Pressure (cm Hg)	*Time (sec)*	*N′ (cm.)*	*Sg (g/cm sec)²*	R_s *(sec⁻¹)* × 10^{-3}
0·25	1551·0	16·8	10·4	0·19
0·91	353·6	17·55	36·3	0·83
1·45	220·1	18·0	55·4	1·32
1·87	173·7	18·5	70·7	1·68
2·48	129·9	19·2	90·5	2·25
2·76	111·3	19·35	99·8	2·53
4·01	80·6	20·6	134·5	3·49
4·61	70·6	21·6	148·0	3·99
5·46	60·2	22·75	168·0	4·68
6·91	49·8	25·1	193·0	5·86
7·81	44·6	26·1	209·6	6·45

Table 2—(contd.)

Instrument : Ostwald Viscometer No. IV.

4·45	28·1	17·55	168·0	4·73
5·3	23·15	18·55	189·3	5·75
6·15	20·35	19·2	212	6·53
6·7	19·0	19·95	222·4	7·0
6·8	18·7	20·2	223	7·11
8·0	16·4	21·65	244·5	8·11
9·15	14·85	23·1	262	8·95
10·35	13·2	24·7	277	10·06
11·55	12·2	25·9	295	10·89
12·1	11·55	26·6	300·5	11·51
13·3	10·7	28·05	313·5	12·42
13·9	10·35	28·55	322	12·85

VOL. 3 1954

Table 3. Viscosity data of 0·25% CMC solution at 42°C.

Instrument : Modified Ostwald Viscometer.

Pressure (cm Hg)	*Time (sec)*	*N′ (cm.)*	*Sg (g/cm sec²)*	R_a *(sec⁻¹)* × 10^{-3}
0·48	578·5	17·65	19·0	0·50
0·805	381·8	17·75	31·8	0·76
1·02	276·1	18·25	39·1	1·055
1·75	157·5	19·5	62·8	1·85
2·75	102·7	20·5	94·0	2·84
4·01	74·0	22·45	130·1	3·94
4·71	64·4	23·5	140·0	4·53
5·41	56·2	25·1	150·7	5·19
5·96	52·05	25·95	160·6	5·60
6·96	45·7	27·7	177·0	6·37
7·71	41·95	29·9	190·5	6·95

Instrument : Ostwald Viscometer No. IV.

4·1	26·95	18·85	144·0	4·93
5·7	20·7	20·35	185·3	6·42
6·3	18·65	21·35	195·4	7·12
6·45	18·2	21·55	198·1	7·30
6·75	17·55	22·1	202	7·57
7·5	16·0	23·2	214	8·30
8·25	14·8	24·45	223	8·98
9·0	14·05	25·0	238	9·45
9·6	13·1	26·1	243	10·13
12·0	11·05	28·75	276	12·02
12·8	10·5	29·5	285	12·66
13·4	10·1	30·3	292·5	13·16

Table 4. Viscosity data of 0·25% CMC solution at 49°C.
Instrument : Modified Ostwald Viscometer.

Pressure (cm Hg)	*Time (sec)*	*N′ (cm.)*	*Sg (g/cm sec²)*	R_s *(sec⁻¹)* × 10^{-3}
0·44	563·4	17·55	17·5	0·52
0·96	263·8	18·6	33·6	1·11
1·66	153·3	19·8	58·7	1·90
2·46	106·2	20·9	79·0	2·75
2·92	90·7	21·85	93·5	3·22
3·32	79·5	22·85	102·5	3·67
4·32	64·05	24·3	124·4	4·55
5·47	52·25	27·2	140·8	5·59

Instrument : Ostwald Viscometer No. IV.

4·2	24·6	20·1	138·3	5·40
4·4	23·5	20·85	139·4	5·65
5·2	20·8	21·55	159·4	6·39
6·05	18·35	22·6	177·2	7·24
6·55	17·25	23·15	187·0	7·70
7·2	15·8	24·5	194·5	8·41
7·3	15·6	24·65	196·0	8·52
8·1	14·4	25·6	209	9·23
9·0	13·2	26·8	222	10·06
9·45	12·85	27·65	225	10·34
9·85	12·3	28·4	229·5	10·80
11·0	11·3	29·75	244·5	11·76
11·65	10·9	30·1	256	12·19
12·9	9·9	32·2	265·5	13·42

Table 5. Viscosity data of 0·25% CMC solution at 56°C.
Instrument : Modified Ostwald Viscometer.

Pressure (cm Hg)	*Time (sec)*	*N′ (cm.)*	*Sg (g/cm sec²)*	R_s *(sec⁻¹)* × 10^{-3}
0·34	635·1	18·3	13·0	0·46
0·555	399·2	18·35	21·2	0·73
1·21	188·15	19·7	43·0	1·55
1·58	146·0	20·5	54·0	2·00
1·88	122·0	21·15	62·2	2·38
2·28	101·3	22·0	72·5	2·88
3·18	75·8	23·9	93·1	3·85
4·23	61·0	25·9	114·2	4·78
5·28	50·95	29·05	127·2	5·72
6·23	45·2	31·1	140·2	6·45

Table 5—(contd.)

Instrument : Ostwald Viscometer No. IV.

3·6	26·0	21·05	118·0	5·11
4·5	21·8	22·6	131·8	6·13
5·25	19·0	23·05	145·0	·00
6·3	16·6	25·65	162·5	8·00
7·3	14·95	26·6	181·4	8·89
7·6	14·3	27·75	181·0	9·30
8·5	13·1	29·25	191·8	10·14
9·65	12·0	30·45	209·6	11·08
10·55	11·05	32·4	215·7	12·03
12·2	9·8	34·3	235·5	13·56

VOL. 3 1954

Table 6. Viscosity data of 0·25% CMC solution at 63°C.

Instrument : Modified Ostwald Viscometer.

Pressure (cm Hg)	*Time (sec)*	*N′ (cm.)*	*Sg (g/cm sec²)*	R_s *(sec⁻¹)* × 10^{-3}
0·24	652·2	18·3	9·2	0·38
0·44	415·6	18·3	16·8	0·70
0·75	260·1	19·55	26·8	1·12
1·41	138·5	21·75	45·4	2·11
2·18	95·1	23.5	65·0	3·07
3·04	70·9	26·8	79·5	4·11
3·84	66·8	28·2	83·0	4·37
4·69	51·5	31·3	104·9	5·66

Instrument : Ostwald Viscometer No. IV.

3·55	24·2	22·8	102·8	5·49
3·95	22·45	23·45	111·2	5·91
4·2	21·3	24·0	115·8	6·24
4·55	20·3	24·6	122·2	6·65
5·2	18·15	25·85	132·9	7·32
5·9	16·3	28·0	139·1	8·15
6·2	15·15	28·2	145·2	8·88
7·0	14·3	30·15	153·6	9·29
7·45	13·9	30·1	163·7	9·56
8·15	12·95	31·2	172·6	10·26
8·5	12·4	32·6	172·7	10·72
9·1	11·8	33·2	181·2	11·26
10·1	10·85	34·7	192·5	12·25
11·05	10·13	35·6	205	13·11

Table 7. Viscosity data of 0·25% CMC solution at 70°C.
Instrument : Modified Ostwald Viscometer.

Pressure (cm Hg)	*Time (sec)*	*N′ (cm)*	*Sg (g/cm sec²)*	R_s *(sec⁻¹)* × 10^{-3}
0·32	489·5	20·5	10·9	0·60
0·70	231·7	21·1	23·2	1·26
1·41	124·7	23·1	42·7	2·34
1·67	108·7	23·8	49·1	2·68
2·50	77·9	27·2	60·1	3·75
3·10	65·3	29·9	72·6	4·47
3·75	56·1	32·8	80·0	5·20
4·30	50·8	33·3	90·5	5·74
Instrument : Ostwald Viscometer No. IV.				
2·35	32·0	21·7	71·6	4·15
4·15	20·15	26·9	102·7	6·60
4·85	18·25	27·65	115·8	7·28
5·4	16·85	28·8	124·0	7·89
5·9	15·5	30·35	128·4	8·57
6·85	13·95	31·95	141·9	9·53
7·2	13·3	33·4	142·6	9·99
7·8	12·55	34·6	149·1	10·59
9·1	11·18	36·5	165·0	11·92
10·5	9·95	39·0	178·0	13·86

Table 8. Viscosity data of 2·5% PVA solution at 30°C.
Instrument : Modified Oswald Viscometer.

Pressure (cm Hg)	*Time (sec)*	*N′ (cm.)*	*Sg (g/cm sec⁻²)*	R_s *(sec⁻¹)* × 10^{-3}
0·71	415·0	17·6	28·2	0·70
1·17	254·6	17·95	45·6	1·14
1·46	206·2	18·30	55·9	1·41
2·02	156·1	18·95	74·6	1·87
2·84	114·0	19·6	101·4	2·56
3·34	96·6	20·2	115·7	3·02
3·89	84·6	20·75	131·2	3·45
4·40	75·4	21·35	147·3	3·87
5·15	66·3	22·15	162·8	4·40
6·04	58·6	22·9	184·7	4·98
6·14	57·8	23·0	187·0	5·05
7·14	50·85	24·25	206	5·74
8·04	46·7	24·8	227	6·25
8·59	44·0	25·35	237·5	6·63

Table 9. Viscosity data of 2·5% PVA solution at 40°C.
Instrument : Modified Ostwald Viscometer.

Pressure (cm Hg)	*Time (sec)*	*N′ (cm)*	*Sg (g/cm sec²)*	R_s *(sec⁻¹)* $\times 10^{-3}$
0·59	398·1	18·15	22·8	0·73
0·74	316·3	18·45	28·1	0·92
1·16	207·9	19·2	42·3	1·41
1·64	149·7	20·1	57·1	1·95
2·35	108·05	21·1	78·0	2·70
2·85	89·2	21·6	91·1	3·27
3·4	78·3	22·7	104·8	3·72
3·8	71·9	23·25	111·4	4·06
4·35	63·1	24·1	126·3	4·62
4·7	60·7	24·7	133·1	4·80
5·65	52·4	26·6	148·6	5·57
6·25	48·35	27·8	157·4	6·04
6·6	47·2	27·5	168·0	6·17
7·2	43·9	29·0	174·0	6·64

Table 10. Viscosity data of 2·5% PVA solution at 50°C.
Instrument : Modified Ostwald Viscometer.

Pressure (cm Hg)	*Time (sec)*	*N′ (cm)*	*Sg (g/cm sec²)*	R_s *(sec⁻¹)* $\times 10^{-3}$
0·48	434·8	18·45	16·3	0·67
0·73	268·0	19·75	25·9	1·09
1·11	175·4	20·8	37·4	1·66
1·61	126·5	21·9	51·4	2·31
2·00	103·0	23·0	60·9	2·83
2·17	92·6	23·5	64·6	3·05
2·34	89·5	24·0	68·3	3·26
2·75	78·55	25·4	75·8	3·71
3·25	69·4	26·3	86·1	4·20
4·25	57·3	28·6	104·0	5·09
4·85	51·9	30·0	113·2	5·62
5·55	47·5	32·95	117·9	6·14
5·9	45·1	33·0	125·1	6·47
6·3	42·7	34·9	126·4	6·83

Table 11. Viscosity data of 2·5% PVA solution at 60°C.
Instrument Modified Ostwald Viscometer.

Pressure (cm Hg)	*Time (sec)*	*N′ (cm)*	*Sg (g/cm sec²)*	R_s *(sec⁻¹)* $\times 10^{-3}$
0·25	622·1	19·85	8·8	0·47
0·64	261·3	20·5	21·8	1·12
1·05	156·8	22·25	33·0	1·86
1·41	122·0	23·5	42·0	2·39
2·01	93·5	25·05	55·9	3·12
2·36	83·6	25·8	64·0	3·49
2·71	72·95	25·4	66·6	4·00
3·08	66·6	29·5	73·1	4·38
3·61	59·1	32·4	78·1	4·94
4·21	52·95	33·5	87·9	5·51
5·26	45·8	36·9	99·8	6·37
5·96	42·15	37·6	110·5	6·92

VOL. 3 1954

Table 12. *Viscosity data of* 2·5% *PVA solution at* 70°*C.*

Pressure (cm Hg)	*Time (sec)*	*N′ (cm)*	*Sg (g/cm sec²)*	R_s *(sec⁻¹)* × 10^{-3}
0·28	492·4	21·2	9·2	0·59
0·43	316·3	21·8	13·8	0·92
0·94	156·2	24·0	27·5	1·87
1·23	123·9	25·3	34·1	2·36
1·41	109·5	27·2	36·3	2·66
1·91	89·05	28·4	47·1	3·28
2·13	81·6	30·0	49·7	3·58
2·59	72·0	31·1	58·8	4·05
3·26	60·8	34·0	66·8	4·80
3·46	58·3	34·3	70·6	5·01
4·31	50·5	37·4	80·5	5·78
4·66	48·0	38·1	85·8	6·08
5·01	45·3	40·7	86·1	6·42

Table 13. *Viscosity data of* 0·025% *SPM solution at* 30°*C.*
Instrument : Modified Ostwald Viscometer.

Pressure (cm Hg)	*Time (sec)*	*N′ (cm)*	*Sg (g/cm sec²)*	R_s *(sec⁻¹)* × 10^{-3}
0·87	422·4	16·65	36·6	0·69
1·19	290·9	17·2	48·4	1·00
1·47	230·5	17·6	58·4	1·27
2·06	153·8	18·75	76·9	1·90
2·42	130·6	19·3	87·8	2·24
2·92	101·9	20·4	100·2	2·86
3·52	83·05	21·5	114·6	3·51
4·07	70·8	22·9	124·8	4·12
4·42	65·6	23·6	131·1	4·45
5·02	58·7	24·7	142·2	4·97
5·27	56·5	25·3	145·7	5·25
6·22	48·1	27·7	157·1	6·07
6·72	45·0	29·3	160·5	6·48
7·37	41·9	30·4	160·1	6·96

Table 14. *Viscosity data of* 0·025% *SPM solution at* 40°*C.*
Instrument : Modified Ostwald Viscometer.

Pressure (cm Hg)	*Time (sec)*	*N′ (cm)*	*Sg (g/cm sec²)*	R_s *(sec⁻¹)* × 10^{-3}
0·64	465·1	17·3	25·9	0·63
0·80	365·9	17·7	31·6	0·80
1·36	211·1	18·55	51·3	1·38
1·65	161·1	19·3	60·1	1·81
2·13	123·6	20·3	73·1	2·36
2·63	98·2	21·5	85·5	2·97
3·08	82·6	22·7	94·9	3·53
3·48	73·7	23·5	103·6	3·96
3·98	64·7	24·7	112·8	4·51
4·73	56·1	27·2	121·8	5·20
5·37	50·7	28·8	130·7	5·75
5·82	47·7	29·9	136·4	6·11
6·43	43·6	32·8	143·0	6·69

Table 15. Viscosity data of 0·025% SPM solution at 50°C.
Instrument : Modified Ostwald Viscometer.

Pressure (cm Hg)	*Time (sec)*	*N′ (cm)*	*Sg (g/cm sec²)*	R_a *(sec⁻¹)* $\times 10^{-3}$
0·58	406·2	18·25	22·3	0·72
1·05	219·9	19·3	38·1	1·33
1·42	160·4	20·3	49·0	1·82
1·72	133·5	20·9	57·6	2·18
2·28	97·6	22·6	70·7	2·99
2·78	81·0	24·2	80·4	3·60
3·18	72·4	25·4	87·6	4·03
3·53	66·05	26·4	93·5	4·42
3·96	59·7	27·1	99·5	4·89
4·33	55·8	29·3	103·7	5·22
4·93	50·8	30·8	112·1	5·74
5·58	46·1	33·4	117·0	6·34
5·68	45·6	33·5	118·6	6·40

Table 16. Viscosity data of 0·025% SPM solution at 60°C.
Instrument : Modified Ostwald Viscometer.

Pressure (cm Hg)	*Time (sec)*	*N′ (cm)*	*Sg (g/cm sec²)*	R_a *(sec⁻¹)* $\times 10^{-3}$
0·51	359·7	19·5	18·3	0·83
0·75	248·7	20·0	26·2	1·17
0·98	190·0	20·7	33·1	1·54
1·33	145·1	21·65	43·0	2·01
1·64	116·0	23·1	49·6	2·52
1·85	102·2	24·0	53·8	2·85
2·23	86·4	25·7	60·7	3·38
2·79	71·8	28·3	69·0	4·06
2·89	71·0	28·0	72·3	4·11
3·19	65·5	29·6	75·5	4·46
3·66	57·6	31·6	80·9	4·98
4·29	51·5	35·0	85·9	5·66
5·04	46·5	37·3	94·6	6·27
5·29	45·0	37·9	97·6	6·48

Table 17. Viscosity data of 0·025% SPM solution at 70°C.
Instrument : Modified Ostwald Viscometer.

Pressure (cm Hg)	*Time (sec)*	*N′ (cm)*	*Sg (g/cm sec²)*	R_a *(sec⁻¹)* $\times 10^{-3}$
0·24	595·3	20·7	8·1	0·49
0·47	303·9	21·7	15·2	0·96
0·74	197·5	22·8	22·7	1·48
1·02	144·5	24·4	29·2	2·02
1·26	117·7	26·9	32·8	2·48
1·72	99·3	27·8	43·3	3·04
2·24	76·85	32·4	48·4	3·80
2·34	75·6	32·3	50·7	3·86
2·54	69·6	33·8	52·6	4·19
2·80	65·2	34·3	57·5	4·48
3·29	56·9	38·0	60·6	5·07
3·49	55·5	38·3	63·6	5·26
3·69	53·5	38·8	66·6	5·45
3·99	49·8	42·3	66·0	5·85
4·74	44·8	43·9	75·5	6·51

VOL. 3 1954

In applying the HAGEN-POISEUILLE equation to the results obtainable from an Ostwald type viscometer, certain sources of error arise, these were discussed in some detail by HALL and FUOSS [7]. They considered the deviations to arise as follows :

1. All the work done by the driving pressure is not dissipated as heat in overcoming the viscous friction.
2. Flow near the ends of the capillary tube is not a laminar.
3. The volume of liquid which flows through the tube is not the volume of the dry bulb.

A method for the analysis of data for a pseudo-plastic fluid to eliminate these errors was considered for the present work, but the results do not lend themselves to extrapolation in the manner recommended. Hence the following method of calibration was employed :

1. The volume of the viscometer bulb (V) between the constrictions at (R) and (S) was measured by filling the bulb with water, draining off the water, and weighing it. The mean of several determinations was used in subsequent calculations. The nipple (Y) on Fig. 4 facilitated this operation.
2. The diameter of the capillary tube was measured, prior to the construction of the viscometer, by two methods : firstly, by direct measurement of the diameter at either end with a travelling microscope ; secondly, by measuring the length of a weighed thread of mercury at various points along the bore of the capillary.
3. The effective or equivalent length (N' cm) was obtained by performing viscosity measurements with solutions of pure cane sugar, the viscosity of which was known (9). The equivalent length was then calculated from the relationship.

$$N' = \frac{\pi g \rho_{Hg} PR\theta}{8\mu v} \qquad (9)$$

In practice, the equivalent length was found to vary with both rate of flow and with viscosity

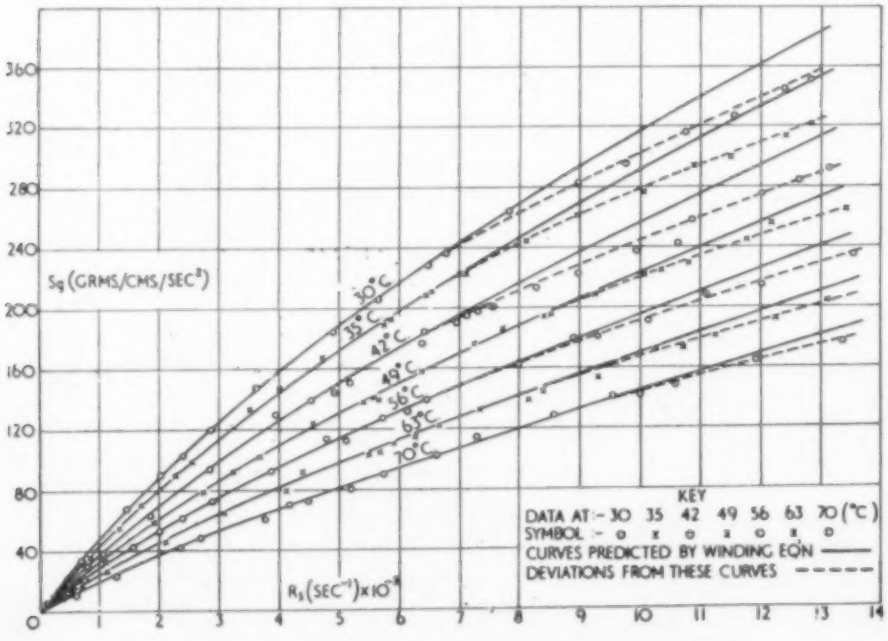

Fig. 6. Temperature effect upon shear rate and stress relation for 0·25 CMC solution in water, with temperature as parameter.

to vary with both rate of flow and with the viscosity of the fluid. Thus it was necessary to established the equivalent length over a range of values for both of these variables. The full procedure is described elsewhere (4).

The data actually recorded were the pressure applied to bulb (V) as shown on the manometer (M) or (N) in Fig. 3, and the time required to empty the bulb (V). From these a plot of applied pressure versus R_s was made (4). The applied pressure was expressed in cm Hg. In the case of the modified Ostwald viscometer an amount equivalent to the hydrostatic pressure head from

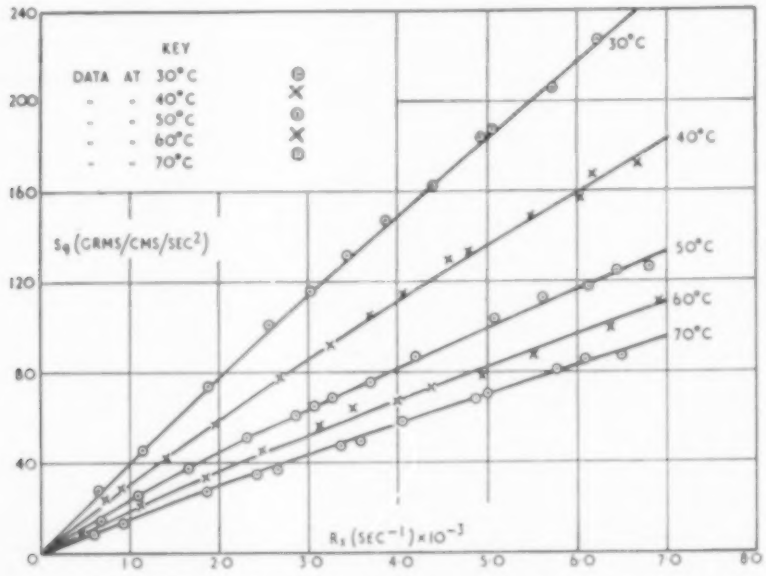

Fig. 7. Temperature effect upon shear rate and stress relation for 2·5% PVA solution in water, with temperatureas parameter.

(R) to the level at (X) in Fig. 4 was subtracted from the manometer reading to give the effective pressure drop across the viscometer. To calculate the resulting viscosities with pseudo-plastic fluids the procedure was as follows : R_s was calculated from the measured values of μ in conjunction with the known values of V and R. A graph of P versus R_s was constructed from data given [4, 6] and on this graph the point corresponding to the data values of P and R_s was located and the value of the parameter τ corresponding to this location was estimated. From graph of N' versus R_s the required value of N' was that which gave the same value for τ, for the datum value of R_s, as that just estimated on the graph of P versus R_s. With N' known, the shearing stress at the wall, Sg, for any given viscosity determination could then be calculated from the relation

$$Sg = \frac{P\rho_{Hg}gR}{2N'} \qquad (10)$$

Discussion of results

As the precautions required to ensure that the viscometers were accurately calibrated were somewhat elaborate, it is appropriate to mention briefly the theoretical background which necessitated this.

It has been fairly well established that the "slip" occurs in a flow of pseudo-plastic fluid in a capillary tube. The term "slip" was described by WINDING *et al.* [7, 14, 16] : "For a given rate of shear, the shearing stress is a function of diameter until a critical value is reached, above which the shearing stress is independent of diameter. This type of behaviour has been designated as 'slip' [16]". The

VOL. 3 1954

viscometers of different diameters are used to determine the relationship between the shear rate and shearing stress. It was found that the minimum diameter of the capillary tube was 0·199 cm in order to be free from the "slip." The viscometer of this minimum diameter was used in the determination of viscosity of the pseudo-plastic fluids.

BAKER [2] established that turbulence losses due to enlargement, contractions, and orifices for pseudo-plastic fluids were substantially similar to the corresponding losses for the simple Newtonian fluids. To compensate for the end effect of the capillary tube, the viscometer of minimum diameter was calibrated with a simple Newtonian fluid.

Fig. 6 shows the result of a test to establish the minimum required diameter. 0·35% CMC solution was used for this test. This solution was of a somewhat higher concentration of CMC than was used in later experiments. It was so selected to give a viscocity higher than that anticipated in the remainder of the work, in order to provide a more severe test of whether errors due to slip were present. Thus a certain margin of safety was introduced into the choice of the minimum suitable diameter.

Fig. 6 shows that providing R_s was less than 7000 sec^{-1} the capillary of 0·199 cm diameter met the required condition. In the paper on heat transfer (5) it will be seen that in the application of the viscosity data to the heat transfer correlations the requirement that R_s should be less than 7000 sec^{-1} was always observed.

Referring to Figs. 6, 7 and 8, it is seen that the range of data are for R_s = 0-7000 sec^{-1} for the PVA and SPM solutions, and R_s = 0-14,000 sec^{-1} for the CMC solution. The data in all three cases for R_s = 0-7,000 sec^{-1} were obtained on the modified Ostwald viscometer, but the additional data on the CMC were obtained on Viscometer No. IV.

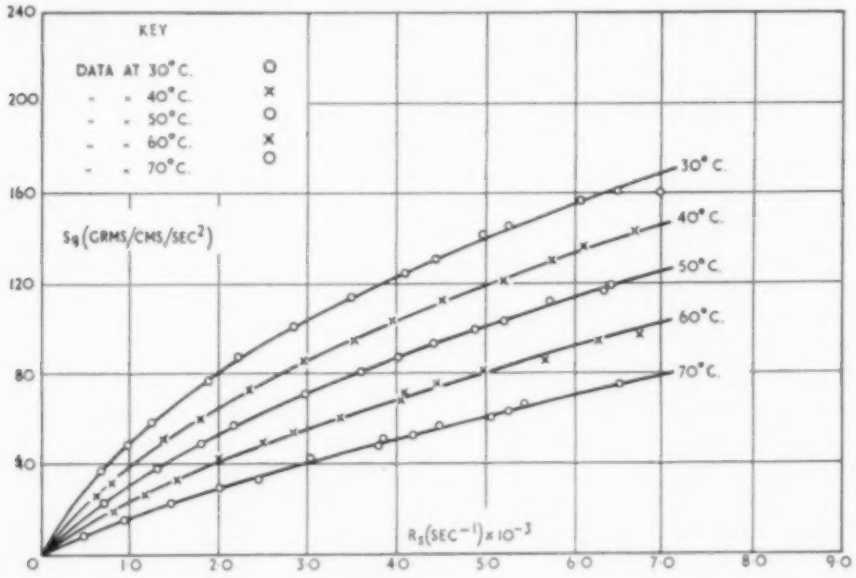

Fig. 8. Temperature effect upon shear rate and stress relation for 0·025% SPM solution in water, with temperature as parameter.

The object of taking the additional data on CMC was two-fold. Firstly, it provided a test of whether the shearing rate vs. stress curve derived from data on Viscometer No. IV was a continuation of that derived from the modified Ostwald viscometer, thus giving a check on the satisfactory operation of this design of instrument. Secondly,

it was desired to have a fairly wide range of data in an attempt to obtain graphically the limit, μ_∞, to which the slope of the shearing rate vs. stress curve approaches as Sg becomes infinity. The results of this attempt were not too satisfactory, and consequently the use of μ_∞ in correlating the heat transfer data [5] was avoided. In view of this conclusion the viscosity data for the PVA and SPM solutions were only taken over a more limited range.

It was preferred to established an analytical relation between the shear rate and the stress at different temperature, rather than to read the date necessary for the heat transfer calculations directly from graphs. By so doing, more accurate values could be obtained for low values of R_s. It also facilitated interpolation between the consistency curves for data required at intermediate temperatures.

None of the standard methods of rectification appeared to give satisfactory results over the whole range of the viscosity data, although a log-log plot such as that used by KRIEGER and MARON [9] resulted in a straight line plot over a limited range. It was thus necessary to consider an empirical equation. The hyperbolic form used previously by WILLIAMSON [15] and WINDING *et al.* [16] was found satisfactory over a sufficient range for the present work.

Considering first the CMC data, it is seen that the dotted lines through the data points at higher values of R_s are substantially straight. Hence "$S_0 g$" and "μ_∞" may be determined graphically. Use of the values thus obtained, plus one other datum point, suffices to solve for the constant "a" and to give an equation of the form used by WINDING.

The resulting equation, however, did not satisfactorily predict the data values for the low values of R_s. An alternative method of fitting the WINDING equation to three selected point values spaced over the range $0 < R_s < 7{,}000$ sec.$^{-1}$ gave a very good prediction of the data over the whole of this range, although the resulting curve gave inaccurate values for $R_s > 7{,}000$ sec.$^{-1}$.

This deviation may be due to three possible causes :

1. Viscosity determinations at high values of R_s were difficult to measure accurately due to the very short time required to empty the viscometer bulb.
2. Due to the "slip" effect, the effect of capillary diameter on the slope of the shearing rate vs. stress curve is no longer negligible at high values of R_s.
3. WINDING's equation is empirical and there may be no theoretical reason why it should hold over the whole range of R_s.

The so called WINDING equation is of the same form as that originally proposed by WILLIAMSON as given by eq. (7). Since the actual shearing stress and shear rate between parallel plates was assumed in WILLIAMSON's original method, the rate of shear R_s calculated at the wall as suggested by WINDING is different from the actual one between the parallel plates. Any method using apparent viscosity alone is bound to be less accurate than those using differential viscosity, though all previous authors have used the former as the easy way out.

The analytical expressions to fit the CMC solution viscosity data at the various temperatures having been derived, it was graphically possible to read off the values of the constants for the Winding equation at any given temperature and so compute the apparent viscosity for the appropriate value of R_s. The same procedure was followed in the development of the viscosity data for the PVA and SPM solutions.

It should be emphasized that the above approach was selected solely because it represented a more convenient and accurate method of obtaining the viscosity data required for the heat transfer correlation. The WINDING equation is empirical, but its application in the present work is justified by the fact that it was only used over the range of data for which it was shown to hold.

ACKNOWLEDGEMENTS

Grateful acknowledgement is made to Prof. WINDING of Cornell University, and Prof. OTHMER of Polytechnic Institute of Brooklyn, for their comments and interest ; to ECA for the Exchange Fellowship awarded to two of the authors.

VOL. 3 1954

NOMENCLATURE

Symbol	*Definition*	*Units*
D	Diameter of tube	cm.
G	Mass velocity	g/sec. $(cm.)^2$
g	Gravitation constant	g/sec. $(cm.)^2$
N	Length of tube	cm.
N'	Equivalent length of capillary tube	cm.
P	Pressure differential along tube	cm of mercury
R	Inside radius of tube	cm
Re	Reynolds number	dimensionless
Re_a	Apparent Reynolds number	"
R_s	Rate of shear $\left(\frac{4V}{\pi R^3}\right)$	$sec.^{-1}$
Sg	Shear stress at wall	g-mass/$(sec)^2$
$S_0 g$	A constant in the WILLIAMSON and WINDING equations	g/cm. $sec.^2$
V	Volume rate of flow	As indicated in text.
v	Linear velocity along the tube	ml/second
ρ_{Hg}	Density of mercury	g/ml
θ	Time of efflux	secs.
μ	Coefficient of viscosity of Newtonian fluid	g/(cm) (sec)
μ_a	Coefficient of apparent viscosity	same
μ_d	Coefficient of differential viscosity	same
μ_∞	A constant in the WILLIAMSON and WINDING equations	same

REFERENCES

[1] ANDRADE, E N. da C. ; " Viscosity and Plasticity " Chemical Publishing Co. Inc., New York (1951), 10.

[2] BAKER, G P. ; Ph.D. Thesis in Chemical Engineering, Cornell University (1950).

[3] BONILLA, C. F., CERVI, AMANDO, Jr., COLVEN, T. J. and WANG, S. J. ; A.I.Ch.E. Symposium Series, 5 " Heat Transfer," p. 390 1953.

[4] BROWN, F. and BURRIDGE, K. G. ; M.Ch.E. Thesis, Brooklyn Polytechnic Institute 1952.

[5] CHU, J. C., BROWN, F. and BURRIDGE, K. G. ; Heat transfer of pseudo-plastic fluids. Ind. Eng. Chem. 1953 **45** 1686.

[6] CHU, J. C., BROWN, F. and BURRIDGE, K. G. ; Data filed with American Institute of Documentation, Washington, D.C.

[7] HALL, M.T. and FUOSS, R. ; J. Amer. Chem. Soc. 1951 **73** 265-7.

[8] HEDSTROM, B.O.A. ; Ind. Eng. Chem., 1952 **44** 651-6.

[9] " International Critical Tables " ; McGraw-Hill Book Co. Inc., New York, 1929 Vo. 5, 23.

[10] KRIEGER, I. M. and MARON, S. H. ; J. Colloid Sci. 1951 **6** 535.

[11] PORTER, A. W. and RAO, P. A. M. ; Trans. Faraday Soc. 1927 **23** 311.

[12] REINER, M. ; " Deformation and flow." H. K. Lewis & Co. Ltd., London 1949, 40.

[13] REINER, M. ; ibid., 109.

[14] REINER, M. ; " Twelve Lectures on Theoretical Rheology," Interscience Publishing Co. Inc., New York 1949.

[15] WILLIAMSON, R. V. ; Ind. Eng. Chem. 1929 **21** 1108.

[16] WINDING, C. C., BAUMANN, G. P. and KRANICH, W. L. ; Chem. Eng. Progress 1947 **43** 527-35.

[17] WINDING, C. C., DITTMAN, F. W. and KRANICH, W. L. ; " Thermal Properties of Synthetic Rubber Latices." Report to Rubber Reserve 1944.

[18] Winding, C. C., KRANICH, W. L. and BAUMANN, G. P. ; Chem. Eng. Progress 1947 **43** 613-22.

Chemical Engineering Science, 1954, Vol. 3, pp. 248 to 259. Pergamon Press Ltd.

The mechanism of mass transfer of solutes across liquid-liquid interfaces

Part I: The determination of individual transfer coefficients for binary systems

J. B. LEWIS

Chemical Engineering Division, Atomic Energy Research Establishment, Harwell, Didcot, Berks.

(*Received September* 1954)

Summary—A new type of transfer cell has been designed and used for the determination of the individual mass transfer coefficients, by the Colburn-Welsh technique, for eight partially miscible binary systems, in six of which one of the phases was water. It was found that the transfer of mass to the interface took place by eddy not molecular diffusion. The individual coefficients for all phases, except furfural, were correlated on one curve by plotting k_1/ν_1 against $Re_1 + Re_2\,\eta_2/\eta_1$. This curve could be represented with a slight loss of accuracy by the expression :

$$60\,k_1/\nu_1 = 6{\cdot}76 \times 10^{-6}\,(Re_1 + Re_2\,\eta_2/\eta_1)^{1{\cdot}65} + 1$$

The effect of adsorbed interfacial films was examined and it was found that while mobile films had little effect rigid protein films caused a retardation of transfer, probably by damping interfacial turbulence.

Since the transfer coefficients are dependent only on the Reynolds numbers and physical properties of the two phases, the correlation enables individual coefficients to be calculated for immiscible solvent-water pairs where the mutual saturation technique cannot be employed.

Résumé—Un nouveau modèle de cellule de transfert a été conçu et utilisé dans la détermination du coefficient individuel du transfert de masses par le procédé COLBURN-WELSH dans le cas de huit systèmes binaires partiellement miscibles pour six desquels l'eau était une des phases. On a trouvé que ce transfert de masse à l'interface se propduit par tourbillon et non par diffusion moléculaire.

Pour toutes les phases, excepté le furfural, les coefficients spécifiques ont été portés sur la courbe $k_1/\nu_1 + f\,(Re_1 + Re_2\,\eta_2/\eta_1$. Cette courbe pourrait être représentée avec un peu moins de précision par l'expression :

$$60\,k_1/\nu_1 + 6{\cdot}76\ .\ 10^{-6}\,(Re_1 + Re_2\,\eta_2/\eta_1)^{1{\cdot}65} + 1$$

On examine l'effect de couches absorbées à l'interface et quoique les couches mobiles aient un faible effet, on trouve que les couches rigides de protéines provoquent un ralentissement du transfert probablement en atténuant la turbulence à l'interface.

Puisque les coefficients de transfert dépendent seulement des nombres de Reynolds et des propriétés physiques des deux phases, la formule permet de calculer les coefficients pour des binaires eau-solvant immiscible dans le cas où le procédé de saturation réciproque ne peut être utilisé.

The transfer of solutes, particularly organic solutes across liquid-liquid interfaces is usually considered to be diffusion controlled. Normally both phases are in turbulent motion but it is assumed that films or layers exist in each phase immediately adjacent to the interface where the flow is laminar, and that diffusion through these layers is slow and rate-determining. When the transfer is followed by a homogeneous chemical reaction the reaction is considered to take place at a zone inside the relevant film. This two film theory, adapted by WHITMAN [1] from the general boundary layer theory of NERNST [2], is used extensively to correlate the performance of extraction equipment. Although various aspects of the theory have been criticised no experiments

VOL. 3 1954

have been carried out to test its validity directly.

Van Name [3] and others have shown that when a chemical reaction occurs at a solid-liquid interface then the process will be chemically controlled if the reaction is very slow, diffusion controlled if the reaction is very fast and of an intermediate complex nature if the chemical reaction rate is of the same order as the diffusion rate. A similar state of affairs must hold for reactions at liquid-liquid interfaces. Since diffusion and first-order chemical reactions have similar kinetics a slow first-order chemical step will be equivalent to diffusion through a fictitious film. In such systems therefore, the two-film theory may be used to correlate data provided that the limitations of the theory are remembered. In general, however, the two film theory should only be used where transport to and from the interface is the controlling factor.

In recent years the hydrodynamics of laminar films at solid-liquid interfaces have been worked out rigorously [4]. The behaviour of films at gas-liquid and liquid-liquid interfaces is less well known but there are indications that turbulence may in some cases persist up to the interface itself [5]. Transport of matter to the interface will then be at least partly by eddy diffusion. Since eddy diffusion is much faster than molecular diffusion there is thus more chance of any chemical step being rate-determining. Chemical steps are known to occur in the extraction of many inorganic solutes and Drickamer has shown that they may even be involved in some apparently simple organic systems [6]. Information as to the mechanism of transfer to the interface and on the magnitude of any chemical step is clearly needed if the performances of different types of extraction equipment are to be compared.

No work has been reported on the nature of transport to liquid-liquid interfaces but a few papers have been published on the extraction of inorganic and organic solutes from water into organic solvents [6, 7, 8]. In these experiments stirring was either absent or else an attempt was made to standardise the effect by making observations at a number of stirring speeds and extrapolating back to zero stirring rate. When stirring was absent effects due to local heating, density gradients, etc., became very important, and the results were sometimes suspect. In some experiments local stirring was prevented by packing the bulk phases with wire gauze [6]. Separate experiments were then necessary to determine the unknown diffusion path lengths. The stirred experiments [7] in general have suffered from non-reproducibility of the turbulence, insufficient attention having been paid to the hydrodynamics of the apparatus. The method adopted of extrapolating the stirring rate back to a fictitious zero rate has recently been shown to be at fault [8].

In the present work the unsteady-state transfer of solutes between phases was investigated using a specially designed transfer cell in which the degree of turbulence could be accurately controlled. Initially the rate of mutual saturation of a number of partially miscible binary systems was measured so that the individual transfer coefficients for these phases could be obtained by the Colburn and Welsh method [9]. The dependence of the individual coefficients on the Reynolds numbers of the two phases, on the diffusion coefficients and other physical properties of the two components and on the temperature, was examined and a method is derived for the approximate correlation of the data. The results of this investigation are summarised below. In Part II [10], this work has been extended to consider the rates of transfer of organic solutes between solvent and water phases.

Experimental

Apparatus

The experiments were carried out with a cylindrical transfer cell in which each phase was independently stirred by a central paddle. Preliminary experiments were first carried out in simple glass vessels to determine the optimum conditions for producing reasonably smooth interfaces of reproducible area at high stirrer speeds. The vessels were closed at the top and completely filled in order to prevent cavitation of the upper liquid surface. It was found necessary to restrict the interface to an annular gap between a central circular baffle and a circumferential wall baffle, the central baffle preventing cavitation and the outer baffle reducing irregular wall effects to a

minimum. The two halves of the cell were made geometrically similar so that the film coefficients for the two phases could be correlated together. Various sizes and shapes of stirrer paddles were tried and the dimensions of the baffles were varied until a satisfactory stirring range could be obtained without break-up of the interface. Both baffles were bevelled to enable drops of either phase accidentally introduced into the other to roll to the interface.

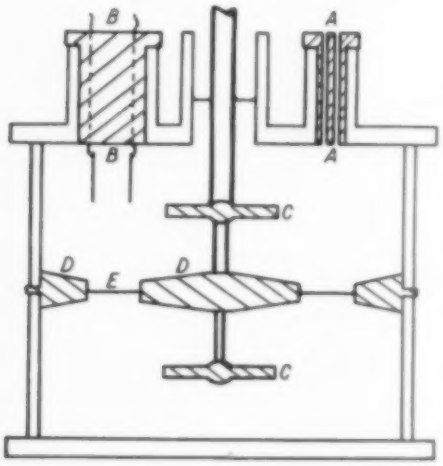

Fig. 1. Transfer cell. *A* – filling plug, *B* – polythene plug supporting electrodes, *C* – stirrers, *D* – baffles, *E* – interface.

The final cell, shown in Fig. 1, consisted essentially of a cylinder 4 in. in diameter and 3 in. high constructed of two 1½ in. lengths of 4 in. i.d. glass pipe clamped between two flat end plates. These and all other metal parts inside the cell were made of stainless steel. The two glass sections were separated by the circumferential baffle, and this together with the central baffle divided the cell into two identical halves each of ca 300 ml. volume, the annular gap area being about 30 sq.cm. Gaskets suitable for the system being examined, e.g. rubber, P.V.C., and polythene-sheathed rubber, were inserted between the various parts. The bottom plate was solid but the upper had three circular holes, a central hole for the stirrer shafts, a filling hole normally closed by a plug and a hole accommodating a polythene plug supporting two platinum electrodes. Both plugs were made to finish flush with the inner surface of the upper plate, and two small holes in the filling plug enabled hypodermic needles to be inserted to sample the two phases. The electrodes were connected to a specially constructed conductivity bridge enabling the conductivity, and hence the concentrations, of suitable inorganic solutions to be determined during an experiment. To reduce interference with the turbulence in the upper compartment the electrodes were parallel to the wall and curved concentrically with the sides.

Three concentric shafts passed through the centre hole, an inner rotating shaft on to which was fixed the stirrer for the lower compartment a fixed central shaft supporting the central baffle at the interface, and an outer rotating shaft driving the upper compartment stirrer. The two stirrers were driven by ¼ h.p. D.C. motors controlled by commercial electronic speed controllers which enabled the speeds of both stirrers to be varied independently from 0 to 1,400 r.p.m. Reversing switches were included in the circuit. The cell was suspended in a water thermostat to enable experiments to be carried out at various accurately-controlled temperatures.

Systems used

Mutual saturation runs were carried out with six different solvent-water systems and also with two non-aqueous systems. For the solvent-water experiments the solvents were aniline, ethyl acetate, ethyl aceto-acetate, ethyl formate, furfural and iso-butanol, while formic acid-benzene and aniline-cyclohexane were used as the non-aqueous systems. The best available grades of solvents were used and with the exception of formic acid, which was purified by fractional freezing, the solvents were all redistilled in a 1 in. i.d. laboratory column packed with 3 ft of 6 mm Raschig rings. Furfural was distilled under filter pump vacuum.

The physical properties of the compounds used

VOL. 3 1954

are tabulated in Table 1, much of the data having been determined experimentally. No diffusion coefficient data were available for the solvent-water systems, and most of these were therefore determined experimentally (full details of this work will be published elsewhere). The dimensionless Schmidt groups ($\eta/\rho D$) were calculated from these values and are included in Table 1. Interfacial tensions of the actual phases used were determined by the pendant drop method [11].

Procedure

Before assembling the cell for an experiment each part was carefully cleaned with a suitable solvent, rinsed in redistilled acetone and dried in a hot air oven. Every few days the components were steeped in chromic acid. It was necessary with some systems to soak the P.V.C. or rubber gaskets in the clean solvent beforehand. Great care was taken to avoid contaminating the cell with grease or surface active agents. The cell was assembled immediately before use, replaced in the bath and the two phases, which had previously been brought to the correct temperature in a thermostat bath, added in such a manner that neither phase wetted the wrong compartment. The heavier phase was run in until the top surface was somewhat above the mid-point of the annulus so that on taking the initial sample from this phase the interface fell to the correct level. Sufficient of the lighter phase was then run into the top compartment to fill it completely and to

Table 1. *Physical properties of solvents.*

Solvent	*Temp.* °C	ρ – *gm/ml*	η *c.p.*	*Schmidt Group*		γ *dynes/cm*	*Remarks*
				In water	*Water in*		
Furfural	20	1·16	1·70	960	1,600	6	
	30	1·15	1·40	620	720	–	
	40	1·14	1·23	–	–	5	
	50	1·13	1·11	–	–	–	
Ethyl acetate	20	0·90	0·46	1,000	160	9	
	30	0·89	0·40	460	130	–	
	40	0·88	0·37	–	–	6·5	
	50	0·86	0·35	–	–	–	
Ethyl formate	20	0·92	0·40	1,000*	100*	10·5	*Estimated values
Ethyl aceto-acetate	20	1·03	1·71	1,400*	1,800*	4·7	
Aniline	20	1·02	4·40	1,090	6,200	5·8	
Isobutanol	20	0·80	3·95	1,200	14,000	2·1	
	50	0·78	1·65	–	–	–	
Formic acid	20	1·21	1·80	–	–	–	
Benzene	20	0·88	0·65	–	–	–	
Cyclohexane	20	0·80	0·96	–	–	–	
Water	20	1·00	1·00				
	30	1·00	0·80				
	40	0·99	0·66				
	50	0·99	0·55				

rise part-way up the filling and centre holes. On inserting the filling plug the excess volume of about 2 c.c. was forced up into the centre hole. This excess volume acted as a reservoir when samples were removed from the upper compartment so that the level did not fall below the top plate. Although this excess liquid was not adequately stirred the error introduced by its somewhat different composition was negligible. Due to the variable thickness of the gaskets the volume of the two phases varied by a maximum of $\pm$ 2 c.c.

The stirring rates necessary to give the correct Reynolds numbers had been previously calculated and the controllers set at this speed. During each run the motor speeds were checked by a tachometer and frequently the stirrer rates were further checked by a stroboscope.

Both phases were sampled immediately after starting the stirrers and subsequently at intervals of 3-5 minutes, by inserting long hypodermic needles through the filling plug and drawing samples from the middle of each phase. Large samples of each phase were also taken at the end of each run. All samples but the last were kept as small as possible consistent with accuracy of analysis, but when only drop samples were required for refractometric analysis at least 1 ml. was taken into a syringe, and after shaking, three or more drops were taken from this. The remainder of the sample was then returned into the cell. If larger samples were required, as e.g. for Karl Fischer titrations of water content, these were kept to a minimum during the run, only three or four intermediate samples being taken, and synthetic solutions of approximately the same composition were injected so as to keep the top compartment full and the interface level constant. The runs normally lasted about 40 minutes.

A number of transfer experiments were carried out with the viscosity of the solvent phase increased by the addition of collodion. The viscosities were determined before and after each run. Transfer runs were also carried out with both mobile and rigid adsorbed films of surface-active agents present at the interface. The cell was filled in the usual manner, the run started then the stirrer stopped and the surface active agent, dissolved in a suitable solvent, injected on to the interface by means of an "Agla" precision syringe connected to a long needle. A long chain quaternary ammonium compound $C_{18}H_{37}N(CH_3)_3$-Cl was used for the mobile film, this being insoluble in either phase.* Enough of a petroleum ether-propanol solution was added to give either 1 or 4 molecules per 150Å^2 of surface area. For rigid films excess of a protein, gliadin, in ethyl alcohol solution was used. In all cases the volumes of the solutions added were negligible.

Analysis

Analysis of both phases in the aniline-cyclohexane, aniline-water and furfural-water systems was by measurement of the refractive index using refractive index/concentration graphs which had been experimentally determined beforehand. An Abbé refractometer was used so that only very small samples were needed. A refractometric method was also used for the analysis of the water phase in the ethyl acetate-water, ethyl acetoacetate-water and isobutanol-water systems, while the water contents of these solvent phases were determined by Kark Fischer titration. It was found convenient to standardise the Karl Fischer reagent by titrating a saturated solution of the solvent after each experiment. The concentration of ethyl formate in water was obtained by hydrolysis of the ester, and this method was also checked by cloud point titration. Formic acid in benzene was determined by titration with N/10 NaOH and the same method was used for the formic acid phase itself.

Calculation of Mass Transfer Coefficients

It was assumed that equilibrium existed at the interface and that the rate-controlling step in the saturation of either phase is the rate of transfer of the other component away from the interface into the bulk of that phase. If equilibrium exists at the interface then the interfacial concentration is constant and substantially equal to the saturation value.

We then have the rate of transfer given by :**

* I am indebted to Dr. J. T. Davies for the supply of this compound.

** The symbols used are defined at the end of this paper.

VOL. 3 1954

$$j = k\,(c_\infty - c) \qquad (1)$$

where $(c_\infty - c)$ is normally taken to be the driving force. Now the transfer rate is also given by :

$$j = \frac{V}{A}\frac{dc}{dt} \qquad (2)$$

$$\therefore k = \frac{V}{A}\frac{dc}{(c_\infty - c)}\frac{1}{dt}$$

$$= \frac{-\,2{\cdot}303\;V}{A} \cdot \frac{d}{dt}\log\,(c_\infty - c) \qquad (3)$$

Hence $\log\,(c_\infty - c)$ was plotted against time and in all cases good straight lines were obtained from the slope of which k could be calculated. Since both phases were sampled, two graphs were plotted for each run from which the two individual transfer coefficients could be obtained. Typical plots are shown in Fig. 2.

Results

The first two systems used, furfural-water and ethyl acetate-water, were studied in much greater detail than the subsequent systems since a wider range of Reynolds numbers could be used before the interface was disrupted. On plotting the coefficients against Reynolds number on logarithmic co-ordinates using the Reynolds number of the other phase as parameter a family of smooth curves were obtained (Fig. 3). Occasionally very low coefficients were obtained and it was assumed that these were due to surface contamination. In order to check on this most experiments were duplicated. With the exception of points of this nature, the scatter was within 10% for furfural-water and 20% for ethyl acetate-water.

Because of the large number of experimental results obtained with these two systems the data

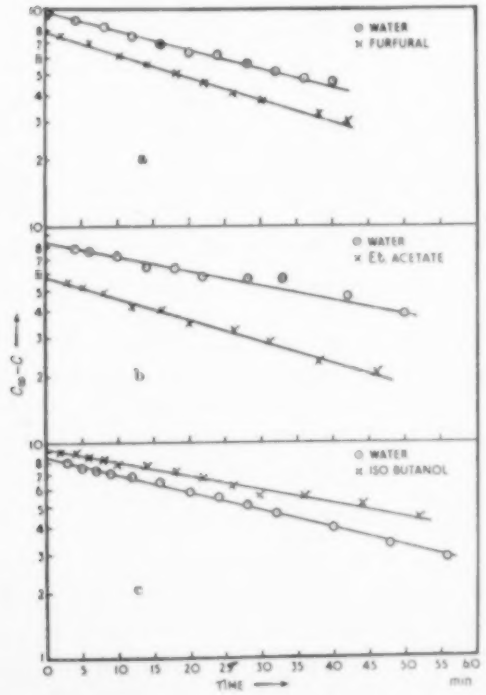

Fig. 2. Typical plots of $\log\,(c_\infty - c)$ v. time. (*a*) Furfural – Water at 50°C, (*b*) Ethyl Acetate – Water at 20°C, (*c*) Isobutanol – Water at 20°C.

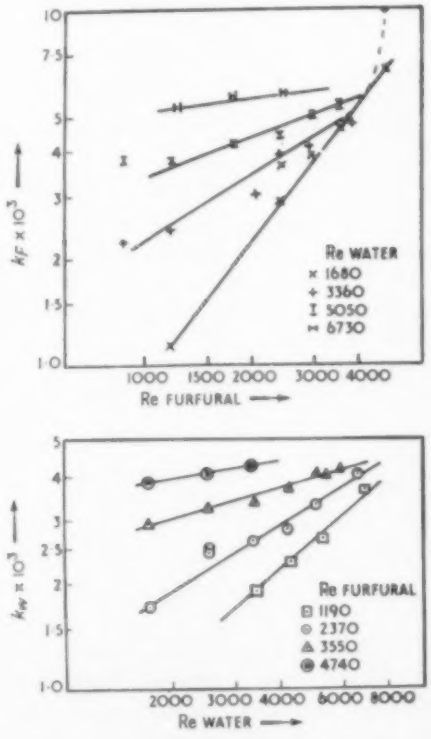

Fig. 3. Plots of individual transfer coefficients v. Reynolds number with Reynolds number of other phase as Parameter – system, Furfural – Water.

plotted in Fig. 4 are smoothed values taken from the graphs. With all other systems the actual experimental data are shown.

With a few exceptions all experiments were carried out with the stirrers contra-rotating. In order to ascertain whether the direction of stirring was important a number of experiments were conducted with the stirrers running in the same direction. There was no marked difference in the transfer coefficients apart from a tendency for the coefficients to be slightly greater.

Interpretation of Results

Correlation of Transfer Coefficients

Due to the complexity of the problem no fundamental theoretical approach was possible, and an attempt was therefore made to correlate the data using dimensional analysis. Thus the mass transfer coefficient for phase 1 may be assumed to be expressed in terms of the variables for phase 1 and 2 as follows :

$$k_1 = f(L, N_1, N_2, \rho_1, \rho_2, \eta_1, \eta_2, \gamma, D_{21}, g) \qquad (4)$$

This takes into consideration the experimental conditions that the stirrer lengths are both equal to L, and that the ratios of L to the cell diameter and to the cell height are constant.

Since there are 10 variables on the R.H.S. of (6) by the π theorem there will be (10-3) i.e. 7 dimensionless groups. The simplest arrangement of these is as follows :

$$\frac{k_1 \rho_1}{\eta_1} = f_1\left[\frac{(\eta_2)}{\eta_1}\frac{(\Delta\rho)}{\rho_1}\frac{(L^3N_1\rho_1)}{\eta_1}\frac{(L^3N_2\rho_2)}{\eta_2}\frac{(L^3N_1^2\rho_1)}{\gamma}\frac{(LN_1^2)}{g}\frac{(\eta_1)}{\rho_1 D_{21}}\right]$$

i.e.

$$k_1/\nu_1 = f_1\left[(\eta_2/\eta_1), (\Delta\rho/\rho_1), (Re_1), (Re_2), (We_1)(Fr_1), (Sch_1)\right] \qquad (5)$$

The values of the various dimensionless groups were calculated for the present systems but with the exception of the Reynolds groups and the viscosity ratio none of the groups on the right hand side appeared to have any relevance ; thus for any given system, $\Delta\rho$ and γ are constant, but widely different values of k/ν were obtained for the two phases when the other groups were approximately equal. If $\Delta\rho$ is not relevant then g can probably be neglected also since these terms should appear as a product with the same exponent. This means that the second, fifth and seventh groups in equation (5) vanish. Again, the Schmidt groups varied from 100 to 14,000 without any particular correspondence to values of k, indicating that this group was not effective. Further evidence that this was the case was obtained from experiments at temperatures up to 50°C when only a slight increase in the transfer coefficients was obtained, at the same Reynolds numbers as at 20°C, despite the large increase in diffusion coefficient.

We have thus found experimentally that

$$k_1/\nu_1 = f_3(Re_1, Re_2, \eta_2/\eta_1)$$

On plotting the transfer coefficients against Reynolds number on logarithmic co-ordinate paper using the second Reynolds number as parameter it was found that both Reynolds numbers were important in determining k_1 (cf. Fig. 3). From the experimental results it was evident that the Reynolds numbers should appear as a sum and not a product. A large number of possible relationships were tested, the dimensionless group k_1/ν_1 being plotted against various combinations of the two Reynolds numbers. The best correlation was obtained when plotting :

$$k_1/\nu_1 \text{ against } (Re_1 + Re_2\,\eta_2/\eta_1)$$

all the coefficients, with the exception of those for the furfural phase falling on a curve with a maximum deviation of about 30%, Fig. 4 (a). This curve can be represented, with a slight loss of accuracy by the equation :

$$60\,k_1/\nu_1 = 6{\cdot}76 \times 10^{-6}(Re_1 + Re_2\,\eta_2/\eta_1)^{1{\cdot}85} + 1 \qquad (6)$$

and a plot of this is given in Fig. 4 (b).

There was a tendency for the data relating to any one phase to lie at a shallow angle to this correlation indictaing that some unknown factor had been omitted. The data also tended to diverge more from the correlation when the two Reynolds numbers were widely different.

The furfural phase coefficients are plotted in

VOL. 3 1954

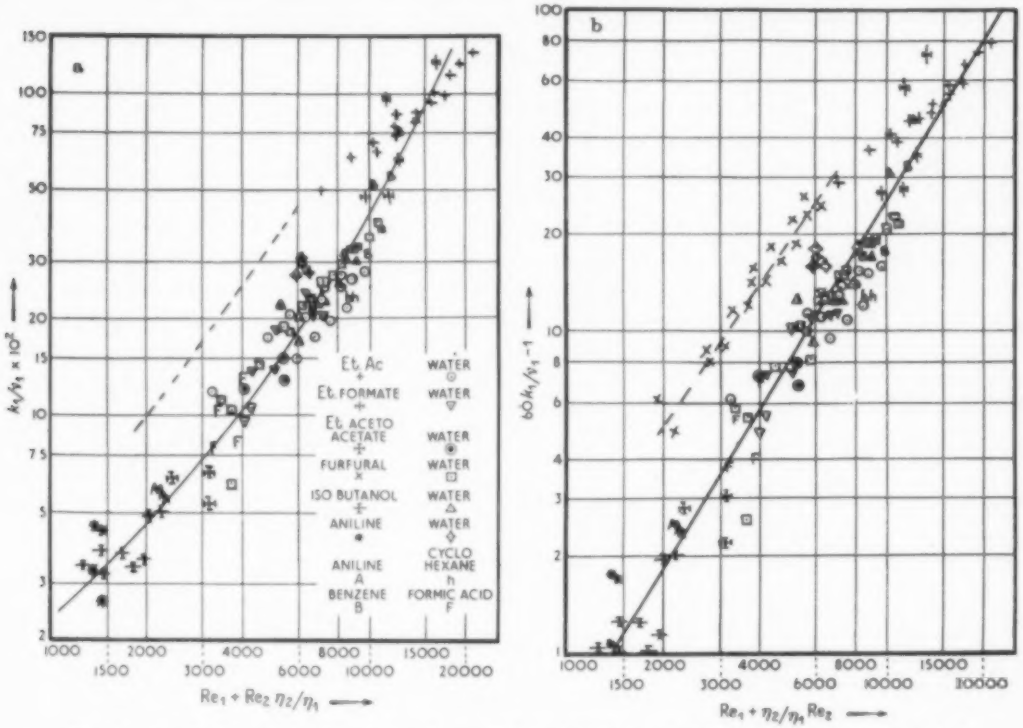

Fig. 4. Correlation of individual transfer coefficients. (*a*) k_1/v_1 plotted against $(Re_1 + Re_2\,\eta_2/\eta_1)$, (*b*) $60\,k_1/v_1 - 1$ plotted against $(Re_1 + Re_2\,\eta_2/\eta_1)$.

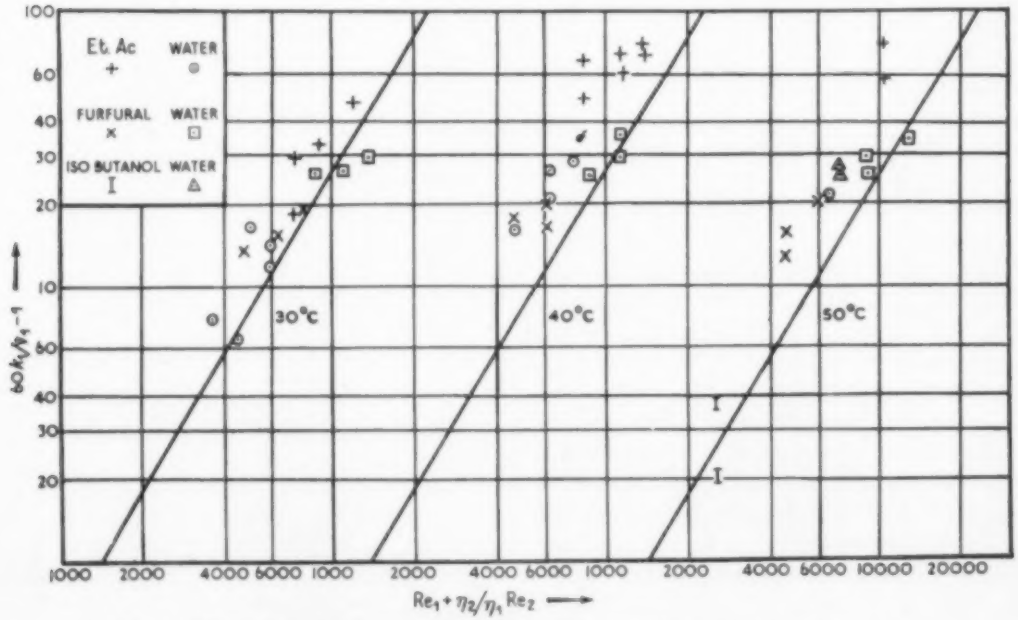

Fig. 5. Effect of temperature on correlation of $60\,k_1/v_1 - 1$ against $(Re_1 + Re_2\,\eta_2/\eta_1)$.

Fig. 4 (b) and it is clear that they do not correspond at all to the correlation. No obvious reason for this discrepancy could be found but since the corresponding aqueous phase coefficients correlate well it cannot be due to any macro interfacial effect. At 30° and above the data for furfural fall in line with the ethyl acetate and water results.

The coefficients obtained at higher temperatures i.e. 30°-50°C were also plotted in the above manner, Fig. 5. These data scattered more than at 20° but there was a definite tendency for k/ν to increase with temperature. When allowance is made for the decrease in ν with temperature it can be seen that k itself remains within about $\pm$ 40% of its value at 20° up to 50°C.

Some of this divergence may be due to the experimental scatter of results. If the rate determining step were a diffusional or a chemical one then the coefficients would increase several fold over this temperature range.

Although the exact relation between the transfer rates, degree of turbulence and physical properties of the two phases is undoubtedly very complicated, it is clear from the lack of dependence on the Schmidt group that transfer takes place by eddy and not by molecular diffusion over the range of Reynolds numbers considered.

Effect of Interfacial Films

Since the diffusion coefficient is normally related to the viscosity it was considered of interest to investigate the effect of changing one without the other. For this purpose collodion was added to the solvent phase in the ethyl acetate-water and furfural-water systems in order to increase the viscosity markedly without altering the diffusion coefficient appreciably. Unfortunately a film of collodion was deposited at the interface. It was found that although the solvent phase coefficients could be predicted satisfactorily from the correlation, the predicted water coefficients were far too low and to ascertain whether the presence of the rigid interfacial film of collodion altered the transfer rate, experiments were carried out with a rigid protein film deposited at the interface. Here there was no change in bulk phase properties but a very large increase in the interfacial viscosity.

It was found that the results both with the protein systems and with the collodion system were best explained by the assumption that rigid interfacial films largely prevent transfer of turbulence across the interface. Hence the second term in the correlation, $Re_2\,\eta_2/\eta_1$, representing the contribution of the turbulence of the second phase to the turbulence in the first phase, is best omitted although a small residual effect remains. With the collodion systems the second term is small when correlating solvent phase transfer since $\eta_2 \ll \eta_1$ and its retention makes little difference. In the water phase, however, the second term is much larger than Re_1 and its retention thus leads to erroneously high predicted values. The results are compared with the correlation in Fig. 6. The

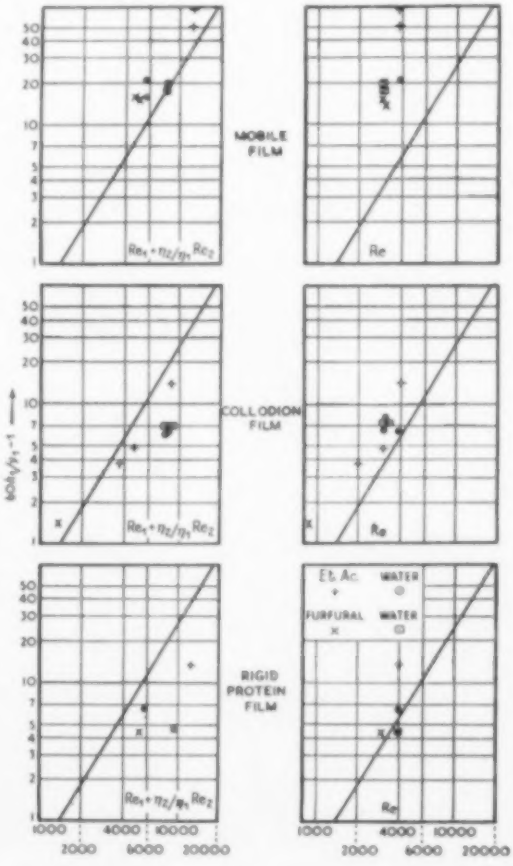

Fig. 6. Effect of interfacial films on correlation.

VOL. 3 1954

experiments with mobile adsorbed films on the interface indicated that there was no significant change in transfer rates with one molecule of quaternary ammonium compound per 150Å^2, but on increasing the concentration fourfold a marked increase was then obtained. This coincided with a noticeable change in the wetting angle at the baffle. Since the interfacial tensions were reduced to very low values the absence of any marked effect is further evidence of the non-dependence of transfer rates on interfacial tensions.

In general these experiments agree with the hypothesis that the transfer mechanism is controlled by eddy not molecular diffusion. The effect of rigid films at the interface suggest that the η_2/η_1 factor should be replaced by some interfacial function possibly involving the interfacial viscosity. Contradictory results reported by various authors on the effect of surface active agents on interfacial transfer rates may be due to the marked difference in effect of mobile and rigid films.

Discussion

The most surprising feature of the present results is that the data for the transfer of water into furfural fail to correlate with the remainder of the results. All attempts to bring the furfural transfer coefficients into line with, for example, the ethyl acetate coefficients, caused the data for other systems to deviate. The furfural water interface was examined by the pendant drop method [12] to see if saturation was accompanied by any marked interfacial turbulence. The effect appeared to be small and less than that observed in the other solvent water pairs used. In any case such turbulence, unless it gave rise to an emulsion in the solvent phase only, should influence the transfer coefficient in the water phase also. The existence of a micro emulsion on the solvent side cannot however be altogether ruled out. It is interesting to note that at 30° and above the furfural coefficients fall in line with the correlation. A possible explanation for this is that polymerisation occurs at this temperature, the viscous polymers formed inhibiting micro emulsification and reducing the transfer rate to the normal value.

The finding that the diffusion coefficient has no influence on the rate of transfer is of great importance, but it is not yet clear whether this is true with other forms of liquid-liquid contactor since Murdoch and Pratt have recently shown that the solvent-phase mass transfer coefficients for wetted wall columns vary approximately as the two-thirds power of the Schmidt group [13]. However, the present correlation gives the purely physical aspects of the transfer which in some respects is analogous to the collision frequency in gas reactions except that here the process is due to eddy, i.e. bulk, and not to molecular transport. If slow chemical stages are involved at the interface the rate will depend on the energy and entropy of activation, but since the transfer coefficients are almost temperature-independent the activation energy must be small. The standard free energies of transfer were calculated from the activity coefficieints at infinite dilution using values derived from solubility data [14]. Table 2. It can be seen that there are marked differences in ΔG_0 between corresponding phases. Although the activation energies would of course be different it might be expected that they would follow the same trend as ΔG_0. Since, however, both phases fit the correlation it is clear that no chemical step can be involved. The value of ΔG_0 for furfural is similar to that for the other solvents.

The effect of entropy changes on the transfer rates cannot be tested directly but since, with one exception, all the phases fit the correlation then either the entropy changes are the same or else they are zero.

It was anticipated in view of the addivity of the Reynolds numbers for the two phases in Fig. 4 and equation (6) that the mass transfer coefficients would be lower when the stirrers were running in the same direction than when they were contra-rotating. However, experiments in which the stirrers rotated in the same direction indicated that the coefficients were, if anything, slightly higher than previously. The most likely explanation is that transfer to the interface is governed by the vertical component of the mixing length, which being perpendicular to the direction of rotation is governed by the absolute and not the

Table 2. Activity coefficients at infinite dilution and standard free energies of saturation.

(a) *Aqueous Systems*

		Ethyl Acetate	*Ethyl Formate*	*Ethyl Acetoacetate*	*Furfural*	*Aniline*	*iso-BuOH*
Solvent Phase	$\log f_0$	1·02	1·17	0·85	0·84	0·73	0·74
	ΔG_0	1·36	1·56	1·14	1·12	0·93	0·99
Water Phase	$\log f_0$	1·80	1·75	1·76	1·82	1·82	1·68
	ΔG_0	2·40	2·34	2·35	2·43	1·76	2·3

(b) *Non-aqueous System*

	Benzene	*Aniline*
$\log f_0$	1·05	0·87
ΔG_0	1·40	1·16
	Formic Acid	*Cyclohexane*
$\log f_0$	1·28	1·21
ΔG_0	1·71	1·62

relative values of the Reynolds numbers. With contra-rotating stirrers a zone will exist where the mean horizontal velocity is zero but in general this will occur at some distance away from the interface in one phase or other depending upon the relative stirring speeds and viscosities of the two phases. Although this might cause a diminution of the turbulence in that plane the effect at the interface would be small and probably swamped by the eddies set up at the sharp edges of the baffles. The net result is therefore that the transfer coefficients would probably be almost independent of the direction of stirring but possibly slightly higher when the stirrers are rotating in the same direction.

Conclusions

(1) A new type of transfer cell has been designed and used for the determination of individual mass transfer coefficients for eight binary systems, in six of which one of the phases was water.

(2) The data for all systems, with the single exception of the transfer of water into furfural, have been correlated graphically by means of a plot of k_1/v_1 against the group $(Re_1 + Re_2 \eta_2/\eta_1)$. This can be approximated by means of equation (6).

(3) Over the range of stirring speeds used the rate of transfer appears to be independent of molecular diffusion coefficient, and the transfer therefore takes place entirely by eddy mixing. The interfacial tension and density difference of the phases also appear to be without effect.

(4) The effect of rigid films at the interface is to suppress the transfer of turbulence from one phase to the other so that the term in the correlation involving Re_2 drops out. On the other hand, the effect of mobile films at the interface is negligible, except at the higher concentration where the transfer rate is somewhat increased.

Most of the experimental work was carried out by Mr. E. W. SHARRATT. The author wishes to thank Mr. A. S. WHITE for his interest in the work and Dr. H. R. C. PRATT for much useful advice particularly on the interpretation of the data.

Nomenclature

- A area of interface in transfer cell – cm².
- c concentration – gm/100 cm³ at time t.
- c_∞ concentration at infinite time, i.e. at equilibrium.
- D diffusion coefficient – cm²/sec.
- f function.
- f_0 activity coefficient at infinite dilution.
- g acceleration of gravity – cm/sec².
- j transfer rate – gm/cm² sec.
- k individual mass transfer coefficient – cm/sec.
- L length of stirrer – cm.
- N stirring rate – revs. per sec.

VOL. 3 1954

t time – secs.
V volume of cell compartments – cm^3.
ΔG_0 standard free energy of saturation – K.cal/mole.
γ interfacial tension – dyne/cm.
η viscosity – gm/sec. cm.
ν kinematic viscosity – η/ρ – cm^2/sec.
ρ density – gm/cm^3.

Dimensionless Groups

Re Reynolds number – $\frac{L^2 N \rho}{\eta}$.

Fr Froude Group – $\frac{LN^2}{g}$.

Sch Schmidt Group – $\frac{\nu}{D}$.

We Weber Group – $\frac{L^3 N^2 \rho}{\gamma}$.

Subscripts

1 phase under consideration.
2 other phase.

References

[1] Lewis and Whitman; Ind. Eng. Chem. 1924 **16** 1215. Whitman; Chem. and Met. Eng. 1923 **29** 146.

[2] Nernst; Z. physik. Chem. 1904 **47** 52; 1905 **53** 235.

[3] van Name and Hill; Amer. J. Science 1916 **42** 301.

[4] Levich; Zh. Fiz. Khimii 1948 **22** 575, 711.

[5] Danckwerts; Ind. Eng. Chem. 1951 **43** 1460. Kischinevskii *et al.*; Zh. Prik. Khimii 1949 **22** 1173; 1951 **24** 413, 542. Levich; Zh. Fiz. Khimii 1948 **22** 721; Doklady 1951 **78** 1105.

[6] Scott, Tung and Drickamer; J. Chem. Physics 1951 **19** 1075. Tung and Drickamer; *ibid.* 1952 **20** 6, 10

[7] Davies; J. Physic. Chem. 1950 **54** 185. Hutchinson; *ibid.* 1948 **52** 897. Sjolin; Acta Physiol. Scand. 1942 **4** 365.

[8] Ward and Brooks; Trans. Faraday Soc. 1952 **48** 1124.

[9] Colburn and Welsh; Trans. Amer. Inst. Chem. Engrs. 1942 **38** 179.

[10] Lewis, Part II, following paper.

[11] Andreas *et al.*; J. Physic. Chem. 1938 **42** 1001; Fordham, Proc. Roy. Soc. A, 1948 **194** 1

[12] Lewis and Pratt; Nature 1953 **171** 1155.

[13] Murdoch and Pratt; A.E.R.E. CE/R 907; Trans. Inst. Chem. Engrs. 1953 **31** 307.

[14] Colburn and Schoenborn: Trans. Amer. Inst. Chem. Engrs. 1945 **41** 421.

Chemical Engineering Science, 1954, Vol. 3, pp. 260 to 278. Pergamon Press Ltd.

The mechanism of mass transfer of solutes across liquid-liquid interfaces

Part II.—The transfer of organic solutes between solvent and aqueous phases

J. B. Lewis

Chemical Engineering Division, Atomic Energy Research Establishment, Harwell, Didcot, Berks.

(*Received September* 1954)

Summary—" Overall " transfer coefficients were determined for a number of organic ternary systems and the results compared with the values predicted assuming zero interfacial resistance and using individual transfer coefficients calculated from the correlation derived in the preceding paper. Although good agreement was obtained in many cases, some systems, notably ethyl acetate-water with acetone, gave larger transfer rates than predicted, whilst others, especially toluene-water systems gave lower results. The faster rates were found to be associated with interfacial turbulence.

The low results are ascribed to slow heterogeneous reactions at the interface, and a method is devised for deriving the rate constants. Experiments were carried out at different temperatures in order to obtain the energies of activation. The probable reason for the slow step is discussed.

Résumé—Pour un certain nombre de systèmes ternaires organiques, on détermine des coefficients de transfert globaux qu'on compare aux valeurs prévues en supposant nulle la résistance à l'interface et en utilisant les coefficients de transfert individuels calculés à partir de la formule établie dans l'article précédent. Quoique la concordance obtenue soit bonne dans de nombreux cas, certains systèmes, notamment acétate d'éthyle – eau, avec l'acétone, donnent des vitesses de transfert plus importantes que prévu tandis que d'autres, particulièrement toluène-eau, donnent des résultats plus faibles. Les vitesses les plus élevées sont dues à turbulence à l'interface. On attribue les faibles résultats à des réactions hétérogènes lentes à l'interface et on imagine une méthode permettent de déduire les constantes de vitesse. On fait des expériences à diverses températures en vue d'obtenir les énergies d'activation. On discute la raison probable d'une marche lente.

VOL. 3 1954

In Part I [1] the factors influencing individual transfer coefficients for the mutual saturation of binary solvent-water systems were examined. Under the experimental conditions used mass transfer from the interface takes place by eddy not molecular diffusion. The individual coefficients were correlated by plotting k_1/v_1 against $[Re_1 + Re_2\,\eta_2/\eta_1]$ (Fig. 4 (a) Part 1). This correlation was represented with a slight loss of accuracy by the expression :

$$60\,k_1/v_1 = 6{\cdot}76 \times 10^{-6}\,[Re_1 + Re_2\,\eta_2/\eta_1]^{1{\cdot}65} + 1$$

Since the transfer coefficients were found to be independent of the molecular diffusivities this correlation will also apply to the transfer of an undistributed solute in solvent-water systems. It is thus possible to predict the individual coefficients for solute transfer in immiscible solvent-water systems where the mutual saturation technique is not applicable.

In any three-component system the overall transfer rate of the undistributed component will depend on the two individual coefficients and on the rate of transfer across the interface itelf. By calculating the overall coefficient, assuming infinitely fast interfacial transfer, and comparing the result with the experimentally determined coefficient, the value of the interfacial rate constant can be determined. This will depend on the nature of the reaction occurring at the interface, i.e. solvation, dimerisation, etc., and hence information can be obtained about this step.

In the present investigation overall transfer coefficients were determined for a number of organic ternary systems and compared with the values predicted by assuming zero interfacial resistance. From the difference in the two coefficients the interfacial transfer coefficients were calculated.

Experimental

Systems Used

The apparatus employed was the same as that described in Part I. Six solvent-water pairs were used, the solvents being ethyl acetate, butyl acetate, iso-butanol, carbon tetrachloride, " chlorex " (bis β chloroethyl ether), and toluene, with acetone, acetic acid, ammonia, aniline, benzoic acid and diethylamine as solutes. The distribution coefficient data for these systems were determined experimentally and are summarised in Table 2 and Figs. 3-9, while the relevant physical properties of the solvents are given in Table 1. Diffusion coefficients were determined for all the systems but since it was demonstrated in Part I that these are not needed for the correlation the results will be reported elsewhere.

The experimental procedure was similar to that used in the case of the mutual saturation experiments, except that solute was added initially to one of the phases. Both phases were sampled as before, but since somewhat larger quantities were needed for analysis samples were only taken every ten minutes. In a few cases, as, e.g., with dilute solutions of acetic and benzoic acids in toluene and carbon tetrachloride, very large samples were needed to obtain accurate analyses and intermediate samples were not therefore taken. In most experiments the phases were not mutually saturated at the start of the experiment, although where the solubility was appreciable, as for ethyl acetate, iso-butanol and butyl acetate, a few duplicate runs were carried out with the phases initially saturated. However, no significant difference in behaviour was observed. A few transfer runs were also carried out with monolayers of a surface active agent adsorbed at the interface, the long chain quarternary ammonium salt $C_{18}H_{37}N(CH_3)_3Cl$ being used as in Part I.

Analysis

The acids and bases were determined by titration with N/10 or N/40 NaOH or HCl, using a potentiometric method for the determination of the end point. (The latter was particularly valuable in the case of the solvent phase as most indicators are soluble in the solvents used.)

Acetone was determined by the hydroxylamine method [2] using N/10 NaOH for the titration, the end point being determined potentiometrically in all but the first few runs. Aniline was determined by bromination in the usual way, using $KBrO_3$-KBr mixture, followed by titration of the excess iodine with N/10 $Na_2S_2O_3$ after addition of KI.

Determination of the Experimental Overall Mass Transfer Coefficients

The transfer of a third component from phase 1 to phase 2 involves transport up to the interface in phase 1, transfer across the interface, and transport away from the interface in phase 2. As the accumulation at the interface due to adsorption must be negligible compared with the bulk concentrations the rates of these three steps will be equal. The concentrations on either side of the interface are normally assumed to be in equilibrium. This assumption is discussed further below. Since the interfacial concentrations cannot be determined it is customary to define an overall transfer coefficient based on the assumption that the resistance to transfer lies entirely in one phase [3]. If, for example, the overall coefficient is based on the water phase, K_{ow}, the assumption is made that there is no concentration gradient in the solvent phase the interfacial concentration being equal to the bulk value c_s. The interfacial concentration on the water side, c_w^*, is taken to be in equilibrium with c_s so that for transfer from solvent to water we can express the rate as :

$$j = K_{ow}(c_w^* - c_w) \qquad (1)$$

Although, in general, this assumption gives a purely imaginary picture of the process the correct transfer rates can be calculated if K_{ow} is known. If the distribution coefficient H is constant c_w^* will be equal to c_s/H. When, however, H varies with concentration a graphical

Table 1. *Physical properties of phases.*

Solvent	*Temp. °C*	*Density gm/ml.*	*Viscosity Centipoise*	*Remarks*
Butyl acetate	20°	0·88	0·72	The effect of adding 5% of various solutes to these solvents was investigated. It was found that the viscosities and densities remained substantially unchanged.
Carbon tetrachloride	20°	1·60	0·97	
	30°	1·57	0·84	
Chlorex (dichlordiethyl ether)	20°	1·22	2·38	
Ethyl acetate	20°	0·90	0·46	
iso-butanol	20°	0·80	3·95	
	30°	0·80	2·90	
Toluene	20°	0·86	0·58	
	30°	0·86	0·53	
	50°	0·84	0·43	
Water	20°	1·00	1·00	
	30°	1·00	0·80	
	50°	0·99	0·55	
Aqueous solutions	20°	1·00	1·06	The densities and viscosities of the other aqueous solutions are substantially the same as pure water.
(i) 4% Acetic acid	30°	1·00	0·84	
(ii) 7% Acetic acid	50°	0·99	0·61	
(iii) 12% Acetic acid	20°	1·00	1·20	
	30°	1·00	0·95	
	50°	0·99	0·63	
(iv) 4% Acetone	20°	0·99	1·13	
(v) 4% Diethylamine	20°	0·99	1·27	
	30°	0·98	0·97	
(vi) 4% Aniline	20°	1·00	1·07	

method of determining c_w^*, or H, must be used. Thus, referring to Fig. 1 (a), the curve AIB represents conditions at equilibrium and the point O the bulk phase concentrations c_w and c_s. The assumed interfacial concentrations c_w^* and c_s are represented by point B on the curve and the corresponding value of H is then the slope of the chord AB. As the bulk concentration varies during an experiment B moves along the curve, producing a family of chords such as AB, corresponding to the change in H. Samples are taken at intervals so that the change of c_w and c_s, and therefore c_w^*, with time can be determined.

Now at any time the transfer rate is given by :†

$$j = \frac{V}{A}\frac{dc_w}{dt}$$

$$\therefore K_{ow} = \frac{V}{A}\frac{1}{dt} \cdot \frac{dc_w}{(c_w^* - c_w)} \qquad (2)$$

When H changes considerably during the course

† The symbols used are defined at the end of this paper.

VOL. 3 1954

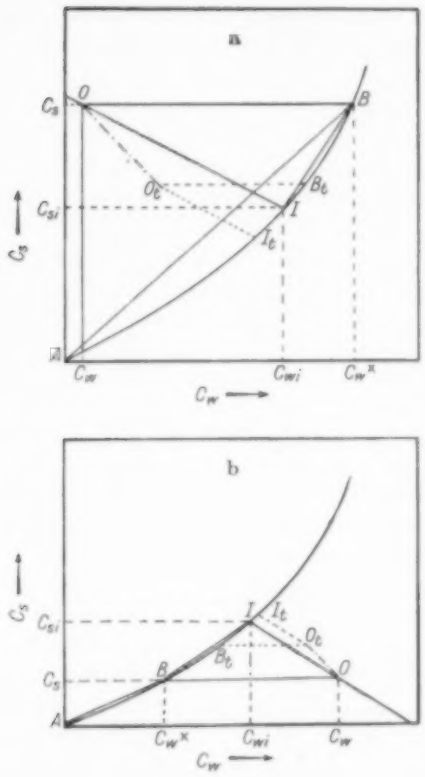

Fig. 1. Relation between the individual and overall resistances when the interfacial transfer is immeasurably fast, (*a*) transfer from solvent to water, (*b*) transfer from water to solvent.

of an experiment it is necessary to integrate this expression graphically. Thus we have :

$$K_{ow}\frac{At}{V} = \int \frac{dc_w}{(c_w^* - c_w)}$$

The right hand integral is evaluated by plotting $\frac{1}{(c_w^* - c_w)}$ against c_w and measuring the area under the curve. Thus, mean values of K_{ow} relating to successive values of c_w can be obtained.

In most cases H was either constant or varied little during the experiments and it was then more convenient to proceed as follows :

If $c_0 = (c_s + c_w)$ is the total initial concentration (since the volumes of the two phases were equal),

$$\therefore K_{ow} = \frac{V}{A}\frac{1}{dt}\cdot\frac{dc_w}{(c_0 - c_w)/H - c_w}$$

$$= \frac{V}{A}\frac{H}{H+1}\frac{1}{dt}\frac{dc_w}{c_0/(H+1) - c_w}$$

$$= -\frac{V}{A}\cdot\frac{H}{H+1}\cdot\frac{d}{dt}\ln(c_0/(H+1) - c_w) \quad (2a)$$

Thus K_{ow} can be obtained from the slope of the curve obtained by plotting $(c_0/(H+1) - c_w)$ against time on semi-logarithmic co-ordinates, using the appropriate values of H corresponding to the concentrations of the samples taken and taking a mean value of $\frac{H}{H+1}$. If K_{ow} is independent of concentration a linear plot will be obtained.

For transfer from water to solvent an exactly analogous equation can be derived thus :

$$K_{ow}\frac{At}{V} = \int \frac{dc_w}{(c_w - c_w^*)}$$

and K_{ow} can be obtained by graphical integration as before. When, as was usually the case, H remained substantially constant during an experiment the expression was integrated directly, giving :

$$K_{ow} = -\frac{V}{A}\cdot\frac{H}{H+1}\frac{d}{dt}\ln\left(c_w - c_0/(H+1)\right) \quad (2b)$$

where H is now the slope of the chord AB in Fig. 1 (b) and the appropriate values are used as before.

Similar equations are obtained when using the overall coefficient based on the solvent phase, i.e. K_{os} ; in this case the equilibrium concentration at the interface is c_s^*.

The experimentally determined transfer coefficients are summarised in Tables 3 to 7.

Interpretation of Results

Theoretical

(a) *Immeasurably Fast Interfacial Transfer*

As stated earlier, the transfer of a solute from, e.g. solvent to water, involves three consecutive processes. When the transfer across the interface is immeasurably fast the concentrations on either

side of the interface will be in equilibrium, i.e. $c_{si}/c_{wi} = H$. If the molecular species are different in the two phases as, for example, acetic acid between toluene and water where the acid is monomeric in water but almost entirely dimeric in toluene the true interfacial equilibrium differs from that determined experimentally since the former refers to the same species in both phases whereas the latter refers to the total concentration. Since however the concentrations used in the rate equations are the total concentrations, the interfacial equilibria considered must be those referring to the total concentrations, i.e. H must be the experimentally determined value. Thus we have :

$$j = k_s (c_s - c_{si}) = k_w (c_{wi} - c_w) \qquad (3)$$

Now we normally define an overall transfer coefficient K_{ow}, equation (1), and it can be shown from equations (1) and (3) that when H is constant.

$$\frac{1}{K_{ow}} = \frac{1}{k_w} + \frac{1}{Hk_s} \qquad (4a)$$

When H varies with concentration a graphical method of analysis is used. Thus, referring to Fig. 1 (a), the point I on the equilibrium curve corresponds to the interfacial concentrations c_{wi} and c_{si}. If we now define H' as the slope of the chord IB

i.e. $$H' = \frac{c_s - c_{si}}{c_w^* - c_{wi}} \qquad (5a)$$

then from equations (1), (3) and (5)

$$\frac{1}{K_{ow}} = \frac{1}{k_w} + \frac{1}{H'k_s} \qquad (4b)$$

The position of I can be obtained if k_w and k_s are known, since :

$$\text{Slope } OI = \frac{c_s - c_{si}}{c_{wi} - c_w} = -\frac{k_w}{k_s} \qquad \text{(from equation 3)}$$

Fig. 4 (a) and equation 6 of Part I enable k_w and k_s to be predicted for any solvent-water system, and the overall transfer coefficient can therefore be predicted whether H varies or not.

During the course of an experiment the bulk phase concentrations will vary, point O moving to some point O_t at time t. Since the volumes of both phases are the same the increase in concentration of the water phase will equal the fall in concentration of the solvent. Hence line $O\,O_t$ will have a slope of $-45°$ and the concentrations of the phases during any experiment will move along this line. For every point O_t there will be a new value of the interfacial concentration I_t and O_tI_t will be parallel to OI. Since the slope of OI is generally not widely different from that of $O\,O_t$ the interfacial concentrations will change much less than the bulk concentration, i.e. while O moves to O_t, I only moves to I_t and B to B_t. Since H' is given by the slope of IB the change in this factor depends on the shape of the curve between I and B. Apart from the toluene-water and carbon tetrachloride-water systems the change in H' was negligible in the present work.

For transfer in the reverse direction we have :

$$j = k_w (c_w - c_{wi}) = k_s (c_{si} - c_s) = K_{ow} (c_w - c_w^*)$$

Referring to Fig. 1 (b), points O, I and B refer to concentrations in the bulk, at the interface and to the hypothetical overall interfacial concentration c_w^* and c_s respectively. Thus defining

$$H'' = \frac{c_{si} - c_s}{c_{wi} - c_w^*} \qquad (5b)$$

$$\therefore \quad \frac{1}{K_{ow}} = \frac{1}{k_w} + \frac{1}{H''k_s} \qquad (4c)$$

The position at I is obtained as before and will again change during each experiment.

(b) *Slow Interfacial Reaction*

When the interfacial transfer rate is slow, e.g. in the case of a slow chemical reaction, the concentrations on either side of the interface are no longer in equilibrium with one another. Since the reaction is heterogeneous it is convenient to express the reaction rate as an equivalent rate either on the water or solvent side of the interface.

For transfer from solvent to water if the reaction is assumed to occur on the water side of the interface the concentration at the interface in equilibrium with the solvent will be $c_{wi}^* = c_{si}/H$. Then for a first order reaction the rate will be

VOL. 3 1954

equal to $k_{rw}(c_{wi}^{*} - c_{wi})$. In most cases the interfacial step involves reaction between the solute and one of the phases and since the latter will be in considerable excess we can assume that the reaction is pseudo-first order. (A possible exception to this is the dimerisation of carboxylic acids in aprotic solvents.) At the steady state there is no build up of solute at the interface and the three steps will take place at the same rate.

$$\therefore j = k_s(c_s - c_{si}) = k_{rw}(c_{wi}^{*} - c_{wi}) = k_w(c_{wi} - c_w) \qquad (6)$$

$$= K_{ow}(c_w^{*} - c_w) \text{ as before.}$$

If H is constant, then

$$H = \frac{c_s}{c_w^{*}} = \frac{c_{si}}{c_{wi}^{*}}$$

and from equation (6) it can be shown that

$$\frac{1}{k_{rw}} = \frac{A}{N}(c_w^{*} - c_w) - \left[\frac{1}{k_w} + \frac{1}{Hk_s}\right]$$

Now the first term on the R.H.S. of this equation is equal to the reciprocal of the overall transfer coefficient, i.e. $1/K_{ow}$, giving :

$$\frac{1}{K_{ow}} = \frac{1}{k_w} + \frac{1}{Hk_s} + \frac{1}{k_{rw}} \qquad (7a)$$

The sum of the first two terms on the R.H.S. of equation (7a) is equal to the reciprocal of the overall coefficient for the case where the reaction is immeasurably fast, i.e. to $1/K_{ow\,(calc.)}$. Hence substituting for the latter in equation (7a),

$$\frac{1}{k_{rw}} = \frac{1}{K_{ow\,(obs.)}} - \frac{1}{K_{ow\,(calc.)}} \qquad (8)$$

If the reaction is not of the first order, it has been shown [4] that for an nth order reaction equation (8) becomes :

$$\frac{(c_w^{*} - c_w)}{k_{rw}(c_w^{*n} - c_w^{n})} = \frac{1}{K_{ow\,(obs.)}} - \frac{1}{K_{ow\,(calc.)}} \qquad (8a)$$

An analogous argument applies when the direction of transfer is from water to solvent.

Instead of considering the overall water film coefficient, K_{ow}, the overall solvent film coefficient, K_{os}, may be used instead. Similar expressions are derived and the reaction is now assumed to occur on the solvent side of the interface. For a first order reaction we have :

$$\frac{1}{k_{rs}} = \frac{1}{K_{os\,(obs.)}} - \frac{1}{K_{os\,(calc.)}} \qquad (8')$$

and for a reaction of the nth order :

$$\frac{(c_s - c_s^{*})}{k_{rs}(c_s^{n} - c_s^{*n})} = \frac{1}{K_{os\,(obs.)}} - \frac{1}{K_{os\,(calc.)}} \qquad (8'b)$$

It is frequently found that the reaction would be of the first order if occurring in one phase but of a higher order in the other. In such cases therefore it is convenient to consider the overall coefficient, and hence the reaction, in terms of

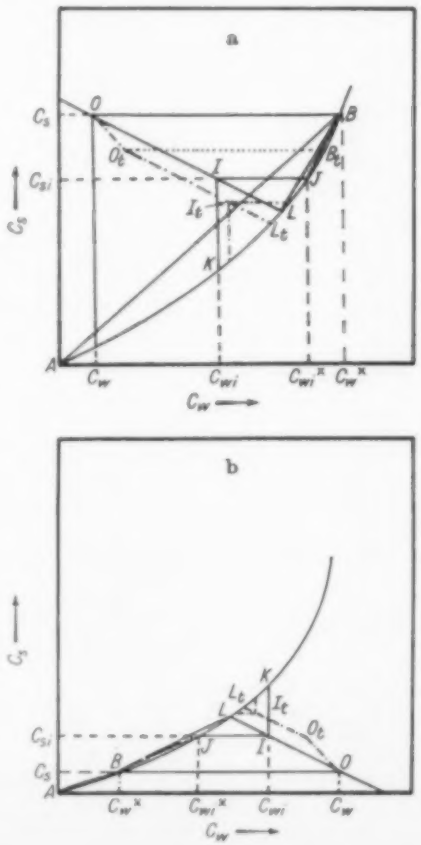

Fig. 2. Relation between the individual and overall resistances in the presence of a slow interfacial reaction, (*a*) transfer from solvent to water, (*b*) transfer from water to solvent.

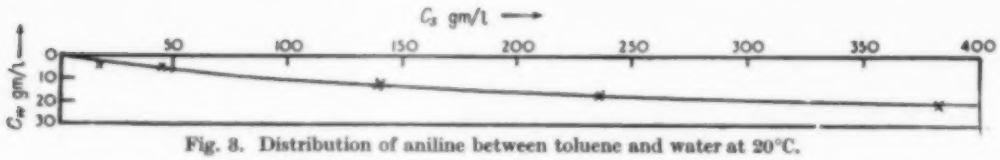

Fig. 3. Distribution of aniline between toluene and water at 20°C.

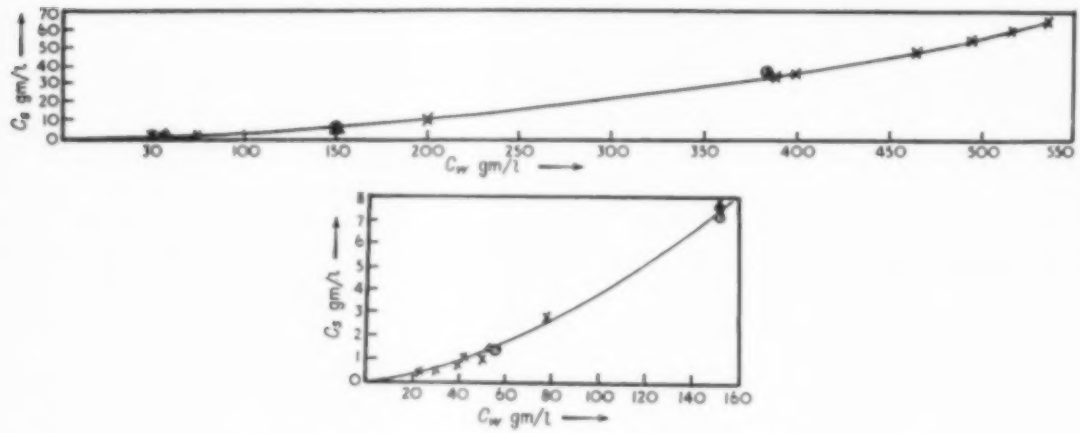

Fig. 4. Distribution of acetic acid between toluene and water, (× 20°C, ○ 30°C, △ 50°C).

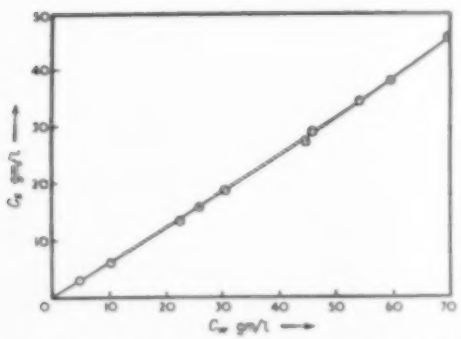

Fig. 5. Distribution of acetone between toluene and water at 20°C.

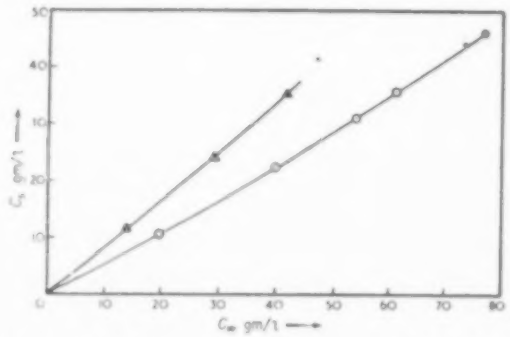

Fig. 6. Distribution of diethylamine between toluene and water, (○ 20°C, △ 30°C).

the phase which would give first order kinetics as this simplifies the calculation and interpretation of results. PRATT and MURDOCH for example [4] considered the overall coefficients for uranyl nitrate transferring between solvents and water in terms of the solvent phase, as this gave first order kinetics, whereas basing the overall coefficients on the water phase gave a third order reaction.

When H varies with concentration it is again necessary to resort to a graphical method of analysis. Referring to Fig. 2 (a), curve $AKJB$ represents the conditions at equilibrium and O the bulk phase concentrations. The point I representing the two interfacial concentrations c_{wi} and c_{si} will not lie on the curve since the two interfacial concentrations are not in equilibrium. If we define H^* as the slope of the chord JB,

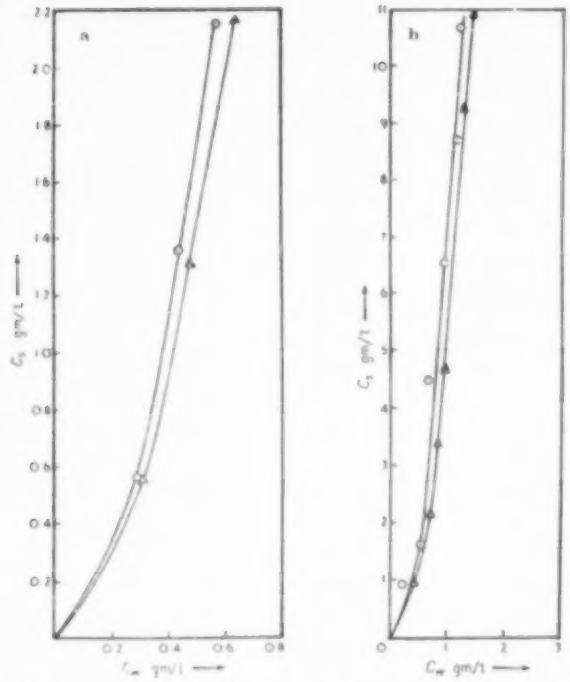

Fig. 7. Distribution of benzoic acid between (*a*) CCl_4 and water, and (*b*) toluene and water (○ 20°C, △ 30°C, □ 50°C)

i.e. $$H^* = \frac{c_s - c_{si}}{c_w^* - c_{wi}^*} \qquad (9a)$$

then it is found from (6) and (9a) that

$$\frac{1}{k_{rw}} = \frac{A}{N}(c_w^* - c_w) - \left[\frac{1}{k_w} + \frac{1}{H^* k_s}\right]$$

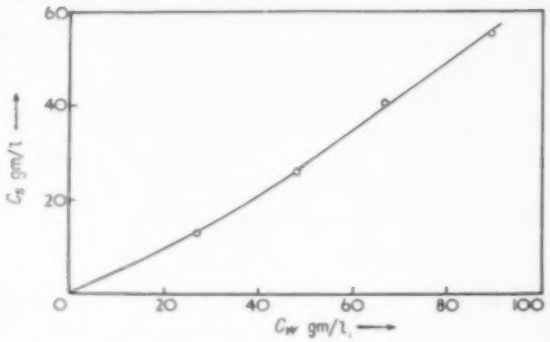

Fig. 9. Distribution of acetone between CCl_4 and watre at 20°C.

Table 2. Systems with constant distribution coefficients.

Solvent – Water	*Solute*	$H = c_s/c_w$	*Temp. °C*
Isobutanol-Water	Acetic acid	1·18	20°
Isobutanol-Water	Ammonia	0·26	20°
Isobutanol-Water	Diethylamine	3·88	20°
Isobutanol-Water	Diethylamine	5·30	30°
Butyl acetate-Water	Acetone	0·81	20°
Butyl acetate-Water	Diethylamine	1·00	20°
Ethyl acetate-Water	Acetic acid	0·84	20°
Ethyl acetate-Water	Acetone	1·24	20°
Chlorex-Water	Acetone	1·20	20°
Toluene-Water	Diethylamine	0·84	30°

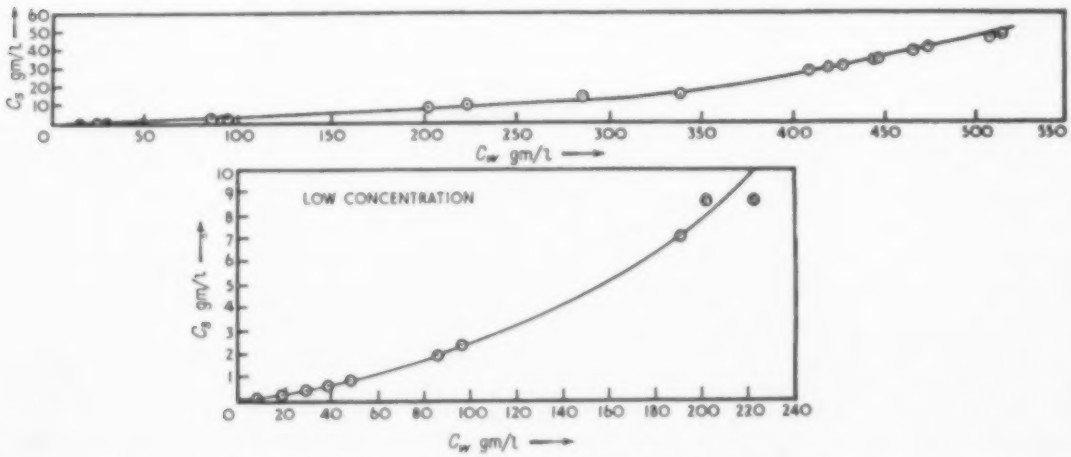

Fig. 8. Distribution of acetic acid between CCl_4 and water at 20°C.

i.e. $$\frac{1}{k_{rw}} = \frac{1}{K_{ow\,(obsd.)}} - \frac{1}{K_{ow\,(calc.)}} \qquad (7b)$$

In order to obtain the second term on the R.H.S. of equation 7 (b), i.e., the predicted value of K_{ow}, it is necessary to know the position of the point J on Fig. 2 (a) so that H^* can be determined. Since I does not lie on the intersection of OI and the equilibrium curve the position of I and therefore of J is uncertain and a series of approximations must be made. The slope of OI is equal to $-k_w/k_s$ as before, and if OI is projected to meet the curve at L we can taken the first value of H^*, H_1^* to be the slope of BL. Using H_1^*, the first value of k_{rw} is calculated, k_{rw1}. Now

$$j = k_{rw}(c_{wi}^* - c_{wi})$$

$$\therefore \quad \frac{j}{k_{rw}} = (c_{wi}^* - c_{wi}),$$

Since the term $(c_{wi}^* - c_{wi})$ corresponds to IJ, using k_{rw1} a first approximation to $(c_{wi}^* - c_{wi})$ is calculated, giving by simple geometry the first position of I and J. Thus a second value of H^*, H_2^* is obtained from the slope of J_1B and the procedure repeated until a constant value of k_{rw} obtained.

During an experiment point O moves along line $O\,O_i$ due to concentration changes, as before, so that both H and H^* change. These variations must be taken into account if the curvature of $AKJB$ is very unsymmetrical between J and B.

For transfer in the reverse direction an analogous situation applies as shown in Fig.2 (b). Defining H° as follows :

$$H^\circ = \frac{c_{si} - c_s}{c_{wi}^* - c_w^*} \qquad (9b)$$

i.e., as the slope of the chord BJ, we can show that equation (8) again applies. A similar series of approximations may be necessary to obtain the correct value of H°. Again the coefficients can be expressed in terms of the solvent phase if more convenient.

Application to Present Data

(a) *Comparison of Calculated and Observed Coefficients*

The experimentally determined overall water coefficients K_{ow} are summarised in Tables 3 to 8 along with the values calculated assuming immeasurably fast interfacial reaction. The ratios of $\frac{K_{ow(obsd.)}}{K_{ow(calc.)}}$ should equal unity if the assumption of immeasurably fast reaction is correct. Values in the range of, say, 0·8-1·2 may well be obtained however because of the uncertainty in k_w and k_s due to the scatter in the correlation and to experimental errors, particularly the difficulty in avoiding interfacial contamination in the transfer cell. Although many results fall in this range it is clear that in some experiments the observed transfer coefficients are much greater, and in others much smaller than the predicted values. The interfacial reaction constants k_{rw} have been calculated where the observed coefficients are significantly lower than the calculated values.

(b) "*Normal*" *Transfer Coefficients*

Good agreement is obtained between the observed and calculated overall coefficients with transfer in the following solvent-water systems :

Isobutanol

(i) Acetic acid from isobutanol to water.

(ii) Ammonia from water to isobutanol.

Butyl Acetate

Acetone transferring in both directions.

Chlorex

Acetone transferring in both directions.

Carbon Tetrachloride

(i) Acetone from water to CCl_4.

(ii) Acetic acid from CCl_4 to water.

Toluene

(i) Acetic acid, diethylamine and acetone from water to toluene (there is a tendency however, with the last two solutes for low values to be obtained at the highest Reynolds numbers, this is discussed further below).

(ii) Aniline from toluene to water.

(c) *High Transfer Coefficients*

Significantly high transfer coefficients are obtained with transfer in the following systems :

Table 3. Isobutanol-Water.

Run No.	Temp. °C	Reynolds Numbers		Conc. gm/l*		K_{ow} cm/sec × 10^3		k_{rw} cm/sec. × 10^3 Φ
		Water	Solvent	Initial	Final	Calc.	Obsd.	
			IIIa. *Diethylamine transfer* Water → Solvent (Interfacial turbulence)					
381	20	2,400	1,000	35·3	26·1	2·17	1·17	
447	20	2,400	1,000	44·7	30·0	2·17	2·34	
453	20	2,400	1,000	86·1	56·1	2·17	2·50	
458	20	2,400	1,000	39·7	25·8	2·17	2·66	
387	30	2,600	1,000	29·4	20·5	1·31	1·83	
484	30	2,600	1,000	31·6	22·6	1·31	1·67	
			Solvent → Water					
380	20	3,000	1,000	27·1	25·5	1·74	1·33	
448	20	3,000	1,000	35·9	34·9	1·74	1·33	
452	20	3,000	1,000	72·3	68·6	1·74	1·33	
459	20	3,000	1,000	34·4	32·1	1·74	1·33	
388	30	3,000	1,000	30·0	28·6	1·38	2·00	
485	30	3,000	1,000	31·1	30·6	1·38	1·67	
			IIIb. *Acetic acid transfer* Water → Solvent (Interfacial turbulence)					
363	20	2,800	1,000	49·8	40·5	1·17	1·33	
368	20	2,800	1,000	52·6	41·7	1·17	1·50	
364	20	2,800	1,500	47·8	35·9	1·64	1·83	
370	20	2,800	1,500	44·8	43·6	1·64	1·83	
			Solvent → Water					
362	20	3,000	1,000	48·0	38·8	1·15	1·67	
366	20	3,000	1,000	38·9	31·4	1·15	1·67	
365	20	3,000	1,500	42·8	32·7	1·69	2·17	
369	20	3,000	1,500	45·4	34·7	1·69	2·33	
			IIIc. *Ammonia transfer* Water → Solvent					
394	20	3,000	1,000	1·9	1·8	0·42	0·25	
486	20	3,000	1,000	1·7	1·6	0·42	0·38	
			Solvent → Water (Interfacial turbulence)					
410	20	3,000	1,000	1·4	0·9	0·42	0·83	
423	20	3,000	1,000	1·2	0·9	0·42	0·50	

* Concentrations of the phase from which transfer is taking place.

Φ Values of k_{rw} are only tabulated where they are markedly significant.

Table 4. Ethylacetate-Water : Interfacial turbulence in both directions in all systems.

Run No.	Temp. °C	Reynolds Numbers		Conc. gm/l*		K_{ow} cm/sec × 10^3		k_{ro} cm/sec. × 10^3
		Water	Solvent	Initial	Final	Calc.	Obsd.	
				IVa. *Acetone transfer* Water → Solvent				
284	20	2,300	2,500	48·0	23·1	0·59	2·5	
287	20	2,300	2,500	47·1	26·4	0·59	2·8	
270	20	3,600	4,000	29·2	15·5	1·16	3·7	
274	20	3,600	4,000	30·4	15·9	1·16	4·2	
275	20	4,600	5,000	32·4	19·2	2·01	3·7	
283	20	4,600	5,000	36·6	19·5	2·01	4·2	
386	20	4,600	5,000	33·6	21·5	2·01	3·8	
460	20	4,600	5,000	40·1	25·2	2·01	4·0	
				Solvent → Water				
285	20	2,500	2,500	41·5	31·0	0·59	2·8	
286	20	2,500	2,500	46·0	33·6	0·59	3·2	
230	20	4,000	4,000	74·0	45·6	1·22	2·7	
263	20	4,000	4,000	44·0	26·7	1·22	4·7	
279	20	5,000	5,000	63·2	43·3	1·77	4·0	
385	20	5,000	5,000	37·7	26·9	1·77	4·2	
461	20	5,000	5,000	41·1	29·9	1·77	3·7	
				IVb. *Acetic acid transfer* Water → Solvent				
437	20	4,700	5,000	40·8	27·9	1·53	3·3	
462	20	4,100	5,000	104·6	67·0	1·47	4·2	
				Solvent → Water				
438	20	5,000	5,000	45·9	29·7	1·56	3·2	
463	20	5,000	5,000	99·0	53·0	1·56	4·2	

Isobutanol

(i) Diethylamine from water to isobutanol.

(ii) Ammonia from isobutanol to water.

Ethyl Acetate

Acetone and acetic acid transferring in both directions.

Carbon Tetrachloride

Acetone transferring from CCl_4 to water.

Toluene

Aniline transferring from toluene to water.

In all these systems transfer was accompanied by marked interfacial turbulence. This effect, which is related to spontaneous emulsification, was frequently seen when the interfacial tensions of the unequilibrated three-component systems were determined [5]. For this purpose, the pendant drop method was used [6], a droplet of the solvent phase being suspended in the aqueous phase and an enlarged image of the drop profile projected on a screen. In several instances the interface could be seen to be in a state of violent agitation during transfer of the undistributed third component. Except with the two ethyl acetate-water

VOL. 3 1954

Table 5. Butyl acetate-Water.

Run No.	Temp. °C	Reynolds Numbers		Conc. gm/l*		K_{ow} cm/sec × 10^3		k_{rw} cm/sec. × 10^3
		Water	Solvent	Initial	Final	Calc.	Obsd.	
				Va. *Acetone transfer* Water → Solvent				
307	20	2,700	3,000	40·0	33·8	0·73	0·5	–
308	20	2,700	3,000	31·0	28·8	0·73	1·0	–
309	20	4,500	5,000	32·0	21·0	1·68	1·9	–
				Solvent → Water				
304	20	3,000	3,000	42·6	28·8	0·76	0·8	–
306	20	3,000	3,000	42·6	25·8	0·76	0·8	–
389	20	5,000	5,000	31·7	21·0	1·73	1·2	–
411	20	5,000	5,000	38·7	25·6	1·73	1·5	–
				Vb. *Diethylamine transfer* Water → Solvent				
428	20	4,000	5,000	33·6	28·7	1·73	0·8	1·5
				Solvent → Water				
427	20	5,000	5,000	27·9	23·4	1·89	1·0	2·1

Table 6. Chlorex-Water.

Run No.	Temp. °C	Reynolds Numbers		Conc. gm/l*		K_{ow} cm/sec × 10^3		k_{rw} cm/sec
		Water	Solvent	Initial	Final	Calc.	Obsd.	
				Acetone transfer Water → Chlorex				
492	20	2,700	3,000	61·6	43·6	1·54	2·32	
494	20	2,700	3,000	48·0	34·1	1·54	1·77	
495	20	3,600	4,000	52·7	33·4	2·41	2·65	
				Chlorex → Water				
491	20	3,000	3,000	44·2	37·8	1·62	1·32	
493	20	3,000	3,000	47·6	36·7	1·62	1·58	
496	20	4,000	4,000	42·8	32·3	2·55	1·82	

Table 7. Carbon tetrachloride-Water.

Run No.	Temp. °C	Reynolds Numbers		Conc. gm/l*		K_{ow} cm/sec × 10^3		k_{rw} cm/sec. × 10^3
		Water	Solvent	Initial	Final	Calc.	Observed	
				VIIa. *Acetone transfer* Water → Solvent				
445	20	3,600	4,000	41·9	38·0	0·66	0·63	
444	20	3,600	4,000	36·9	34·1	0·66	0·52	
468†	20	3,600	4,000	41·0	39·5	0·66	0·35	
470†	20	3,600	4,000	40·5	38·6	0·66	0·32	
				Solvent → Water (interfacial turbulence obsd.)				
443	20	4,000	4,000	37·3	24·0	0·85	1·67	
446	20	4,000	4,000	31·2	25·4	0·85	1·00	
				VIIb. *Benzoic acid transfer* Water → Solvent				
454	20	4,000	4,000	1·8	1·6	2·02	0·92	1·8
477	20	4,000	4,000	1·0	0·95	1·77	0·62	1·0
456	30	4,000	4,000	1·9	1·7	1·64	0·70	1·2
479	30	4,000	4,000	1·0	0·95	1·44	0·43	0·6
				Solvent → Water				
455	20	4,000	4,000	1·95	1·85	2·23	1·33	1·3
469	20	4,000	4,000	1·93	1·87	2·23	0·67	1·0
476†	20	4,000	4,000	3·59	3·35	2·23	0·17	0·2
457	30	4,000	4,000	2·0	1·90	1·85	3·04	
480	30	4,000	4,000	3·69	3·37	1·85	1·95	
				VIIc. *Acetic acid transfer* Water → Solvent				
467	20	3,300	4,000	119·5	118·8	0·038	0·03	0·14
465†	20	3,300	4,000	103·4	103·0	0·038	0·02	0·04
478	20	3,300	4,000	121·6	120·2	0·038	0·05	–
481	30	3,300	4,000	120·5	120·0	0·032	0·05	–
				Solvent → Water				
464	20	4,000	4,000	40·9	28·6	0·14	0·15	–
466	20	4,000	4,000	49·7	28·9	0·14	0·20	–
482	30	4,000	4,000	50·6	35·2	0·13	0·17	–

† Interface probably contaminated.

VOL. 3 1954

Table 8. Toluene-Water

Run No.	Temp. °C	Reynolds Numbers		Conc. gm/l*		K_{ow} cm/sec × 10^3		k_{rw} cm/sec. × 10^3
		Water	Solvent	Initial	Final	Calc.	Obsd.	
		VIIIa. *Acetic acid transfer* Water → Solvent						
371	20	2,800	3,000	53·2	52·8	0·033	0·050	–
375	20	2,800	3,000	53·3	53·0	0·033	0·033	–
475	20	2,500	3,000	114·5	112·8	0·078	0·098	–
397	30	2,900	3,000	47·5	47·2	0·025	0·042	–
418	50	2,700	3,000	71·5	70·8	0·033	0·075	–
376	20	4,700	5,000	53·4	53·0	0·084	0·050	0·12
379	20	4,700	5,000	54·8	54·2	0·084	0·067	0·33
414	20	4,700	5,000	61·5	61·3	0·084	0·033	0·06
435*	20	4,700	5,000	40.1	39·8	0·084	0·017	0·02
436(a)†	20	4,700	5,000	42·5	42·3	0·084	0·017	0·02
436(b)†	20	4,700	5,000	42·4	42·2	0·084	0·033	0·06
474	20	4,200	5,000	123·5	121·7	0·20	0·67	–
398	30	4,800	5,000	54·2	54·0	0·062	0·025	0·04
417	50	4,800	5,000	66·1	65·5	0·077	0·10	–
487	50	4,600	5,000	131·0	128·9	0·11	0·83	–
		Solvent → Water (Interfacial turbulence observed)						
373	20	3,000	3,000	45·9	33·3	0·176	0·183	–
374	20	3,000	3,000	43·7	32·5	0·176	0·130	0·5
396	30	3,000	3,000	43·2	33·0	0·144	0·15	–
416	50	3,000	3,000	43·6	28·8	0·103	0·167	–
377	20	5,000	5,000	41·6	30·6	0·418	0·012	0·02
378	20	5,000	5,000	45·0	33·4	0·418	0·083	0·10
412	20	5,000	5,000	46·5	28·5	0·418	0·167	0·28
413	20	5,000	5,000	51·7	28·4	0·418	0·217	0·45
434(a)†	20	5,000	5,000	42·0	30·7	0·418	0·167	0·28
434(b)†	20	5,000	5,000	28·3	21·4	0·367	0·13	0·20
399	30	5,000	5,000	44·7	29·2	0·343	0·233	0·72
400	30	5,000	5,000	46·1	32·6	0·343	0·183	0·39
415	50	5,000	5,000	43·6	26·5	0·23	0·20	1·36
488	50	5,000	5,000	56·9	37·6	0·23	0·25	–
		VIIIb. *Diethylamine transfer* Water → Solvent						
347	20	1,600	2,000	32·3	30·2	0·31	0·28	–
313	20	1,600	2,000	39·5	37·9	0·31	0·18	–
392	20	1,600	2,000	32·7	30·2	0·31	0·35	–
296	20	2,400	3,000	52·7	46·9	0·56	0·43	–
297	20	2,400	3,000	40·3	35·9	0·56	0·50	–
383	30	2,500	3,000	38·0	33·9	0·58	0·52	–
489	30	2,500	3,000	35·6	31·4	0·58	0·57	–
310	20	3,900	5,000	39·5	34·3	1·20	0·57	1·0
390	20	3,900	5,000	32·6	27·8	1·20	1·03	7·1
391	20	3,900	5,000	32·5	28·7	1·20	0·78	1·8
		Solvent → Water						
312	20	2,000	2,000	40·8	36·4	0·35	0·27	1·8
348	20	2,000	2,000	35·5	31·0	0·35	0·27	1·8
294	20	3,000	3,000	44·0	36·1	0·63	0·47	1·9
295	20	3,000	3,000	33·8	28·2	0·63	0·37	0·9
382	30	3,000	3,000	31·9	27·7	0·59	0·42	1·5
490	30	3,000	3,000	34·2	31·2	0·59	0·52	4·4
298	20	5,000	5,000	40·4	31·4	1·49	0·42	0·6
311	20	5,000	5,000	40·7	32·3	1·49	0·50	0·8

† Monolayers on interface.

Table 8 cont. Toluene-Water.

Run No.	Temp. °C	Reynolds Numbers		Conc. gm/l*		K_{ow} cm/sec × 10^3		k_{rw} cm/sec. × 10^3
		Water	Solvent	Initial	Final	Calc.	Obsd.	
				VIIIc. *Acetone transfer* Water → Solvent				
333	20	2,700	3,000	42·6	38·5	0·61	0·75	–
353	20	2,700	3,000	40·3	36·7	0·61	0·60	–
346	20	4,500	5,000	33·7	32·6	1·44	0·22	0·3
409	20	4,500	5,000	35·2	27·8	1·44	1·17	6·2
420	20	4,500	5,000	29·8	26·5	1·44	0·72	1·4
				Solvent → Water (Interfacial turbulence observed)				
332	20	3,000	3,000	48·9	39·5	0·69	1·27	–
352	20	3,000	3,000	31·6	29·9	0·69	0·67	–
351	20	5,000	5,000	37·9	28·4	1·55	0·98	2·7
419	20	5,000	5,000	29·7	24·5	1·55	0·80	1·7
				VIIId. *Benzoic acid transfer* Water → Solvent				
432	20	5,000	5,000	1·79	1·46	2·38	1·17	2·3
508	20	5,000	5,000	0·62	0·45	2·32	1·08	2·0
499	50	5,000	5,000	3·51	2·65	1·52	0·95	2·5
502	50	5,000	5,000	2·91	2·15	1·50	1·13	8·5
507	50	5,000	5,000	1·22	0·75	1·25	1·38	–
509	50	5,000	5,000	3·14	2·04	1·51	1·18	5·5
				Solvent → Water				
431	20	5,000	5,000	1·95	1·86	2·62	1·3	2·6
433	20	5,000	5,000	2·04	1·94	2·62	1·17	2·1
500	50	5,000	5,000	1·64	1·38	1·59	2·62	–
501	50	5,000	5,000	1·68	1·53	1·59	1·48	4·0
506	50	5,000	5,000	7·37	6·85	2·97	2·33	4·1
510	50	5,000	5,000	6·74	6·29	2·87	1·17	2·0
				VIIIe. *Aniline transfer* Water → Solvent (Interfacial turbulence observed)				
432	20	2,900	3,000	17.6	13.2	1.16	1.67	–
426	20	2,900	3,000	20·8	15·4	1·16	1·67	–
				Solvent → Water				
421	20	3,000	3,000	19·0	18·7	1·17	1·00	6·6
425	20	3,000	3,000	21·6	21·3	1·17	0·83	2·8

systems, where transfer of acetone and acetic acid in either direction caused turbulence, this effect if obtained at all was confined to transfer across the interface in one direction only. The direction of transfer causing turbulence is recorded in Tables 3 to 8, for those systems where this effect was found.

The increased turbulence and larger area arising from this effect will increase the observed transfer rate by an unpredictable amount so that in the absence of a slow interfacial reaction the ratio of $K_{ow\,(obsd.)}/K_{ow\,(calc.)}$ will be greater than unity. If, however, a slow reaction does occur then the net result will be complicated and ratios equal to or less than unity might be obtained. Thus, in a system where this effect is found a value of the obs./calc. ratio near unity indicates the probable existence of a moderately slow interfacial reaction. When a ratio significantly lower than unity is obtained this is still greater than the value that

VOL. 3 1954

would be obtained if allowance could be made for the additional turbulence and increased area. Consequently the value of k_{ro} calculated will be too great in all systems where interfacial turbulence arises. The effect on the calculated activation energy cannot be predicted.

(d) *Low Transfer Coefficients*

Significantly low transfer coefficients are obtained in a number of instances and for these the reaction rate constants were calculated as described above. Where this could be done at more than one temperature an approximate value of the activation energy E was obtained. In a few instances the rates are low at 20°C but " normal " at higher temperatures so that only the 20° value of the reaction constant could be obtained. It was thus not possible to calculate the activation energies but either these were very small or else the low coefficients at 20° were not significant. A few transfer coefficients were also obtained that were ' normal ' at Reynolds numbers of 2,000 and 3,000, but somewhat low at 5,000. It is clear that here the reaction constants are of the same order as the turbulent transfer coefficients at Reynolds numbers of 5,000 but sufficiently greater than the turbulent coefficients at lower Reynolds numbers not to have a marked effect on the transfer rate.

The transfer of acetic acid from water to isobutanol and from toluene to water gives rise to marked interfacial turbulence. In these cases therefore high transfer coefficients should be obtained and their absence indicates a slow reaction. With isobutanol the coefficients are approximately " normal " so that no reaction constant can be calculated. Low coefficients are obtained with the toluene system but the calculated reaction constant will be too large and the activation energy very approximate.

The systems where slow reactions probably occur are :

Isobutanol

(i) Diethylamine from isobutanol to water at 20°C.

Since obs./calc. ratios greater than unity are obtained at 30° either the activation energy is small or else the low values at 20° are not significant.

(ii) Acetic acid from water to isobutanol.

Ratios slightly greater than unity are actually obtained but since an appreciable interfacial turbulence was observed these values indicate the probable presence of a slow interfacial reaction. The rate constant cannot be obtained but it is probably of the same order as the turbulent transfer coefficients.

Butyl Acetate

Diethylamine transfer in either direction.

Since experiments were only carried out at 20° no value of the activation energy was obtained.

Carbon Tetrachloride

(i) Benzoic acid in either direction at 20°C.

For transfer from solvent to water at 30° ratios greater than unity were obtained thus either E is small or the 20° result is of no significance. In the other direction the position is not clear as slow transfer also occurs at 30° with a similar reaction constant to that at 20°. This may well be due to experimental inaccuracies.

(ii) Acetic acid from water to CCl_4 at 20°C.

A ratio greater than unity is obtained at 30° so that again either E is small or the 20° results are of no significance.

Toluene

(i) Acetic acid from toluene to water.

Interfacial turbulence was present in this system so that the observed overall coefficient and the calculated reaction constants are both too large. The apparent energy of activation is about 4 K.cals./mole but due to the turbulence no assessment of the accuracy of this value can be made.

(ii) Diethylamine from toluene to water.

E is somewhere between 5 and 7 K.cals./mole.

(iii) Benzoic acid from water to toluene. E is about 10 K.cals./mole.

(iv) Benzoic acid from toluene to water. E is about 13 K.cals./mole.

In addition to these results low values were also obtained with transfer of acetic acid between toluene and water when the interface was coated with a monolayer of $C_{18}H_{37}N(CH_3)_3Cl$. For transfer from toluene to water the rate was approximately the same as in the absence of a film but in the other direction a marked retardation in transfer was obtained as compared with transfer across the clean surface.

Discussion

Of 32 systems studied 15 gave reasonable agreement between the calculated and observed coefficients, while 8 transfer rates were faster and 9 slower than predicted. All the fast transfer rates were obtained in systems exhibiting marked interfacial turbulence and since none of the " normal " and only two of the slow rates exhibited any interfacial effect this phenomenon is considered to be the cause of the high rates. Since " normal " rates were obtained, in some cases at least, for every solvent-water pair investigated, with the exception of ethyl acetate-water which was, however, actually used in obtaining the correlation, the results were considered to be a justification of the use of the correlation in predicting third-component transfer in the transfer cell. The diminution in the rate of transfer of acetic acid from water to toluene caused by the monolayer was unexpected since a similar film had little effect on rates of mutual saturation of ethyl acetate-water and furfural-water. It may be however that such monolayers are very specific in their action. Recent work on the retardation of evaporation from water surfaces covered with unimolecular films tends to support this view [7].

Except for transfer between toluene and water at the highest Reynolds numbers, the acetone transfer coefficients were either in agreement with the predicted values or else high due to interfacial turbulence. The only effect likely to occur with acetone transfer would be energy and entropy changes arising from the different type of solvation in the two phases. This should be most marked with toluene-water and CCl_4-water where the solvents and water are most dissimilar. It is interesting to note that the distribution coefficient of acetone between toluene and water has a marked temperature coefficient, unlike distribution between the ethyl acetate-water and butyl acetate-water phases. The slight retardation in transfer between toluene and water is thus probably due to such a solvation effect. Since the effect is small it would not be noticeable at the lowest stirring speeds. The interfacial energy barrier would of course be higher in one direction than the other and if this is in the direction toluene to water, the retardation in transferring from water to toluene may be negligible. In the analogous case of transfer from carbon tetrachloride to water a marked interfacial turbulence is obtained which will mask any small interfacial effects.

Acetic and benzoic acids are known to dimerise in aprotic solvents such as toluene and carbon tetrachloride whereas in water, alcohols, ketones, etc. the monomeric molecules are stabilised by hydrogen bonding to the solvent molecules. The transfer of these acids between the toluene-water and CCl_4-water phases will thus involve a dimerisation reaction at the interface which will be absent in the other systems investigated. It is significant therefore that slow transfer rates have been obtained (with the exception of acetic acid from CCl_4 to water) for the transfer of acetic and benzoic acids between toluene and water and CCl_4 and water. Transfer of acetic acid between the other solvents was not slow, except possibly from water to isobutanol where turbulence may have masked a small effect.

The reaction constants have been calculated assuming first order kinetics. This may well be incorrect but in the absence of other evidence this is probably the best way of expressing the results. The values of k_{rw} and E obtained are only approximate as the aim of the present work was to examine the general behaviour of a large number of systems rather than obtain very accurate data on a limited number. (More detailed investigations are now being carried out on a few systems of particular interest.) No data are

VOL. 3 1954

available as to the free energy and heats of dissociation of acetic and benzoic acids in toluene but in benzene the values are 4·3 and 8·2 K.cals./-mole respectively for acetic acid and 5·2 and 8·4 K.cals./mole for benzoic acid [8]. Similar values apply for acetic acid in carbon tetrachloride. Since however the interfacial reaction occurs in the presence of water the nature of the reation will be different and these values of no relevance. Transfer from solvent to water must involve a reaction between dimeric acid molecules and water whilst transfer in the other direction involves a reaction between monomeric acid molecules hydrogen bonded to water molecules. Ward [9] has calculated the increase in free energy of acetic acid transferring from water to toluene at 25°C from distribution data. This is about 3 K.cals./-mole but no value of the activation free energy can be computed ; allowance has also to be made for the energy of adsorption. Since benzoic acid is much less soluble in water than acetic acid the degree of solvation may be widely different and this may alter the reaction rate appreciably as compared with acetic acid. Further, with increasing concentration of acetic acid in the toluene phase the solubility of water will increase. This will then reduce the extent of dimerisation in this phase and hence accelerate the rate of reaction, as was actually found. Further information as to the nature of the rate-controlling step is clearly desired. It is interesting that the turbulent transfer technique is able to demonstrate activation energy barriers when the technique of diffusion across a plane interface fails [9].

Diethylamine was found to transfer slowly between butyl acetate and water and from toluene to water. A small effect was also found in transferring from isobutanol to water. The effect here is almost certainly associated with the presence of the amine group which presumably forms hydroxyl compounds in water. Diethylamine being a stronger base than ammonia should thus have a more marked retardation of transfer. This appears to be the case as the observed ammonia transfer coefficients agree with the calculated value for transfer from isobutanol to water whereas the corresponding diethylamine values are somewhat low.

Conclusions

(1) Overall transfer coefficients were determined for various solutes transferring between six different solvent-water pairs, 16 systems, i.e. 32 cases being investigated in all. The results were compared with values calculated using the correlation derived in Part I. In 15 cases the two sets of data agreed well, in 8 the observed rates were faster and in 9 slower than predicted.

(2) The high coefficients were found to occur only in systems where marked interfacial turbulence arose and it was concluded that this phenomenon was the reason for the high values.

(3) The low coefficients were associated with the transfer of those solutes which might reasonable be expected to be involved in reaction at the interface. Approximate values of the first-order reaction constant k_{rw} were calculated, and in a number of instances very approximate values of the activation energy of the reaction also.

(4) It is concluded that the correlation of Part I is quite satisfactory for predicting individual turbulent transfer coefficients in the transfer cell used. In the absence of any interfacial turbulence and slow chemical reaction, the overall transfer coefficient can then be calculated. Conversely if interfacial turbulence is absent, the chemical rate constant can be obtained if the observed and calculated overall transfer coefficients are known.

(5) It is thus demonstrated that the behaviour of two different systems should not be compared even in the same equipment unless it is known that interfacial turbulence is absent and that no slow interfacial reaction is present.

The bulk of the experimental work was carried out by Mr. E. W. Sharratt. Thanks are due to Mr. A. S. White for his continued interest in this work, and to Dr. H. R. C. Pratt for many helpful discussions.

Nomenclature

A	area of interface in transfer cell – cm^2
c	concentration – gm/100 cm^3, at time t.
c_0	total initial concentration.
c^*	concentration in equilibrium with other phase.
E	activation energy – K.cals/mole.
H	distribution or partition coefficient – c_s/c_w
H', H'', H^*, H°	defined by equations (5a), (5b), (9a) and (9b).
j	transfer rate – gm/cm^2 sec.
K_{os}	" overall " mass transfer coefficient based on solvent phase – cm/sec.
K_{ow}	corresponding overall coefficient based on water phase – cm/sec.
k	individual mass transfer coefficient – cm/sec.
k_{rs}	velocity constant for first order interfacial reaction based on solvent phase – cm/sec.
k_{rw}	corresponding velocity constant based on water phase – cm/sec.
L	length of stirrer – cm.
N_1, N_2	stirring rates in phase 1 and phase 2 respectively – revs. per sec.
t	time – secs.
V	volume of cell compartments – cm^3.
Re_1	Reynolds number in phase 1 $= \dfrac{L^2 N_1}{\nu_1}$.
Re_2	Reynolds number in phase 2 $= \dfrac{L^2 N_2}{\nu_2}$.
η	viscosity – gm/sec cm.
ν	kinematic viscosity $= \eta/\rho$ – cm^2/sec.
ρ	density – gm/cm^3.

Subscripts

1	phase under consideration.
2	other corresponding phase.
s	solvent phase.
si	value in solvent phase at interface.
w	water phase.
wi	value in water phase at interface.

VOL. 3 1954

References

[1] Lewis, Part I, preceding paper.

[2] Morasio; Ind. Eng. Chem. 1926 **18** 701.

[3] See e.g. Treybal: Liquid Extraction (McGraw-Hill, New York, 1951) p. 120.

[4] Murdoch and Pratt; A.E.R.E. CE/R 907; Trans. Inst. Chem. Engrs. 1953 **31** 307.

[5] Lewis and Pratt; Nature 1953 **171** 1155.

[6] Andreas, Hauser and Tucker; J. Phys. Chem. 1938 **42** 1001; Fordham; Proc. Roy. Soc. A 1948 **194** 1.

[7] Sebba; J. Chem. Soc. 1940 106; 1952 2513.

[8] Allen and Caldin; Quart. Rev. 1953 7 255.

[9] Ward and Brooks; Trans. Faraday Soc. 1952 **48** 1124.

Chemical Engineering Science, 1954, Vol. 3 pp. 279 to 286. Pergamon Press Ltd.

A rapid method of measuring absorption rates and its application to CO_2 absorption into partially carbonated ammonia liquor

S. P. S. Andrew

Imperial Chemical Industries Ltd., Billingham Division, Billingham

(*Received September* 1954)

Summary—An experimental absorption system designed to simplify the investigation of processes in which the absorption rate is limited by liquor reaction is described.

Data from an investigation into the mechanism of absorption of carbon dioxide into partially carbonated ammonia liquor is utilised to illustrate the operation of this absorption system and is then employed for determining the kinetic constant for the reaction controlling the absorption rate in this process. The values obtained agree satisfactorily with those previously measured by other techniques.

Résumé—L'auteur décrit une méthode expérimentale d'absorption conçue pour simplifier l'étude des processus dans lesquels la vitesse d'absorption est limitée par la réaction en phase liquide.

Il utilise les résultats d'un travail sur le mécanisme d'absorption du CO_2 dans une solution ammoniacale partiellement carbonatée, pour illustrer le mécanisme de cette méthode d'absorption et calculer ensuite la constante cinétique de la réaction contrôlant la vitesse d'absorption. Les valeurs obtenues sont en bon accord avec celles qui avaient été mesurées auparavant par d'autres procédés.

Introduction

Any thorough experimental investigation into a particular case of absorption accompanied by chemical reaction in a packed tower usually involves a considerable number of measurements of absorption rates under differing conditions of gas composition, liquor flow rate, liquor composition and temperature. The large number of liquor and gas analyses which must be made accurately in order to obtain absorption rates and driving forces, together with the necessity of possessing comprehensive vapour pressure data for the liquor, are liable to deter the intending investigator whose time is limited. The apparatus to be described greatly simplifies the task of measuring absorption rates, and obviates the necessity of using vapour pressure data for the interpretation of the absorption mechanism. This apparatus has been used for determining the mechanism of the absorption of carbon dioxide into partially carbonated ammonia liquor, and results of this investigation will be utilised in order to illustrate its method of operation. Data from these measurements are also used to obtain the temperature variation of the kinetic constant for the second order liquor reaction between free ammonia and free carbon dioxide.

The Experimental Method

A flowsheet of the apparatus is given in Fig. 1. The absorption tower consists of a 1 in. diameter vertical glass tube containing 76 ceramic discs threaded on a vertical wire running down the axis of the tube. Each disc is set with its face at right angles to the faces of the discs immediately above and below it. The gas stream passes up the tube and surrounds the discs which are wetted by the descending liquor stream. The tube walls are not wetted. The general arrangement of the absorption tower is similar to that described in Ref. [1], and is particularly suited to the measurements of absorption rates where the liquid film is controlling. The design shown has a gas/disc interfacial area of 355 sq. cm.

The gas flow up the tower is maintained by a positive displacement rotary gas booster which circulates gas through the tower at a rate of about 4 M^3/hr. This corresponds to a gas velocity of

about 8 ft/sec up the tower. The gas leaving the top of the tower passes through a reservoir vessel fitted with a by-pass and purge connections before re-entering the booster. The circulating gas is virtually at atmospheric pressure, but is isolated from the atmosphere by the small lute filled with transformer oil shown teed in to the descending gas pipe.

When the absorption tower was in use for absorbing carbon dioxide in partially carbonated ammonia liquor, pure carbon dioxide was fed into the circulating gas stream through the connection to the descending pipe at a rate that was sufficient to replace the carbon dioxide absorbed in the liquor passing down the tower. The feed rate was manually adjusted so as to maintain the circulating gas pressure at the lute equal to atmospheric, the carbon dioxide absorption rate being then directly indicated on the capillary flowmeter.

As the process of carbon dioxide absorption is liquid-film limited, the rate of absorption is not increased by increasing the gas flow rate up the absorption tower. With the design of tower shown, the amount of carbon dioxide absorbed from the gas stream in a single pass up the tower was only a small fraction of the total amount passing up the tower due to the high gas circulation rate and the low absorption rate; the partial pressure of carbon dioxide in the gas stream decreasing by less than 5% between the bottom and top of the tower. Variation in the liquor composition and temperature between top and bottom of the tower was also small. The absorption tower is thus virtually an element of packing surface of known area in which gas of a constant composition is contacted with liquor of a known composition and where the resultant absorption rate is directly measured.

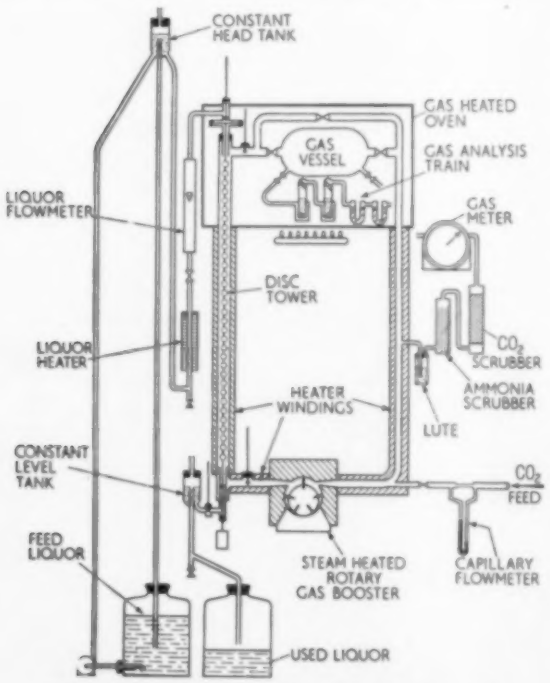

Fig. 1. Arrangement of experimental apparatus.

In order to promote absorption it is, of course, necessary for the partial pressure of the absorbing gas in the gas stream (p_g) to be higher than its partial pressure in equilibrium with the liquor (p_l). The difference in partial pressure ($p_g - p_l$) $= \Delta p$ is known as the driving force promoting absorption, and must be evaluated in order to analyse the results of absorption rate measurements. This quantity is usually obtained from the results of a gas analysis, which gives p_g, and the use of vapour pressure data for the liquor in conjunction with measurements of the liquor temperature and composition which gives p_l. This procedure is unnecessary with the apparatus described as the absorption train and gasmeter attached on the outlet side of the lute enable the driving force (Δp) to be read directly. Their use is best described by considering the circulating gas content of the system, firstly, when the gas is in equilibrium with the liquor passing down the absorption tower, and secondly, when carbon dioxide is admitted into the circulating system and absorption is taking place.

In the first case, the circulating gas contains partial pressures of carbon dioxide, ammonia and water vapour in equilibrium with the liquor, together with sufficient air to bring the total pressure up to one atmosphere. In the second case, the circulating gas contains partial pressures of ammonia and water vapour in equilibrium with the liquor as before, a partial pressure of carbon dioxide exceeding the previous value by the driving force (Δp) and a partial pressure of air less than the previous value by the amount

VOL. 3 1954

Δp. Provided that the circulating gas and liquor temperatures are maintained the same by suitable adjustments to the heaters fitted to the absorption tower, gas pipes, gas reservoir and circulating pump, then the volume of air displaced from the circulating stream through the lute and into the gas meter is $(\Delta p)(V)$ where V is the volume of the gas circulating system. As a certain amount of ammonia, carbon dioxide and water vapour are also displaced through the lute, a small acid filled ammonia scrubber and a Sofnolite packed carbon dioxide absorber are interposed between the lute and the gas meter to ensure that the meter only records the displaced air. Knowing the volume of the gas circulating system and the temperature of the meter and the circulating gas, the constant of proportionality between meter reading and partial pressure driving force is readily obtained.

In order to measure the rate of absorption of carbon dioxide into a liquid of known composition and temperature flowing at a known rate down the absorption tower and under a known partial pressure driving force, it was thus merely necessary to set the liquor flow rate by the rotameter, start the gas booster and adjust the gas and liquor temperatures by means of the heaters, and then by admitting carbon dioxide into the system displace sufficient air through the gas meter to give the required driving force. The capillary flowmeter reading when the gas meter pointer was stationary on the correct driving force and the lute had ceased blowing was then equal to the carbon dioxide absorption rate.

In order to check values of the driving force obtained in the above manner it was possible to isolate the gas reservoir and analyse its contents when the apparatus was running. In this connection it may be noted that it was essential to maintain the whole of the apparatus in contact with the circulating gas at a temperature slightly above the liquor temperature in order to prevent condensation on the walls. The gas reservoir and gas analysis train were placed in a gas heated air oven, the absorption tower and descending gas pipe were wound with heating elements and the gas booster was surrounded by steam coils. All measurements were made with circulating gas compositions and temperature for which the formation of ammonium carbamate was impossible.

Analysis of The Mechanism of Absorption

Theorectical investigations into the process of absorption with chemical reaction [2] have distinguished certain limiting mechanisms to which actual systems approach in behaviour. The recognition of the particular limiting mechanism which best describes the characteristics of the absorption system under study is most easily effected by setting down the behaviour of these limiting cases in response to variations in experimental constraints. The most readily variable constraints are : liquor flow rate (L), partial pressure driving force (Δp) and concentration of the uncombined liquor reactant (B). The following table gives the criteria which characterise the three limiting mechanisms distinguished in [2].

Table 1. *List of absorption criteria.*

Mechanism		*Influence on absorption rate*		
Description	*Conditions**	*Of L*	*Of* Δp	*Of B*
Reaction rate in film slow compared with interchange of B or A across film	$k_l \frac{B}{Z}$ or $k_l A > A\sqrt{kDB^n}$	$\propto L^{0.5}$ to $L^{0.9}$	$\propto \Delta p$	Small
Reaction rate in film slow compared with interchange of B but fast compared with A	$k_l \frac{B}{Z} > A\sqrt{kDB^n} > k_l A$	None	$\propto \Delta p$	$\propto B^{n/2}$
Reaction rate in film fast compared with interchange of both B and A across film	$A\sqrt{kDB^n} > k_l \frac{B}{Z} > k_l A$	$\propto L^{0.5}$ to $L^{0.9}$	Small	$\propto B$

* For list of symbols see end of article.

Of the above three mechanisms, the first is very similar to the simple process of absorption without chemical reaction, inasmuch as a negligible amount of reaction of the dissolving gas takes place in the liquid film, and consequently the rate of transfer is solely determined by diffusion. If the reaction is very slow indeed then the absorption rate will become limited by the rate of reaction in the liquor held up in the tower packing. In the limit this fourth mechanism results in an absorption rate proportional to the product of the reaction rate and $L^{0.3}$. The last term expresses the fact that the hold up in a fully wetted packed tower is roughly proportional to the one third power of the liquor flow rate.

In general, an actual case of absorption with chemical reaction will not follow any one of the fixed limiting mechanisms exactly. Its behaviour will rather tend towards one or other of the limiting cases as the experimental constraints are varied. Thus, the second of the tabulated limiting mechanisms is favoured by a low driving force and a high reactant concentration, whereas the third is rendered likely by the opposite conditions. A theoretical analysis based on the classic film theory of cases intermediate between the limiting mechanism quoted in Table 1 is given in [2]. Analyses based on the unsteady state theory of absorption give rather different expressions for absorption rates from the classic theory. All theories are, however, agreed on the general features of the criteria listed in Table 1, and agree exactly on the expression for absorption rates for the second limiting mechanism, but there is some uncertainty as to the value of the index of the liquor rate effect for the first and third mechanisms. The indices of 0·5 to 0·9 which are given have been taken as covering the range of values found experimentally.

The Carbonation of Ammonia Liquor

Laboratory investigations into the absorption of carbon dioxide into ammonia liquor in a packed tower have previously been reported by Van Krevelen *et al.* [3] and recently in a wetted-wall tower by Silver [4]. Both these investigations were concerned with dilute (less than 2·2 N) virtually uncarbonated ammonia liquor such as is used in gas works practice. The measurements reported here extend the range of liquor compositions up to 11 N ammonia liquor, whilst dealing systematically with the effects of driving force, of liquor flow rate, of liquor temperature and of degree of reaction, on the carbon dioxide absorption rate.

The effect of partial pressure difference driving force on the absorption rate for three different liquor compositions is shown in Fig. 2. The values

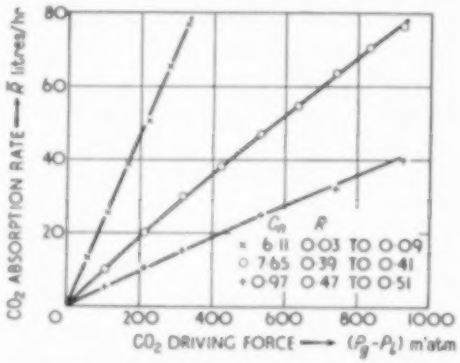

Fig. 2. Effect of CO_2 driving force on CO_2 absorption rate.

plotted are the direct experimental readings, the absorption rate being the capillary flowmeter readings, and the driving force being the reading of the specially calibrated gasmeter. The series of readings for one of the liquor strengths is given in Table 2. In making this series the absorption tower was run continuously with a feed liquor of constant composition, and the driving force increased at intervals by 100 m.atm. steps. Due to this procedure both R, the mean carbonation ratio of the liquor in the tower (the mol ratio of CO_2 to NH_3), and the mean liquor temperature increased slightly between the first measurement at 106 m.atm. driving force and the last at 927 m.atm. Apart from this small effect it is, however, quite clear from Fig. 2 that the carbon dioxide absorption rate is proportional to the driving force Δp. It is also evident that the liquor composition has a pronounced influence on the constant of proportionality between absorption rate and driving force. Reference to the table of criteria characterising the three limiting mechanisms indicates that the only mechanism likely to satisfy the above conditions is the second.

VOL. 3 1954

Table 2. Experimental results showing effect of CO_2 driving force on CO_2 absorption rate.

Liquor flow rate			lit./hr.	7·7									
Liquor Temperatures	Inlet		°C	20									
	Exit		°C	26	26	26·5	27	27·5	28·5	29	29·5	30·5	
	Mean		°C	23	23	23·2	23·5	23·7	24·2	24·5	24·7	25·2	
Liquor Compositions	Total NH_3	(C_n)	mol./lit.	7·65									
	Carbonation Ratio (C_c/C_n)	Inlet	-	0·390									
		Exit	-	0·398	0·404	0·411	0·417	0·424	0·430	0·435	0·440	0·445	
		Mean	-	0·394	0·397	0·401	0·404	0·407	0·410	0·412	0·415	0·418	
Driving force ($p_g - p_i$) = Δp			m. atm.	106	213	320	427	533	634	741	882	927	
CO_2 absorption rate		(N_c)	K lit./hr.	10·6	20·0	30·0	38·0	47·0	54·5	68·5	70·0	76·5	

This conclusion gains further support when the effect of liquor flow rate on absorption rate is studied. The results of tests made with four different liquor compositions showing the effect of liquor flow rate are plotted in Fig. 3. In order to reduce the measured absorption rates to a common basis and eliminate the influence of liquor composition, the ordinate is taken as the ratio of the absorption rate measured at a given liquor flow rate to the absorption rate measured using the same liquor and driving force at a standard flow rate, which was taken to be 10 litres/hr. All the points obtained fall on a smooth curve which is divisible into two parts, a steeply rising curve in which the absorption rate increases rapidly with increase in liquor rate followed by an almost flat line where the absorption rate increases only slightly with increase in liquor rate. The sharp fall off in absorption rate below about 7 litres/hr is ascribed to incomplete wetting of the packing at these low liquor flow rates, the gas/liquor interfacial area decreasing as the liquor rate decreases. The slow increase in

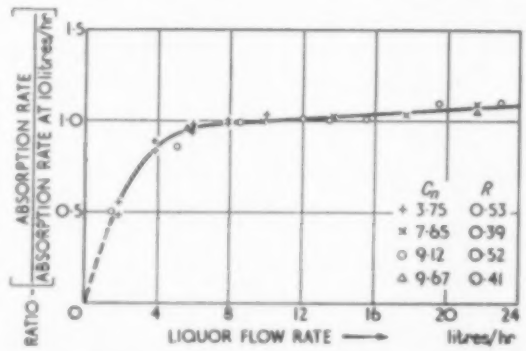

Fig. 3. Effect of liquor flow rate on CO_2 absorption rate.

absorption rate with liquor flow rate when once the packing is fully wetted is further confirmation that the controlling mechanism is the second listed in Table 1. The final criterion for the mechanism was the non-existence of any influence of liquor flow rate on absorption rate. The small influence measured is probably solely due to the greater interfacial area at high liquor rates consequent upon the greater thickness of the liquor layer on the discs.

Having shown that the mechanism controlling the absorption rate over the range of liquor compositions, driving forces and flow rates investigated closely agrees with the second limiting type, it is then possible to determine the kinetics of the liquor reaction from measurements of the effect of liquor composition and temperature on the absorption rate. Reference to Table 1 shows that the order n of the liquor reaction with respect to concentration of the uncombined reactant (ammonia in this case) is double the index of the variation of absorption rate with reactant concentration. Thus, if the absorption rate divided by the driving force is proportional to the square root of the total ammonia strength of the liquor for a given temperature and degree of reaction, this indicates that the reaction is first order with respect to ammonia. Two such plots of experimental values for virtually uncarbonated ammonia liquor (carbonation mol ratio circa 0·05) at temperatures of 20·7°C and 60·5°C are given in Fig. 4. Satisfactory straight lines are obtained up to a liquor strength of 11 N which was the highest used. The rate controlling absorption reaction is thus first order with respect to ammonia, as was also shown by VAN KREVELEN *et al.* and SILVER, for weak liquors [3, 4].

Now for the absorption of a component A from the gas stream into a liquor in which it reacts with component B, under conditions such that the absorption mechanism is of the second type, and the liquor reaction has a velocity given by the kinetic equation $-\frac{dA}{dt} = kAB$, it has been shown [2] that the absorption rate per unit area of interface is :

$$\text{Absorption rate} = N_A = p_g H_A \sqrt{kBD} \quad (1)$$

where H_A = Henry's law constant for solution of A
D = diffusion coefficient of A in liquor
k = second order kinetic constant
p_g = partial pressure of carbon dioxide in gas
B = concentration of reactant in liquor

In the present case this gives :

$$\text{Absorption rate of carbon dioxide per unit interface} = N_c = H_c \sqrt{kD(NH_3)} \cdot p_g \quad (2)$$

where (NH_3) is the concentration of free dissolved ammonia in the liquor.

Equation (2) may be re-arranged so as to enable the kinetic constant to be calculated from the absorption rate measurement, thus :

$$k = \frac{1}{D H_c^2} \left(\frac{N_c}{\sqrt{(NH_3)}} \cdot \frac{1}{p_g} \right)^2 \quad (2a)$$

The last term in the above equation may be obtained from the slope of the lines in Fig. 4 divided by the interfacial area of the disc tower, which was 355 cm². In consistent units values for the two lines are :—

$9{\cdot}8 \times 10^{-5}$ mol/cm² sec atm (mol/cm³)$^{\frac{1}{2}}$ at 20·7°C
and
$20{\cdot}5 \times 10^{-5}$ mol/cm² sec atm (mol/cm³)$^{\frac{1}{2}}$ at 60·5°C

Taking values of

$D = 1{\cdot}82 \times 10^{-5}$ cm²/sec at 20·7°C,
$D = 4{\cdot}53 \times 10^{-5}$ cm²/sec at 60·5°C,
and $H_c = 3{\cdot}85 \times 10^{-5}$ mol/cm³ atm at 20·7°C,
$H_c = 1{\cdot}55 \times 10^{-5}$ mol/cm³ atm at 60·5°C,
then $k = 3{\cdot}56 \times 10^5$ cm³/mol sec at 20·7°C,
$k = 38{\cdot}6 \times 10^5$ cm³/mol sec at 60·5°C.

From these two values of the kinetic constant its

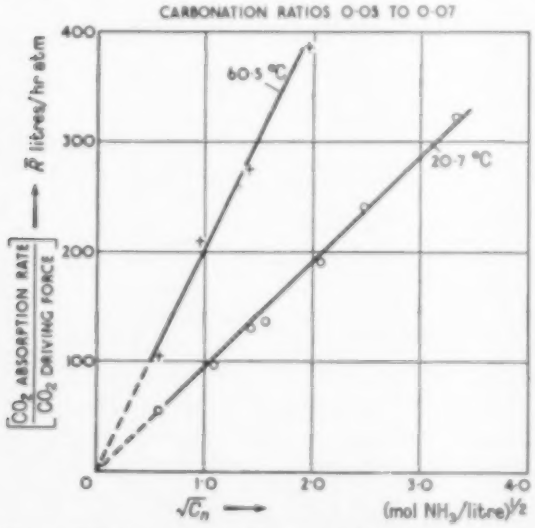

Fig. 4. Effect of strength of liquor on CO_2 absorption rate.

VOL. 3 1954

variation with temperature is found to be given by the equation :

$$\log_{10} k = 14{\cdot}23 - \frac{2{,}550}{T}$$

Values from this equation are found to agree well with those directly measured for the liquor reaction $CO_2 + NH_3 \rightarrow NH_2COOH$ by FAURHOLT [5] and more recently by PINSENT, PEARSON and ROUGHTON [6].

For partially carbonated ammonia liquors it is to be expected that Equation (2), in a modified form, will similarly correlate absorption rates. The ammonia concentration will be the uncombined ammonia content of the liquor, not the total content, and the carbon dioxide partial pressure driving force will be the difference $(p_g - p_l)$ as the partially carbonated liquor exerts a partial pressure of carbon dioxide of magnitude p_l. The modified form of equation (2) is :

$$N_c = H_c \sqrt{kD\,(NH_3)}\,(p_g - p_l) \qquad (3)$$

As the reacted carbon dioxide combines in more than one form with ammonia and an equilibrium between the various ions is set up in the liquor, the relationship between the free ammonia content, the total ammonia content and the carbonation ratio of the liquor is complex. In these circumstances the uncombined ammonia concentration is best calculated from vapour pressure data for the liquor using Henry's law ; whence equation (3) becomes :

$$N_c = H_c \sqrt{kD\,H_n p_n}\,(p_g - p_l) \qquad (3a)$$

where H_n = Henry's law constant for NH_3
p_n = partial pressure of ammonia over liquor.

For dilute liquors, where the solubilities and the diffusion coefficient are little affected by the amount of carbon dioxide dissolved in the liquor, it follows from equation (3a) that :

$$\frac{N_c}{\Delta p} \propto \sqrt{p_n} \qquad (4)$$

The applicability of this law is demonstrated in Fig. 5 where the effect of carbonation ratio on the absorption rate at constant total ammonia concentration is plotted according to equation (4).

At higher total ammonia concentrations (> 2 mol NH_3/litre) appreciable deviations occur from the simple law of equation (3), and equation (3a) must be used, making appropriate allowances for the lower diffusion coefficient and lower solubilities in liquors containing much carbon dioxide.

With the above qualifications it appears that the mechanism of absorption corresponds closely with the limiting case defined by equation (3a) for a range of liquor compositions from 0·25 to 11 N on total NH_3 and up to carbonation ratios of 0·6 for the range of temperatures of from 20°-60°C and driving forces of up to 0·8 atm and for the whole range of liquor flow rates possible in the experimental absorption tower. In this connection it is interesting to note that even with the very different hydraulic conditions obtaining in a wetted wall tower, SILVER found a similar mechanism to operate. It is, therefore, likely that for similar liquor and gas compositions and temperatures, the controlling mechanism will be the same in any type of packed absorption tower. Absorption rate measurements made in the experimental tower are, therefore, directly applicable to the design of large scale packed towers in these circumstances.

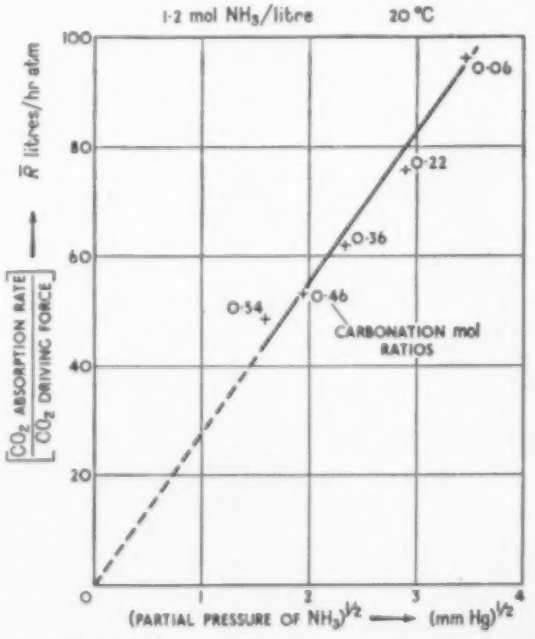

Fig. 5. Effect of carbonation ratio on CO_2 absorption rate.

Notation

A = Concentration of absorbed component in liquor	mol/cm³	n = Order of the liquor reaction with respect to the liquor reactant	
B = Concentration of reactant in liquor	mol/cm³	N_A = Absorption rate per unit of interface of absorbed component	mol/cm² sec
C_c = Concentration of total CO_2 in partially carbonated ammonia liquor	mol/cm³	N_c = Absorption rate per unit of interface of CO_2	mol/cm² sec
C_n = Concentration of total NH_3 in partially carbonated ammonia liquor	mol/cm³	p_g = Partial pressure of CO_2 in gas stream	atm
D = Diffusion coefficient of absorbed component in liquor	cm²/sec	p_l = Partial pressure of CO_2 in equilibrium with liquor	atm
H_A = Henry's law constant for solution of A	mol/cm³ atm	p_n = Partial pressure of ammonia in equilibrium with liquor	atm
H_c = Henry's law constant for solution of CO_2	mol/cm³ atm	Δp = Partial pressure driving force	atm
H_n = Henry's law constant for solution of NH_3	mol/cm³ atm	R = Ratio C_c/C_n, the carbonation ratio of the liquor	
k = Kinetic constant for the absorption reaction (2nd order)	cm³/mol sec	t = Time	sec
k_l = Liquid film matter transfer coefficient	cm/sec	T = Absolute Temperature	°K
L = Liquor flow rate	cm³/sec	Z = Number of molecules of B reacting per molecule of A	
		(NH_3) = Concentration of free dissolved NH_3 in the liquor	mol/cm³
		$\overline{R}$ = Refers to gas volumes at 20°C and 1 atm. pressure.	

VOL. 3 1954

References

[1] Stephens, E. J. and Morris, G. A.; Chem. Eng. Prog. 1951 **47** 232.

[2] Van Krevelen, D. W. and Hoftijzer, P. J.; Rec. Trav. chim. Pays-Bas 1948 **67** 563.

[3] Van Krevelen, D. W. and van Hooren, C. J.; Rec. Trav. chim. Pays-Bas 1948 **67** 587.

[4] Silver, L.; Proc. Inst. Chem. Eng. 1954, Symposium on Gas Absorption.

[5] Faurholt, L.; J. Chim. Phys. 1925 **22** 1.

[6] Pinsent, Pearson and Roughton, private communication to author.

Chemical Engineering Science, 1954, Vol. 3, pp. 287 to 298. Pergamon Press Ltd.

Equilibrium calculations

S. R. M. Ellis

Chemical Engineering Dept., The University, Birmingham.

(*Received August* 1954)

Summary—A simplification is suggested of the Ponchon and Savarit difference-point construction method for distillation at constant molal overflow by using a reflux-concentration diagram. This method is particularly applicable to dilute solutions and for graphical tray-to-tray analysis in azeotropic, extractive, and multicomponent separations. The difference-point construction is common to most unit operation equilibrium calculations.

Résumé—Dans le cas de la distillation à flux moléculaire constant, l'auteur simplifie la méthode graphique de Ponchon et Savarit en se servant d'un diagramme reflux-concentration. Cette méthode est applicable en particulier aux solutions diluées et pour l'analyse graphique " plateau à plateau " dans les séparations azéotropiques, extractives et des systèmes complexes.

Cette construction est commune aux calculs d'équilibre de beaucoup d'opérations fondamentales.

Equilibrium Calculations

Numerous graphical procedures have been proposed for calculating the number of equilibrium stages in countercurrent mass transfer operations. In the field of distillation one of the classical methods is that of Ponchon [10] and Savarit [13], using an enthalpy concentration diagram. This method allows for varying molal overflow and so takes into account heats of mixing, varying molal latent heats, etc.

The method can only be used, however, in the limited number of cases in which the requisite enthalpy data are available. The well-known McCabe-Thiele method overcomes this difficulty by making the assumption, which is approximately valid in a number of systems, of constant molal overflow. The object of this paper is to suggest a graphical construction, using a reflux-concentration diagram similar to that of the Ponchon-Savarit method, but incorporating the assumption of constant molal overflow.

The use of a reflux concentration diagram involving the difference-point construction is useful in the stripping of very dilute solutions and for tray-to-tray analysis in ternary and multicomponent distillation. Interest in this method of calculation also arises in the teaching of chemical engineering since the difference point construction is common to several unit operations, i.e. adsorption, absorption, liquid extraction, leaching, ion exchange, etc.

Graphical Representation

In Fig. 1 two horizontal lines are drawn at any convenient distance apart. The lower line is used to represent the liquid (X) and the upper line to represent the vapour (Y). If the liquid is at the boiling point, mark off on the (X) line the compositions of the bottoms, feed and distillate, namely X_w, X_f and X_D. Draw a vertical line from X_D and mark off the reflux ratio $\frac{MA}{AB}$. Join MX_f and extend to the

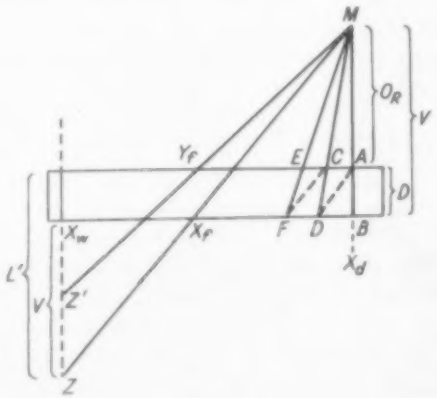

Fig. 1.

line through X_w at Z. The difference point Z is located on the line through X_w by the reflux ratio below the feed tray. Starting from the top of the column the tie-line AD represents the top plate. The line MD is now drawn, and cuts the Y-line at C, representing the vapour leaving the second plate down. The line CF represents this plate, while E represents the vapour rising to it from the third plate, and so on. A similar construction, using lines drawn through Z, gives the composition of vapour and liquid leaving plates below the feed.

When the feed is a vapour, join MY_f and extrapolate to cut the X_w line at Z'. The actual location of the feed point on the vertical line from Y_f to X_f is determined by q, the total heat needed to convert one mole of feed into saturated vapour divided by the molal latent heat. If the feed is a vapour, i.e. $q = 0$ and the feed point is Y_f. If the feed is a liquid at the boiling point, i.e. $q = 1$, the feed point is at X_f. If the feed is partially vapourised q will be between zero and 1 with the feed point being a fraction q of the distance from Y_f to X_f. If the feed is a cold liquid q will be greater than 1 with the feed point below X_f on the vertical line Y_f to X_f, while if it is a superheated vapour the feed-point will be above Y_f.

It can be shown by simple geometrical considerations that the construction gives the same results as the McCabe-Thiele diagram, with straight operating lines. It may be noted that the X- and Y-lines need not be horizontal as long as they are parallel. The condition for constant molal overflow is that the vapour and liquid lines on the enthalpy-composition chart should be straight and parallel.

Benzene-Toluene Separation

Fig. 2 shows the graphical construction for determining the number of equilibrium stages when the feed composition at the boiling point is 30·0 mole % benzene, the overhead composition is 95·0 mole % benzene, and the bottoms composition 5·0 mole % benzene. For a reflux ratio of 3:1 the number of theoretical trays is 12·7. The McCabe-Thiele construction also gives 12·7 theoretical trays.

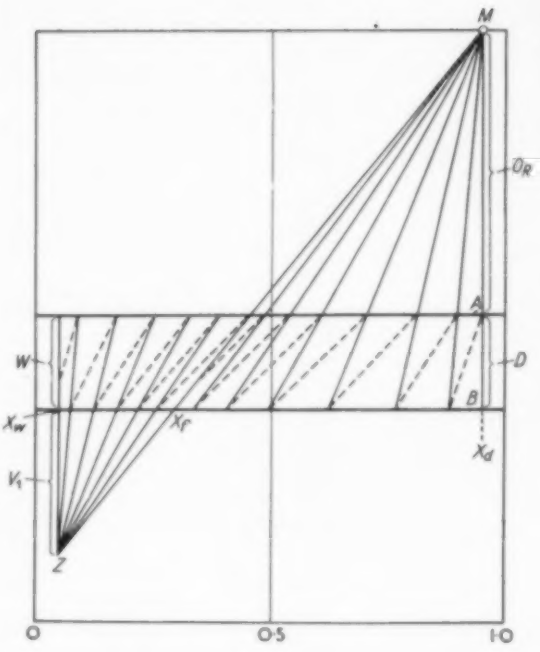

Fig. 2.

Stripping of Dilute Solutions

For the stripping of alcohol or phenol from water the mole fraction of component remaining in the water is often very low indeed, i.e. 0·00001-0·0001 mole fraction. This low concentration makes it almost impossible to enlarge the McCabe Thiele graphical plot sufficiently to determine the number of equilibrium stages in the column. To overcome this difficulty various workers have suggested the use of a log-log plot to facilitate the calculations. This log-log construction suitably spreads the equilibrium curve but makes the location of the resulting curved operating line somewhat difficult.

A simpler and probably more accurate graphical procedure than the log-log plot is suggested for determining the number of theoretical or equilibrium stages in the column. The procedure, involving the difference point construction, is best illustrated by the following example :

It is desired to strip an alcohol feed of approximately 0·03 mole fraction of ethyl alcohol in water to a final concentration of 0·00004 mole fraction ethyl alchohol. The number of theoretical

VOL. 3 1954

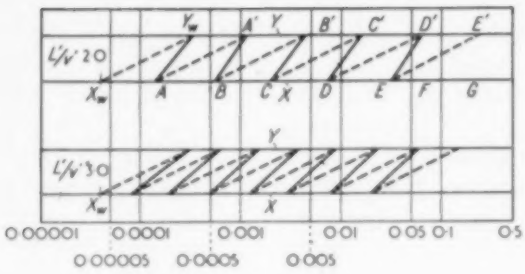

Fig. 3.

plates are required for $\frac{L'}{V'}$ reflux ratios of 2·0 and 3·0 respectively.

Firstly a vapour (Y) and liquid (X) line is drawn on log-rectangular paper as shown on Fig. 3. Equilibrium relationships are shown plotted by dotted lines. For most systems at very low concentrations the equilibrium ratio is constant and consequently as seen on Fig. 3 the equilibrium tie lines are parallel. The vapour (Y) and liquid (X) lines can be placed any convenient distance apart.

Starting from X_w, the still composition, the equilibrium composition Y_w is evaluated. Using equation (1) the solid line on Fig. 3 relates the liquid composition (A) to the vapour composition Y_w. After the first one or two trays at the base of the column the solid lines, or operating lines, become parallel thus leading to a simplification of the graphical construction.

From the general operating line equation

$$L'X_{m+1} = V'Y_m + WX_w \qquad (1)$$
$$= V'Y_m + (L' - V')X_w$$

if $\frac{X_{m+1}}{X_w} \geqslant 1 - \frac{V'}{L'}$, then equation (1) reduces to

$$\frac{Y_m}{X_{m+1}} = \frac{L'}{V'} = \text{constant} \qquad (2)$$

Thus for reasonable reflux ratios the operating lines become parallel when $X_{m+1} \geqslant X_w$. This condition is usually fulfilled after one or two trays if X_w itself is very small.

From Fig. 3 the number of theoretical stages is 6·0 for $\frac{L'}{V'} = 2{\cdot}0$ and 8·5 for $\frac{L'}{V'} = 3{\cdot}0$.

Rectifying Section

The rectification of components of low relative volatility often requires a diagram to be plotted on a large scale. This is well illustrated by Robinson and Gilliland ([12] p. 210) in the purification of alcohol. The scale on Fig. 4 can be conveniently enlarged and when the reflux ratio is high the following construction is sometimes useful.

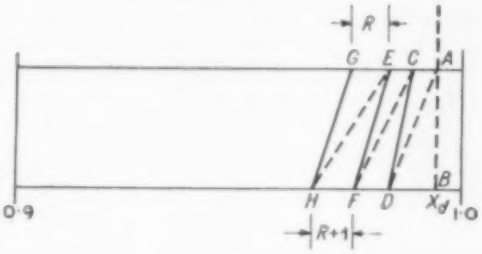

Fig. 4.

The vapour (Y) and liquid (X) scales can be placed any distance apart with the dashed lines AD, CF, EH, etc., representing the tie equilibrium lines. The operating lines are located by the following relationships

$$\frac{AC}{BD} = \frac{EC}{FD} = \frac{GE}{HF} = \frac{R}{R+1} \qquad (3)$$

The number of equilibrium stages is determined as before by zig-zagging between the equilibrium and operating lines.

Ternary Mixtures

Most ternary graphical methods for equilibrium calculations are based on the binary key component McCabe-Thiele construction or use the triangular graph difference point construction, i.e. Bonilla [1], White [18]. Chambers [4] uses McCabe-Thiele constructions for ternary tray-to-tray analysis but the overall plots are somewhat confusing.

The difference point construction used on Fig. 1 lends itself to tray-to-tray analysis in ternary mixtures. A single graph is constructed for each component.

Consider the example of Robinson and Gilliland ([12] p. 219) for the system benzene-toluene-xylene. The feed composition is 60·0

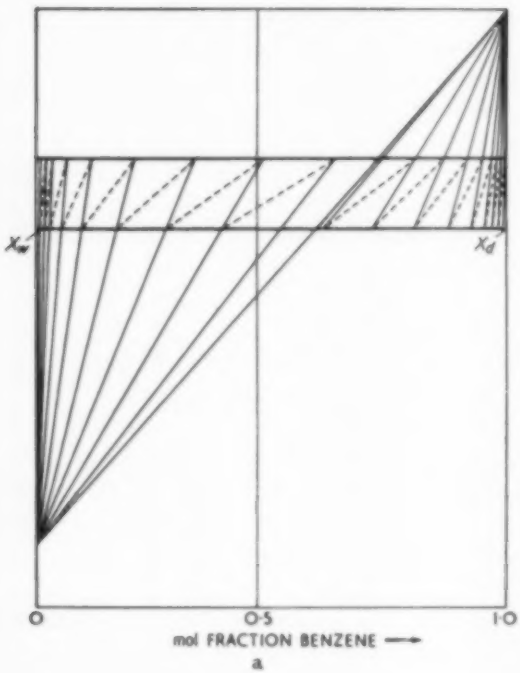

Fig. 5a.

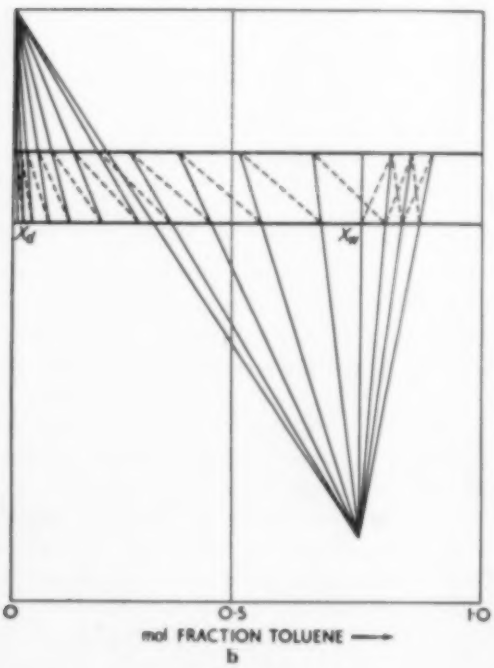

Fig. 5b.

mole % benzene, 30·0 mole % toluene, 10 mole % xylene, the overhead product 99·5 mole % benzene, 0·5 mole % toluene and the bottoms composition 0·5 mole percent benzene, 74·4 mole % toluene and 25·1 % xylene. The tray-to-tray analysis construction is shown on Fig. 5. On Fig. 5c for the xylene component it is to be

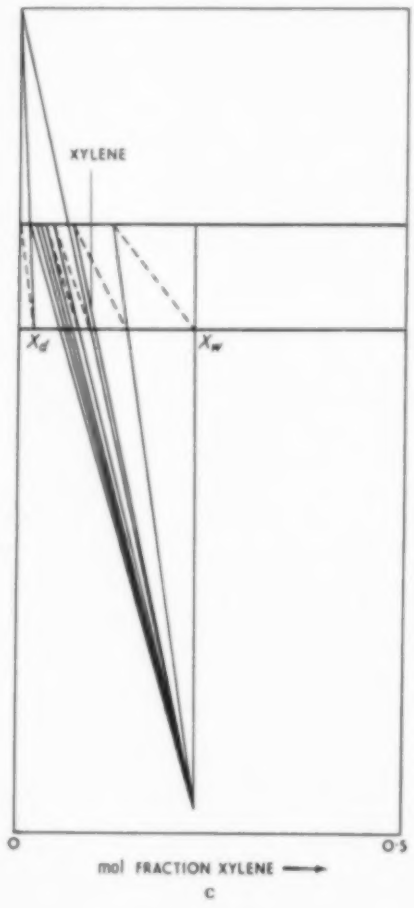

Fig. 5c.

noted that the change over from the stripping to the rectifying operating line occurs at the composition of xylene on the feed tray and not at the composition of xylene in the entering feed. Such constructions as shown on Fig. 5 help to give a clear picture how each component distributes itself throughout the column.

VOL. 3 1954

Fig. 6 gives the tray-to-tray analysis for example 1 quoted by Chambers [4]. A feed of 50·0 mole % methyl alcohol, 20 mole % ethyl alcohol, 30·0 mole % water enters the column to give an overhead distillate of 92·0 mole % methyl alcohol, 8·0 mole % water and a bottoms composition of 8·0 mole % methyl alcohol, 32·0 mole % ethyl alcohol, 60·0 mole % water. Chambers has expressed the ternary vapour liquid equilibria on Y-X diagrams for methyl alcohol-water, ethyl alcohol-water, with the third component as parameter. This representation of the equilibrium data for azeotropic and extractive distillation systems permits the rapid use of equilibrium data in the graphical constructions outlined in this paper.

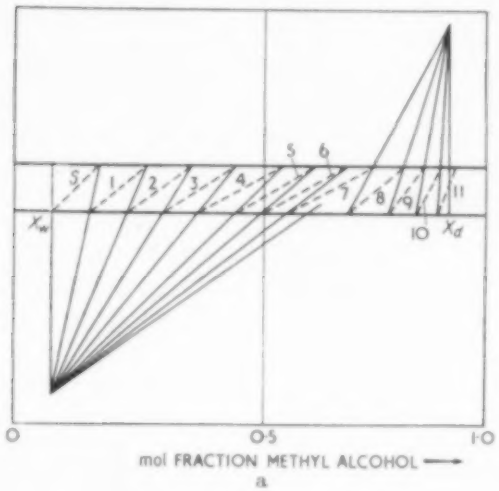

a

Fig. 6a.

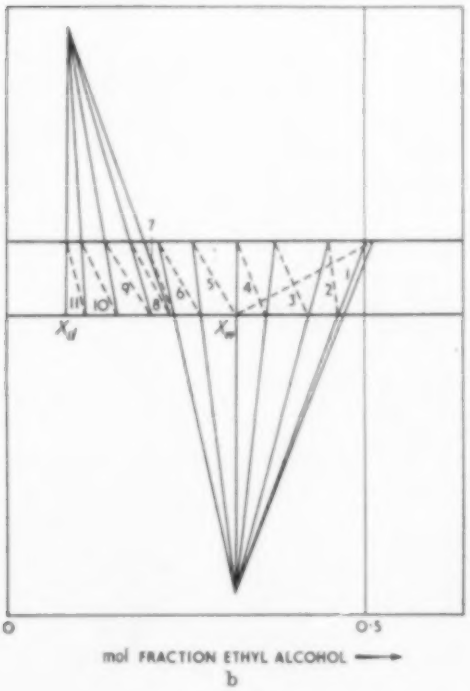

b

Fig. 6b.

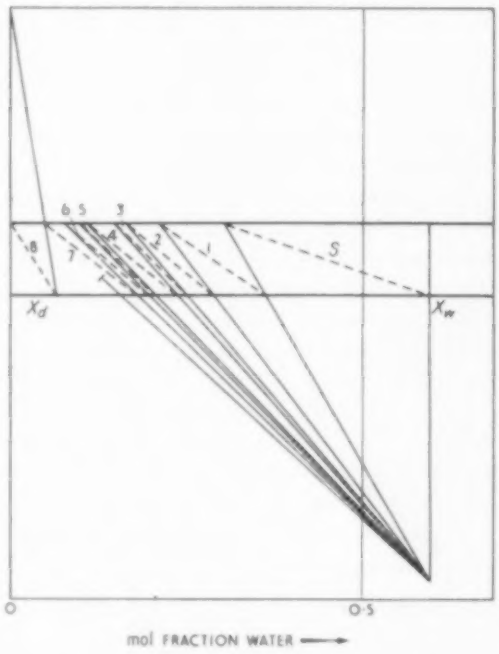

c

Fig. 6c.

From Fig. 6 it will be seen that the feed enters tray 7. The composition entering the tray is a mixture of the feed and the composition leaving tray 8 and corresponds to 62.0 mole % methyl alcohol, 21·5 mole % ethyl alcohol and 16·5 mole % water. The composition leaving the feed tray is in approximate agreement with the composition leaving tray 7. In the location of the feed tray in this example, it is important that there should be the correct percentage of water on the feed tray since the amount of water influences the equilibrium relationships and thus the

obtaining of the correct overhead and bottoms compositions.

The representation of tray-to-tray analysis as shown on Figs. 5 and 6 can also be applied to azeotropic and multicomponent distillation. In the case of azeotropic distillation the reflux ratio in the rectifying section is often high, due to the presence of the entrainer and consequently the use of the construction shown on Fig. 4 for above the feed tray avoids the difficulty of the rectifying section difference point being off the graph paper.

Gas Absorption

Sherwood [15] uses the McCabe-Thiele construction, whereas Brown [3] and Edmister [5] use the absorption factor graphical plot for calculating the number of equilibrium stages.

The difference point construction has not been widely applied to gas absorption equilibrium calculations although Ross [13] has used this construction on triangular graph paper. However, this method is not particularly suitable for low concentrations of solute in the gas stream.

The same graphical constructions as here described for distillation can also be used for gas absorption equilibrium calculations. Gas and liquid composition lines are drawn parallel, the compositions being expressed as lbs. of solute per lb. of non-solute. Fig. 7 shows the plot for the absorption of ammonia from air into water. The gas enters at a concentration of 0·1775 lbs of ammonia/lb. of air and the water leaves at a concentration of 0·125 lbs. of ammonia/per lb. of water. The ratio of water entering to gas leaving is 1·35.

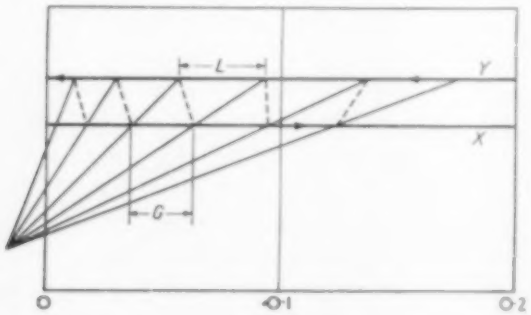

Fig. 7.

Liquid Extraction

The Ponchon and Savarit difference point construction has been extensively used in liquid-liquid extraction calculations. Nash and Hunter [8] have used triangular graphs whereas Thiele [16], Rasdal and Longmarton [11], Treybal [17], Maloney and Schubert [7] and other workers have used rectangular co-ordinates.

Elgin [6] and Brown [2] have used similar graphical constructions for leaching.

Ion Exchange Units

Peeiffer [9] has proposed a difference point construction method for evaluating the number of equilibrium stages in a continuous counter current ion-exchange unit.

Notation

X = mole fraction in the liquid phase.
Y = mole fraction in the vapour phase.
O_R = moles of liquid reflux from the condenser.
L = moles of liquid reflux from tray-to-tray above the feed.
L^1 = moles of liquid reflux below the feed.
V = moles of vapour above the feed.
V^1 = moles of vapour below the feed.
D = moles of distillate.
W = moles of bottoms.
M = difference point above the feed.
Z = difference point below the feed.
A, B, C, D, E, F, G, points of intersection of the operating line on the vapour and liquid lines.
X_D, X_f, X_W, subscripts refer to distillate, feed, and bottoms.
q = total heat to convert one mole of feed into saturated vapour divided by the molal latent heat.

References

[1] Bonilla, C. F.; Trans. Amer. Inst. Chem. Eng. 1941 **37** 664.
[2] Brown, G. G.; "Unit Operation," John Wiley and Sons, 1950, p. 291.
[3] Brown, G. G.; Souders, M., Ind. Eng. Chem. 1932 **24** 519.
[4] Chambers, J. M.; Chem. Eng. Progress 1951 **47** 555.

VOL. 3 1954

[5] Edmister, W. C. ; Ind. Eng. Chem. 1943 35 837.

[6] Elgin, J. C. ; Trans. Amer. Inst. Chem. Eng. 1936 32 451-70.

[7] Maloney, J. O. and Schubert, A. E. ; Trans. Amer. Inst. Chem. Eng. 1940 36 741.

[8] Nash, A. W. and Hunter, T. G. ; J. Soc. Chem. Ind. 1934 53 95.

[9] Peeiffer, P. W. ; Chem. Eng. Sci. 1953 2 45.

[10] Ponchon, M. ; Tech. Moderne 1921 13 20.

[11] Randall, M. A. and Longton, B. ; Ind. Eng. Chem. 1938 30 1063,1188,1311.

[12] Robinson, C. S., Gilliland, E. R. ; " Elements of Fractional Distillation," McGraw-Hill, 1950.

[13] Ross, T. K. ; " An Introduction to Chemical, Engineering," Sir Isaac Pitman & Sons Ltd. London.

[14] Savarit, R. ; Arts et Metiers, 1922, p. 65, 142, 178.

[15] Sherwood, T. K. ; "Absorption and Extraction," McGraw-Hill, 1937.

[16] Thiele, E. W. ; Ind. Eng. Chem. 1935 27 392.

[17] Treybal, R. E. ; " Liquid Extraction," McGraw-Hill, 1951.

[18] White, R. R. ; Petroleum Processing, 1948, February, p. 143.

Book review

Clayton's The Theory of Emulsions and Their Technical Treatment. Fifth edition by C. G. Sumner. Pp. viii + 669. J. & A. Churchill Ltd., London, 1954. 72s. net.

For all who are interested in the theory and the practical applications of emulsions, the appearance of a new edition of Clayton's handbook must necessarily be a matter of interest. Earlier editions have been remarkable for the thoroughness with which they have covered the literature of the subject. "Clayton" has never been a book for the uninitiated, since it accepts most authors at their own valuation. Nevertheless, it has been, and remains, the leading book in English, and probably in any language, as a work of reference, since very few relevant publications are not mentioned in its pages.

The present edition has been prepared by Dr. C. G. Sumner, for many years a collaborator of Dr. Clayton and himself a notable contributor to the literature of the subject. The book has been brought well up to date and now includes chapters on emulsion polymerization and paint emulsions which provide adequate introductions to extensive new fields of literature.

The most serious fault of the book, persisting in the new edition, lies in the mode of presentation of the theoretical material. This is distributed over the first 300 pages and constitutes in effect a complete text-book of surface chemistry, with exhaustive lists of references to literature often of doubtful relevance to the main theme of the book. It is difficult to conceive that the average reader, seeking a succinct account of current emulsion theory, could remain unconfused by this mass of material, most of which is not subjected to critical evaluation by the author.

All this, of course, does not reduce the value of the treatise as a work of reference, and we must be grateful to Dr. Sumner for the meticulous character of his revision. It is to be hoped that, in a future edition, he will discard the superfluous and attempt a critical approach to the theory of emulsions.

D. F. Cheesman.

VOL. 3 1954

CORRECTION

A convenient method for the evaluation of vapour-liquid equilibria of binary mixtures

by W. Jost and H. Rock

On page 18, *right column*, two addition symbols have been inserted in formula (9) instead of multiplication symbols (cf. the corresponding formulae on page 20).

On page 23, *this volume*, the correct reading for $\overset{4}{\underset{0}{\Sigma}}$ at 35°C (middle of the page) is :

1·8798 ; 1·223 ; 1·1150 ; 1·0443 ; 0·9992 ; 0·9709 ; 0·9522 ;
0·9386 ; 0·9271 ; 0·9172 ; 0·9102.

The figures given under the heading $\overset{4}{\underset{0}{\Sigma}}$ are actually those for $\overset{5}{\underset{0}{\Sigma}}$. Comparison shows that it is not reasonable to carry the approximation beyond $\overset{4}{\underset{0}{\Sigma}}$.

The missing number in $\overset{3}{\underset{0}{\Sigma}}$ at 25°C is 0·9333, in $\overset{3}{\underset{0}{\Sigma}}$ at 55°C 0·9500 and in $\overset{4}{\underset{0}{\Sigma}}$ at 55°C 0·9423

END